

# Renormalizable Enhanced Tensor Field Theory: The quartic melonic case

Joseph Ben Geloun<sup>a,c,†</sup> and Reiko Toriumi<sup>b,‡</sup>

<sup>a</sup>*Laboratoire d'Informatique de Paris Nord UMR CNRS 7030*

*Université Paris 13, 99, avenue J.-B. Clement, 93430 Villetaneuse, France*

<sup>b</sup>*Institute for Mathematics, Astrophysics, and Particle Physics, Radboud University,  
Heyendaalseweg 135, 6525 AJ, Nijmegen, the Netherlands*

<sup>c</sup>*International Chair in Mathematical Physics and Applications  
(ICMPA-UNESCO Chair), University of Abomey-Calavi,  
072B.P.50, Cotonou, Rep. of Benin*

E-mails: <sup>†</sup>bengeloun@lipn.univ-paris13.fr, <sup>‡</sup>reiko.toriumi@science.ru.nl

## Abstract

Amplitudes of ordinary tensor models are dominated at large  $N$  by the so-called melonic graph amplitudes. Enhanced tensor models extend tensor models with special scalings of their interactions which allow, in the same limit, that the sub-dominant amplitudes to be “enhanced”, that is to be as dominant as the melonic ones. These models were introduced to explore new large  $N$  limits and to probe different phases for tensor models. Tensor field theory is the quantum field theoretic counterpart of tensor models and enhanced tensor field theory enlarges this theory space to accommodate enhanced tensor interactions. We undertake the multi-scale renormalization analysis for two types of enhanced quartic melonic theories with rank  $d$  tensor fields  $\phi : (U(1)^D)^d \rightarrow \mathbb{C}$  and with interactions of the form  $p^{2a}\phi^4$  reminiscent of derivative couplings expressed in momentum space. Scrutinizing the degree of divergence of both theories, we identify generic conditions for their renormalizability at all orders of perturbation. For a first type of theory, we identify a 2-parameter space of just-renormalizable models for generic  $(d, D)$ . These models have dominant non-melonic four-point functions. Finally, by specifying the parameters, we detail the renormalization analysis of a second type of model. Lying in between just- and super-renormalizability, that model is more exotic: all four-point amplitudes are convergent, however it exhibits an infinite family of divergent two-point amplitudes.

March 13, 2022

Pacs numbers: 11.10.Gh, 04.60.-m, 02.10.Ox

Key words: Renormalization, tensor models, tensor field theories, quantum gravity

# Contents

<b>1</b>	<b>Introduction</b>	<b>1</b>
<b>2</b>	<b>Enhanced <math>p^{2a}\phi^4</math> tensor field theories</b>	<b>5</b>
<b>3</b>	<b>Amplitudes</b>	<b>8</b>
<b>4</b>	<b>Power counting theorems for <math>p^{2a}\phi^4</math>-models</b>	<b>12</b>
<b>5</b>	<b>Analyses of the potentially renormalizable models</b>	<b>17</b>
5.1	Models + . . . . .	18
5.2	Models $\times$ . . . . .	22
<b>6</b>	<b>Rank <math>d</math> just-renormalizable models +</b>	<b>27</b>
6.1	List of divergent graphs . . . . .	27
6.2	Renormalization . . . . .	29
<b>7</b>	<b>A rank <math>d = 3</math> renormalizable model <math>\times</math></b>	<b>33</b>
7.1	List of divergent graphs . . . . .	34
7.2	Renormalization . . . . .	35
<b>8</b>	<b>Conclusion</b>	<b>36</b>
<b>A</b>	<b>Spectral sums</b>	<b>38</b>
<b>B</b>	<b>Divergences in model + (<math>d = 3, D = 1, a = \frac{1}{2}, b = \frac{3}{4}</math>)</b>	<b>39</b>
<b>C</b>	<b>Divergences in model <math>\times</math> (<math>d = 3, D = 1, a = \frac{1}{2}, b = 1</math>)</b>	<b>42</b>

## 1 Introduction

Tensor models [1, 2, 3, 4, 5], and their field theory version, tensor field theories are approaches to Quantum Gravity (QG) which propose a background-independent quantization and, in the field theory case, an ultraviolet-consistent completion of General Relativity. They study a discrete-to-continuum transition for discretized path integrals summing over not only metrics of a discretized Einstein-Hilbert action, but also over topologies. The partition function of tensor models spans weighted triangulations for every piecewise-linear manifold in any dimensions, hence they are naturally a random-geometric approach to QG. In this regard, they can be considered to fall under the umbrella of discretization approaches to QG, such as quantum Regge calculus [6, 7] and (causal) dynamical triangulations [8, 9, 10].

Historically, tensor models were introduced as higher dimensional generalizations of matrix models which saw their celebrated success in describing 2-dimensional QG [11]. It was, however, not so straightforward to generalize matrix models' achievements to higher dimensions mainly because the organizing principle of and computational tools for the partition

function of tensor models were lacking; diagonalization of tensors is not obvious and techniques on which matrix model calculations relied on did not find extensions to tensors. In particular, matrix models generate maps sorted by their genus. Their partition function then admits a genus expansion and, at large size  $N$  of the matrix [12], calculations can be made exact and matrix models become solvable. The large  $N$  limit is crucial to achieve the continuum limit of matrix models, as a 2D theory of gravity coupled with a Liouville conformal field [13, 14, 15, 16, 17, 18]. This is one of the most acclaimed results pertaining to 2D QG.

The large  $N$  limit for tensor models [19, 20, 21] was finally unveiled after the advent of colored tensor models generating triangulations shown to be pseudo-manifolds [22, 23, 24, 25]. The partition function of colored tensor models can be catalogued in terms of a new quantity called the degree of the tensor graph which plays the role of the genus in higher dimensions. Such a discovery, as anticipated, led to a wealth of developments in random tensors in areas as diverse as statistical mechanics, quantum field theory, constructive field theory, combinatorics, probability theory, geometry and topology [26]–[104]. The following references provide comprehensive reviews on random tensors and tensor field theories [60, 42, 47, 77]. Furthermore, more recently, tensor models gathered an attention in a new direction: they turn out to be desirable toy models for holographic duality [105, 106, 107, 108, 109, 110, 111]. The large  $N$  limit in range of the disorder of the famous Sachdev-Ye-Kitaev (SYK) model [112, 113, 114, 115], corresponds to the large  $N$  limit of colored tensor models thought of as quantum mechanical models without disorder [105].

Despite all its remarkable achievements, colored tensor models have not yet succeeded to define a “nice” continuum limit in which an emergent 3D or 4D space could be identified. In colored tensor models, some graphs which are particular triangulations of a sphere, called melons, are found to be dominant at large  $N$  [26]. In the world of melons, colored tensor models undergo a phase transition towards the so-called branched polymer phase which is not of the characteristics (*e.g.*, Hausdorff and spectral dimensions) that our large and smooth space-time manifold holds [70]. In order to improve the critical behavior of tensor models, it was then put forward to go beyond the melonic sector, by modifying the weights of interactions in order to include a wider class of graphs that could be resummed at large  $N$ . Such a proposal has been called “enhancing” tensor models and has first been investigated in the work by Bonzom et al. [71, 72]. The upshot of this analysis is somehow encouraging: some enhanced tensor models undergo a phase transition from branched polymers to a 2D QG phase (with positive entropy exponents). Let us be more specific at this point: the previous studies on enhanced tensor models focused on increasing the statistical weights of non-melonic tensor interactions called necklaces (which are only present in the tensor rank  $d \geq 4$ ). In a different perspective along with its very own set of questions, our proposal is to use the framework of field theories, therefore working in tensor field theories rather than in tensor models, and to explore new ways of building enhanced models in which non-melonic graphs could contribute to the analysis at large  $N$ .

Once one promotes tensor models to field theories, which possess now with infinite degrees of freedom, we call them tensor field theories. Note that, from the 90’s, Boulatov introduced a gauge invariant version of tensor models by embedding them in lattice gauge field theory over  $SU(2)$  [4]. This approach was considerably appealing to make contact with other QG approaches and was at the inception of Group Field Theory (GFT) [116, 117, 59].

Hence, chronologically, the first field theoretic approach of tensor models was GFT. GFT implements a constraint (referred to as the gauge invariance constraint) on the fields to achieve a geometrical interpretation of the combinatorial simplices associated with the tensor field and their interactions, along with a flatness condition for the gluing of simplices. On the other hand, in GFT, as the name refers to it, the group as a manifold where the fields live is a central concept: the group law is used in the underlying lattice gauge field theory. Tensor field theory distinguishes itself with GFT as it might not have these constraints.

There are other motivations for introducing fields in the search of an emergent spacetime. For instance, one makes another progress by regarding the simplicial complex associated with the tensor (in a tensor model) as a true (combinatorial) quantum of space. These fields live in an abstract internal space and are endowed with a given dynamics and consequently a flow. The goal is then to provide a phase portrait of that theory space and, in particular, to detect the presence of interesting (fixed) points. Such fixed points would be associated with interesting physics. Thus, rather than tuning a given tensor model at criticality and seeing a new phase for geometry emerging, we might give initial conditions of a model in a field theory space and let it flow towards the corresponding fixed point. To define a flow, a parameter or a scale is needed. This makes the presence of propagators or regulators of paramount importance in usual field theory. Hence embedding tensor models into a field theoretic context, that is giving them a propagator, provides them with a flow. This naturally steer us towards other interesting questions.

Quantum field theories have many well-established tools in order to reveal the properties of high energy physics and condensed matter systems. However, tensor field theory as a quantum field theory also inherits several of its drawbacks like divergent amplitudes due to the existence of infinitely many degrees of freedom. The treatment of divergences, hence the renormalization program for tensor field theories becomes even more intricate because they are non-local field theories, *i.e.*, their interactions occur in a region of the configuration space. As a result, to import the quantum field theoretic methods to tensor field theories was an important axis of investigations in the recent years.

The Renormalization Group (RG) program has been successfully applied to tensor field theory and also GFT leading to the discovery of entirely new families of renormalizable non-local quantum field theories [80, 88, 87, 89, 90, 93, 91]. These models can be regarded as a rightful extension of matrix field theories like the Grosse and Wulkenhaar model [119, 120, 121], an asymptotically safe non-local quantum field theory stemming from non-commutative geometry. The parametric representation and the ensuing dimensional regularization have been extended to tensor field theory with the emergence of new Symanzik polynomial invariants for tensor graphs [61]. Moreover, the computations of the perturbative  $\beta$ -functions for  $\phi^4$ - and  $\phi^6$ -like models were achieved in the UV [88, 86, 89, 91, 96, 95, 97]. The perturbative results [86, 88, 97] suggested a generic asymptotic freedom for tensor field theories. This result was somehow surprising at first as they are not gauge theories, however, the (combinatorially) non-local nature of the tensor interactions drives the presence of a non-trivial wave-function renormalization, which then eventually dominates the renormalization of coupling constants. Afterwards, careful (perturbative) studies on  $\phi^6$ -like models hinted that the asymptotic safety may be possible in GFT [95, 96]. As a consequence, this last result strongly prompted that  $\phi^6$  theories could have a more complicated behavior in the UV even for tensor field theories and the fact that asymptotic freedom might not hold for these

particular models.

The perturbative renormalization reveals interesting UV properties for tensor field theories which were encouraging to proceed to the next level. The exact renormalization group equations via Polchinski [62, 63] and via Wetterich (Functional Renormalization Group (FRG)) equations were fruitfully applied in all rank  $d \geq 2$  matrix and tensor models with compelling corroborations on the existence of Gaussian and non-Gaussian UV and IR points [64, 65, 66, 44, 46, 45, 68, 69]. Within the ordinary consistency checks on the FRG methods (*i.e.*, extensions of the truncation at higher orders and a change of the theory regulator), non-perturbative calculations show that several  $\phi^4$  models are asymptotically free and a  $\phi^6$  model is asymptotically safe [65, 67, 68]. In the GFT setting, similar conclusions were reached using the same tools with an extension of the truncation [46, 69]. Hence, we conclude with a certain degree of confidence that, generically in tensor field theory, renormalizable  $\phi^4$  models are UV asymptotically free, and renormalizable  $\phi^6$  models are UV asymptotically safe.

The notable UV behavior of renormalizable tensor field theories is only one interesting aspect among other results brought by the FRG analysis. Another result concerns strong evidences for the existence of infrared (IR) fixed points. For tensor field theories, the existence of a IR fixed point could play an important role. Indeed, one aim of the FRG program is to identify the phase portrait of field theories. Stable IR and UV fixed points define complete trajectories which allow to distinguish different regimes of the theory, in other words, the existence of such trajectories could provide evidences for phase transitions in the models. A known mechanism characterizing a phase transition in ordinary field theory is spontaneous symmetry breaking. In fact, from preliminary calculations in [65, 68], the phase diagrams of some tensor field theories show a IR fixed point which is similar to the Wilson-Fisher fixed point of a scalar field theory (it however occurs in different dimensions). This would likely imply that there is a phase transition in tensor field theory. If one shows that this phase transition results from a spontaneous symmetry breaking in these models, this transition will be described in terms of a symmetric phase and a broken or a condensed phase. The broken phase would correspond to a new vacuum state corresponding to some geometry, characterized by a non-zero expectation value of the field. This may validate the scenario in which homogeneous and isotropic geometries emerge as a condensate in GFT [79].

In this paper, we undertake the study of the theory space of enhanced tensor field theories by addressing the perturbative renormalization of classes of enhanced models. We study tensor field models with quartic melonic interactions with a momentum weight mimicking derivative couplings. The effect of the new couplings is to make the non-melonic graph amplitudes larger than or as large as the melonic graph amplitudes. Note that derivative couplings are well established in ordinary renormalizable quantum field theory *e.g.* appearing as in non-Abelian Yang-Mills theories. The issue addressed in this work is to find a class of renormalizable theories endowed with non-local and weighted interactions. As one can expect, the presence of these interactions bears additional subtleties as it naturally tends to increase the divergence degree of a graph.

The enhanced models that we study radically differ from that of [72] and [69], as we do not enhance non-melonic interactions of the necklace type but melonic interactions. We could apply the same idea of derivative-type couplings over necklaces and expect that the resulting kind of enhanced tensor field theories to be closely related to the one of the above

references.

Specifically, we focus on  $\phi^4$ -melonic couplings which are endowed with extra powers of momenta  $|p|^{2a}$ ; we call the resulting models  $p^{2a}\phi^4$ -models, where  $a \geq 0$  is a parameter. The study is put on a very general ground, at any rank  $d$  of the tensor field defined on a Abelian group of dimension  $d \times D$ . The propagator of the model is of the form  $(\sum |p|^{2b} + \mu)^{-1}$ , where  $b > 0$ . Hence our model is parametrized by  $(d, D, a, b)$ . The case  $a = 0$  stands for the standard tensor field theory. Initially proposed by [73], these models were found tractable at fixed ranks  $d = 3, 4$ ,  $D = 1$ , and  $b = 1$ , and there were indications of their super-renormalizability without a full-fledge proof of this statement. We carry on detailed analyses for these models, extending them at any rank and any dimension. The method that we use is the so-called multi-scale renormalization [122]. It proves to be efficient enough to address non-local field theories (like tensor field theories) by achieving a perturbative power counting theorem and then the renormalization at all orders. Using the multi-scale analysis, we then find conditions on the tuple  $(d, D, a, b)$  for potentially renormalizable enhanced models of two different types.

- For the first type of theory, quite remarkably, we show that for generic  $(d, D)$  parameters, there exists a just-renormalizable model at all orders. Theorem 1 summarizes this result.

- For the second type of theory, we prove the renormalizability at all orders of a specific model for a choice of parameters. Theorem 2 is another main result of our analysis.

The plan of the paper is as follows: In section 2, we introduce two models: the model  $+$  and the model  $\times$  with different enhancements in the  $\phi^4$ -tensor interactions. In section 3, preparing for the power counting analyses, we give an explicit expression for the amplitudes of a given graph  $\mathcal{G}$ . Section 4 addresses the multi-scale analysis: we optimally bound a generic graph amplitude in terms of combinatorial quantities of the graph. In section 5, we determine the parameter spaces of  $(d, D, a, b)$  which could potentially give rise to renormalizable models  $+$  and  $\times$ . Concretely, we investigate further instances of renormalizable models: (1) section 6 presents a generic model  $+$  with arbitrary  $D$ ,  $d$ ,  $a = D(d - 2)/2$ , and  $b = D(2d - 3)/4$ ; (2) section 7 addresses a model  $\times$  with  $D = 1$ ,  $d = 3$ ,  $a = 1/2$  and  $b = 1$ . We prove that these models determined by such parameters are indeed renormalizable at all orders of perturbation theory. We give a summary of our results and future prospectives in section 8. Closing the manuscript, in appendix A, the reader will find the detail of the spectral sums to be used for bounding the amplitudes, and appendices B and C respectively illustrate some representative and divergent graphs appearing in specific models  $+$  and  $\times$ .

## 2 Enhanced $p^{2a}\phi^4$ tensor field theories

We consider a field theory defined by a rank  $d$  complex tensor  $\phi_{\mathbf{P}}$ , with  $\mathbf{P} = (p_1, p_2, \dots, p_d)$  a multi-index, and  $\bar{\phi}_{\mathbf{P}}$  denotes its complex conjugate. From a field theory standpoint, introducing a complex function  $\phi : (U(1)^D)^{\times d} \rightarrow \mathbb{C}$ , where  $D$  will be called dimension of the group  $U(1)^D$ ,  $\phi_{\mathbf{P}}$  is the Fourier component of the field and the indices  $p_s$  are by themselves multi-indices:

$$p_s = (p_{s,1}, p_{s,2}, \dots, p_{s,D}), \quad p_{s,i} \in \mathbb{Z}. \quad (1)$$

Let us make a few remarks. First, considering  $\phi_{\mathbf{P}}$  as a rank  $d$  tensor is a slight abuse because the modes  $p_{k,s}$  range up to infinity. Cutting sharply off all modes to  $N$ , then the resulting

multi-index object  $\phi_{\mathbf{P};N}$  transforms under the fundamental representation of  $U(N)^{D \times d}$  and hence is a tensor. For convenience, we keep the name of tensor for the field  $\phi_{\mathbf{P}}$ . Second,  $\phi_{\mathbf{P}}$  could be considered as a  $d \times D$  multi-index tensor, we shall call it a rank  $d$  tensor, because  $d$  and  $D$  will play different roles in the following. Third, several of the results derived hereafter could be extended to any compact Lie group  $G_D$  of dimension  $D$  admitting a Peter-Weyl decomposition (see, for instance, how a treatment for  $SU(2)^{D'}$ ,  $D = 3D'$ , can be achieved using tools in [93]). The treatment of the corresponding models could have been achieved with some extra work. Finally, a last remark is that the dimension  $D$  has nothing to see with the space dimension associated with the discrete geometry encoded by the tensor contractions as we will discuss soon. Thus referring in the following to UV and IR should be related with small and large distances on the group  $U(1)^D$ .

A general action  $S$  built by a sum of convolutions of the tensors  $\phi_{\mathbf{P}}$  and  $\bar{\phi}_{\mathbf{P}}$  can be written as:

$$\begin{aligned} S[\bar{\phi}, \phi] &= \text{Tr}_2(\bar{\phi} \cdot \mathbf{K} \cdot \phi) + \mu \text{Tr}_2(\phi^2) + S^{\text{int}}[\bar{\phi}, \phi], \\ \text{Tr}_2(\bar{\phi} \cdot \mathbf{K} \cdot \phi) &= \sum_{\mathbf{P}, \mathbf{P}'} \bar{\phi}_{\mathbf{P}} \mathbf{K}(\mathbf{P}; \mathbf{P}') \phi_{\mathbf{P}'}, \quad \text{Tr}_2(\phi^2) = \sum_{\mathbf{P}} \bar{\phi}_{\mathbf{P}} \phi_{\mathbf{P}}, \\ S^{\text{int}}[\bar{\phi}, \phi] &= \sum_{n_b} \lambda_{n_b} \text{Tr}_{n_b}(\bar{\phi}^{n_b} \cdot \mathbf{V}_{n_b} \cdot \phi^{n_b}), \end{aligned} \quad (2)$$

where  $\text{Tr}_{n_b}$  are sums over all indices  $p_{k,s}$  of  $\mathbf{P}$  of  $n_b$  tensors  $\phi$  and  $\bar{\phi}$ . Then  $\text{Tr}_{n_b}$  are considered as traces over indices of the tensors. In (2), the kernels  $\mathbf{K}$  and  $\mathbf{V}_{n_b}$  are to be specified,  $\mu$  is a mass coupling and  $\lambda_{n_b}$  is a coupling constant. If  $\mathbf{V}_{n_b}$  corresponds to a simple pairing between tensor indices (by delta functions identifying indices), then  $\text{Tr}_{n_b}(\bar{\phi}^{n_b} \cdot \mathbf{V}_{n_b} \cdot \phi^{n_b})$  spans the space of unitary invariants [27, 35, 33].

There is a geometrical interpretation of the interaction  $\text{Tr}_{n_b}(\bar{\phi}^{n_b} \cdot \mathbf{V}_{n_b} \cdot \phi^{n_b})$ . If each tensor field is regarded as a  $d$ -simplex, the generalized trace  $\text{Tr}_{n_b}$  corresponds to a pairing or an identification of the  $(d-1)$ -simplices on the boundary of the  $d$ -simplexes to form a  $d+1$  dimensional discrete geometry. If the kernel  $\mathbf{V}_{n_b}$  is not a simple pairing, it then assigns a weight to each of those discrete geometries.

A model is specified after giving the data of the kernels  $\mathbf{K}$  and  $\mathbf{V}_{n_b}$ . Let us introduce some convenient notations:

$$\begin{aligned} \delta_{\mathbf{P}; \mathbf{P}'} &= \prod_{s=1}^d \prod_{i=1}^D \delta_{p_{s,i}, p'_{s,i}}, \quad \mathbf{P}^{2b} = \sum_{s=1}^d |p_s|^{2b}, \quad |p_s|^{2b} = \sum_{i=1}^D |p_{s,i}|^{2b}, \\ \phi_{12\dots d} &= \phi_{p_1, p_2, \dots, p_d} = \phi_{\mathbf{P}}. \end{aligned} \quad (3)$$

for a real parameter  $b \geq 0$ , and where  $\delta_{p,q}$  is the usual Kronecker symbol on  $\mathbb{Z}$ .

We introduce the following class of kernels for the kinetic term

$$\mathbf{K}_b(\mathbf{P}; \mathbf{P}') = \delta_{\mathbf{P}; \mathbf{P}'} \mathbf{P}^{2b}. \quad (4)$$

$\mathbf{K}_b$  therefore represents a sum of the power of eigenvalues of  $d$  Laplacian operators over the  $d$  copies of  $U(1)^D$ . The case  $b = 1$  corresponds precisely to Laplacian eigenvalues on the torus. Seeking renormalizable theories, from the fact that we are dealing with a nonlocal

model, we might be led to choose values of  $b$  different from integers. In usual quantum field theory (QFT)  $b$  should have an upper bound  $b \leq 1$  to ensure the Osterwalder-Schrader (OS) positivity axiom [122]. Whether or not such a condition (or any OS axioms) might be kept for tensor field theories is still in debate [47]. Thus, for the moment, to avoid putting strong constraints on the models, we let  $b$  as a free strictly positive real parameter.

We will be interested in 2 models distinguished by their interactions. Introduce a parameter  $a \in (0, \infty)$  and write:

$$\text{Tr}_{4;1}(\phi^4) = \sum_{p_s, p'_s \in \mathbb{Z}^D} \phi_{12\dots d} \bar{\phi}_{1'23\dots d} \phi_{1'2'3'\dots d'} \bar{\phi}_{12'3'\dots d'} , \quad (5)$$

$$\begin{aligned} \text{Tr}_{4;1}([p^{2a} + p'^{2a}] \phi^4) &= \sum_{p_s, p'_s \in \mathbb{Z}^D} \left( |p_1|^{2a} + |p'_1|^{2a} \right) \phi_{12\dots d} \bar{\phi}_{1'23\dots d} \phi_{1'2'3'\dots d'} \bar{\phi}_{12'3'\dots d'} , \\ &= 2 \sum_{p_s, p'_s \in \mathbb{Z}^D} |p_1|^{2a} \phi_{12\dots d} \bar{\phi}_{1'23\dots d} \phi_{1'2'3'\dots d'} \bar{\phi}_{12'3'\dots d'} = 2 \text{Tr}_{4;1}(p^{2a} \phi^4) , \end{aligned} \quad (6)$$

$$\text{Tr}_{4;1}([p^{2a} p'^{2a}] \phi^4) = \sum_{p_s, p'_s \in \mathbb{Z}^D} \left( |p_1|^{2a} |p'_1|^{2a} \right) \phi_{12\dots d} \bar{\phi}_{1'23\dots d} \phi_{1'2'3'\dots d'} \bar{\phi}_{12'3'\dots d'} . \quad (7)$$

Note that in (5), (6) and (7), the color index 1 plays a special role. We sum over all possible color indices and obtain colored symmetric interactions:

$$\begin{aligned} \text{Tr}_4(\phi^4) &:= \text{Tr}_{4;1}(\phi^4) + \text{Sym}(1 \rightarrow 2 \rightarrow \dots \rightarrow d) , \\ \text{Tr}_4(p^{2a} \phi^4) &:= \text{Tr}_{4;1}(p^{2a} \phi^4) + \text{Sym}(1 \rightarrow 2 \rightarrow \dots \rightarrow d) , \\ \text{Tr}_4([p^{2a} p'^{2a}] \phi^4) &:= \text{Tr}_{4;1}([p^{2a} p'^{2a}] \phi^4) + \text{Sym}(1 \rightarrow 2 \rightarrow \dots \rightarrow d) . \end{aligned} \quad (8)$$

The momentum weights in the interactions  $\text{Tr}_4(p^{2a} \phi^4)$  and  $\text{Tr}_4([p^{2a} p'^{2a}] \phi^4)$  can be viewed as derivative couplings for particular choices of  $a$ . This is why, at times, we will call them coupling derivatives. Written in the momentum space, the interactions are however put in a more general setting using  $|p|^{2a}$ , for positive values of  $a$ . Once again, achieving renormalizability will be our sole constraint for fixing  $a$ . These interactions are called enhanced compared to  $\text{Tr}_4(\phi^4)$  (the usual quartic melonic graph studied for instance in [86]) because they can generate amplitudes which are more divergent, and so enhanced, compared to those generated by  $\text{Tr}_4(\phi^4)$  alone. As a second property, we discussed that enhanced interactions represent weighted discrete geometries. The contraction pattern of the four tensors shows us that the weight here has a subtle sense: we are weighting a particular  $(d-1)$ -simplex in the  $(d+1)$ -simplex representing the interaction.

It turns out that the renormalization analysis performed in sections 6 and 7 leads us to new 2-point diverging graphs. Then we must add to the kinetic term the new terms:

$$\text{Tr}_2(p^{2\xi} \phi^2) = \text{Tr}_2(\bar{\phi} \cdot \mathbf{K}_\xi \cdot \phi) , \quad \xi = a, 2a , \quad (9)$$

in addition to the kinetic term  $\text{Tr}_2(p^{2\xi} \phi^2)$ , where  $\xi = b$ .

We will need counter-terms for each term in the action. In particular, the counter-term  $CT_2$  of the form of the mass,  $CT_{2;b}$  for the wave function, and new 2-point interactions  $CT_{2;a}$



and  $CT_{2;2a}$ , that will be important for renormalizing two-point functions. We define

$$CT_2[\bar{\phi}, \phi] = \delta_\mu \text{Tr}_2(\phi^2), \quad CT_{2;\xi}[\bar{\phi}, \phi] = Z_\xi \text{Tr}_2(p^{2\xi} \phi^2), \quad \xi = a, 2a, b, \quad (10)$$

where  $\delta_\mu$  and  $Z_\xi$  are counter-term couplings. Note that, in the following,  $Z_b$  is called wave function renormalization.

The models that we will study have the following kinetic terms and interactions:

$$\begin{aligned} \text{model } + : \quad S_+^{\text{int}}[\bar{\phi}, \phi] &= \frac{\lambda}{2} \text{Tr}_4(\phi^4) + \frac{\eta_+}{2} \text{Tr}_4(p^{2a} \phi^4) + CT_2[\bar{\phi}, \phi] + \sum_{\xi=a,b} CT_{2;\xi}[\bar{\phi}, \phi] \\ S_+^{\text{kin}}[\bar{\phi}, \phi] &= \sum_{\xi=a,b} \text{Tr}_2(p^{2\xi} \phi^2) + \mu \text{Tr}_2(\phi^2), \end{aligned} \quad (11)$$

$$\begin{aligned} \text{model } \times : \quad S_\times^{\text{int}}[\bar{\phi}, \phi] &= \frac{\lambda}{2} \text{Tr}_4(\phi^4) + \frac{\eta_\times}{2} \text{Tr}_4([p^{2a} p'^{2a}] \phi^4) + CT_2[\bar{\phi}, \phi] + \sum_{\xi=a,2a,b} CT_{2;\xi}[\bar{\phi}, \phi], \\ S_\times^{\text{kin}}[\bar{\phi}, \phi] &= \sum_{\xi=a,2a,b} \text{Tr}_2(p^{2\xi} \phi^2) + \mu \text{Tr}_2(\phi^2) \end{aligned} \quad (12)$$

where  $\lambda$ ,  $\eta_+$  and  $\eta_\times$  are coupling constants.

It is an interesting question to list the classical symmetries of the models  $+$  and  $\times$  given by the generalized Noether theorem for such non-local theories [99, 98]. To apply the Lie symmetry algorithm as worked out in these references could be an interesting exercise for derivative coupling theories and could bear important consequences for the Ward identities.

The present theory space is clearly much more involved than the usual unitary invariant theory space where the vertices of the model do not have any momentum weight. It will result from our analysis that a new combinatorics provides our models with a genuinely different renormalization procedure. Then, the comparison could be made with the models in Table 8 in [93] which are unitary invariant models. We seize this opportunity to correct that table: the just-renormalizable  $\phi^6$ -models should be UV asymptotically safe (rather than free) under the light of many recent results [95, 96, 44, 45, 46, 69].

In [73], a power counting theorem was proved for the model  $+$  restricted at rank  $d = 3$  and  $d = 4$  and  $D = 1$ . Nevertheless, the optimization procedure to reach a power counting was quite complicated. There were indications of potentially super-renormalizable enhanced models without finalizing the proof of such a renormalizability. In this work, we will improve that analysis by noting that the relevant interaction is rather  $\text{Tr}_4(p^{2a} \phi^4)$  (8). Before reaching this point, our next task is to express generic amplitudes in the enhanced models.

### 3 Amplitudes

Models  $+$  and  $\times$  associated with actions given by (11) and (12), respectively, give the quantum models determined by the partition function

$$Z_\bullet = \int d\nu_{C_\bullet}(\bar{\phi}, \phi) e^{-S_\bullet^{\text{int}}[\bar{\phi}, \phi]}, \quad (13)$$

where  $\bullet = +, \times$ , and  $d\nu_{C_\bullet}(\bar{\phi}, \phi)$  is a field Gaussian measure with covariance  $C_\bullet$  given by the inverse of the kinetic term:

$$C_\bullet(\mathbf{P}; \mathbf{P}') = \tilde{C}_\bullet(\mathbf{P}) \delta_{\mathbf{P}, \mathbf{P}'} , \quad \tilde{C}_\bullet(\mathbf{P}) = \frac{1}{\sum_\xi \mathbf{P}^{2\xi} + \mu} . \quad (14)$$

where, if  $\bullet = +$ ,  $\xi = a, b$  and if  $\bullet = \times$ ,  $\xi = a, 2a, b$ . Dealing with the interactions, we have the vertex kernels  $\mathbf{V}_{4;s}$  and  $\mathbf{V}_{+;4;s}$  associated with (11) and  $\mathbf{V}_{4;s}$  and  $\mathbf{V}_{\times;4;s}$  associated with (12). These kernels are given by

$$\begin{aligned} \mathbf{V}_{4;s}(\mathbf{P}; \mathbf{P}'; \mathbf{P}''; \mathbf{P}''') &= \frac{\lambda}{2} \delta_{4;s}(\mathbf{P}; \mathbf{P}'; \mathbf{P}''; \mathbf{P}''') , \\ \mathbf{V}_{+;4;s}(\mathbf{P}; \mathbf{P}'; \mathbf{P}''; \mathbf{P}''') &= \frac{\eta_+}{2} |p_s|^{2a} \delta_{4;s}(\mathbf{P}; \mathbf{P}'; \mathbf{P}''; \mathbf{P}''') , \\ \mathbf{V}_{\times;4;s}(\mathbf{P}; \mathbf{P}'; \mathbf{P}''; \mathbf{P}''') &= \frac{\eta_\times}{2} |p_s|^{2a} |p'_s|^{2a} \delta_{4;s}(\mathbf{P}; \mathbf{P}'; \mathbf{P}''; \mathbf{P}''') , \end{aligned} \quad (15)$$

$s = 1, 2, \dots, d$ , where the operator  $\delta_{4;s}(-)$  is a product of Kronecker deltas identifying the different momenta according to the pattern dictated by the interaction  $\text{Tr}_{4;s}(\phi^4)$ . Note that  $\mathbf{V}_{\bullet;4;s}$  has a color index. The vertex operator  $\mathbf{V}_2$  associated with the mass counter-term is a delta function  $\delta_{\mathbf{P}, \mathbf{P}'}$ ; the vertex operators  $\mathbf{V}_{2;\xi;s}$   $\xi = a, 2a, b$ , associated with the counter-terms  $CT_{2;\xi}[\bar{\phi}, \phi]$  are delta functions weighted by momenta  $|p_s|^{2\xi}$ .

**Feynman tensor graphs.** There are two equivalent graphical representations of Feynman graphs in tensor models. The first one is called “stranded graph” and it incorporates more details of the structure of the Feynman graph (used and explained in [22] and [93]). The other representation of a Feynman graph in this theory is a bipartite colored graph [22, 70, 33, 25]. We mostly use the latter because it is convenient and economic. The first representation will be used in this section to make explicit the notion of faces associated with momentum loops.

At the graphical level the propagator is drawn as a collection of  $d$  segments called strands (see Figure 1).

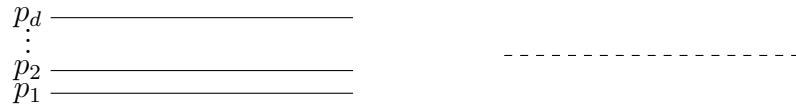


Figure 1: The propagator of the theory: the stranded representation (left) made with  $d$  segments representing  $d$  momenta; the colored representation (right) denoted by a dotted line.

Each interaction is sketched as a stranded vertex or by a  $d$ -regular colored bipartite graph called a “bubble.” The bipartiteness of the graph comes from the representation of each field  $\phi$  as a white vertex and each field  $\bar{\phi}$  by a black one. For instance, see bubbles corresponding to  $\phi^2$  vertices (mass and wave functions vertices), and  $\phi^4$ -interactions in Figure 2. Note that, the bubbles representing the vertex kernel  $\mathbf{V}_{\bullet;4;s}$ ,  $\bullet = +, \times$ , appear with one or two bold edges, respectively. The color of a bold edge corresponds to the color index of the enhanced

momentum. The bubbles that describe the vertices are particular contractions of tensors and are called melons.

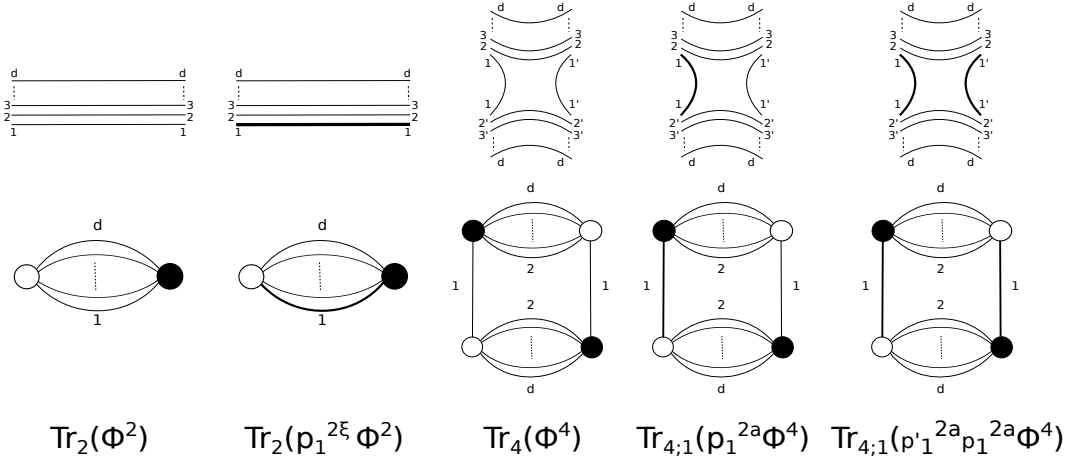


Figure 2: Rank  $d$  vertices of the mass,  $\phi^2$ - and  $\phi^4$ -terms.

Perturbation theory tells us that, via the Wick theorem, we should glue vertices by propagator lines to produce a Feynman graph. Some examples of Feynman tensor graphs by the above rule are depicted in Figure 3. We put half-lines or external legs on vertices to reflect the presence of external fields. In the following, a Feynman tensor graph is simply called a graph and is denoted by  $\mathcal{G}$ .

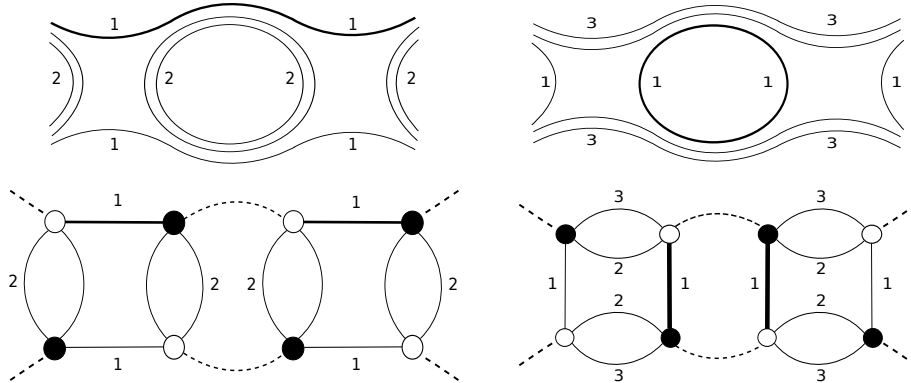


Figure 3: Rank  $d = 3$  Feynman graphs.

In the stranded picture, closed cycles (homeomorphic to circles) in the graphs are called closed or internal faces and strands homeomorphic to segments are called open or external faces. The set of closed faces is denoted by  $\mathcal{F}_{\text{int}}$  and the set of open faces  $\mathcal{F}_{\text{ext}}$ . As expected, the presence of an internal face is associated with a sum over infinite values of momenta which can make the amplitude divergent, hence the need of regularization and renormalization for the model. In the colored graph representation, note that an extra color 0 could be attributed to all dotted propagator lines. The cycles in that  $(d+1)$  colored graph have two colors. The internal faces of  $\mathcal{G}$ , elements of  $\mathcal{F}_{\text{int}}$ , are associated with bicolored cycles of colors 0s, with  $s = 1, 2, \dots, d$ . To obtain the subset of  $\mathcal{F}_{\text{int}}$  (or of  $\mathcal{F}_{\text{ext}}$ ) of faces of colors 0s from the  $d+1$

colored graph, we remove all edges except those of colors 0 and  $s$  and observe the remaining cycles (or open strands, respectively). In the end, for simplicity, we omit the color 0 in the couple 0s and claim that a (internal or external) face is of color  $s$ .

**Amplitudes.** Given a connected graph  $\mathcal{G}$  with vertex set  $\mathcal{V}$  (with  $V = |\mathcal{V}|$ ) and line or propagator set  $\mathcal{L}$  (with  $L = |\mathcal{L}|$ ), we formally write the amplitude of  $\mathcal{G}$

$$A_{\mathcal{G}} = \sum_{\mathbf{P}_v} \prod_{l \in \mathcal{L}} C_{\bullet, l}(\mathbf{P}_{v(l)}; \mathbf{P}'_{v'(l)}) \prod_{v \in \mathcal{V}} (-\mathbf{V}_v(\{\mathbf{P}_v\})). \quad (16)$$

The above formula shows that propagators  $C_l$  have a line index  $l$  and momentum arguments  $\mathbf{P}_{v(l)}$ , with  $v(l)$  the source or target of the line  $l$ . The vertex constraints  $\mathbf{V}_v$  convolute the set of momenta and can be of the form  $\mathbf{V}_{4;s}$ ,  $\mathbf{V}_{\bullet;4;s}$ ,  $\mathbf{V}_2$ ,  $\mathbf{V}_{2;\xi;s}$ ,  $\xi = a, 2a, b$ . The presence of these weights makes the amplitude quite different from those of unitary invariant theories. For instance, as opposed to the ordinary situation, the amplitudes do not directly factorize in terms of internal faces.

To derive a power counting theorem we need to study graph amplitudes  $A_{\mathcal{G}}$  coming from the perturbative expansion of correlators of the form

$$\langle \phi_{\mathbf{P}} \bar{\phi}_{\mathbf{P}'} \phi_{\mathbf{P}''} \bar{\phi}_{\mathbf{P}'''} \rangle, \quad (17)$$

$$\langle |p_1|^{2a} \phi_{\mathbf{P}} \bar{\phi}_{\mathbf{P}'} \phi_{\mathbf{P}''} \bar{\phi}_{\mathbf{P}'''} \delta_{4;s}(\mathbf{P}; \mathbf{P}'; \mathbf{P}''; \mathbf{P}''') \rangle \quad (18)$$

$$\langle |p_1|^{2a} |p_{1'}|^{2a} \phi_{\mathbf{P}} \bar{\phi}_{\mathbf{P}'} \phi_{\mathbf{P}''} \bar{\phi}_{\mathbf{P}'''} \delta_{4;s}(\mathbf{P}; \mathbf{P}'; \mathbf{P}''; \mathbf{P}''') \rangle. \quad (19)$$

In tensor graphs, consider the faces as previously introduced. A face  $f_s$  with color  $s$  has an  $s$ -colored  $\mathbb{Z}^D$  conserved momentum  $p_{f_s}$ , and passes through some vertices  $v_s$ , with vertex kernel of the form  $\mathbf{V}_{4;s}$ ,  $\mathbf{V}_{\bullet;4;s}$ ,  $\mathbf{V}_2$ , or  $\mathbf{V}_{2;\xi;s}$ ,  $\xi = a, 2a, b$ . This face may also pass through some other vertices with color  $s' \neq s$ . More generally, a face  $f$  can pass through a vertex  $v$  a number of times, say  $\alpha$ . Denote this statement by  $v^\alpha \in f$ . Because of the coloring,  $\alpha$  can only be 0, 1, 2 ( $v_s \in f_s$  will mean  $v_s^1 \in f_s$ ). We therefore define the incidence matrix between faces and vertices by

$$\epsilon_{v_s f_{s'}} = \begin{cases} \alpha, & (s = s') \wedge (v_s^\alpha \in f_s), \\ 0, & \text{otherwise.} \end{cases} \quad (20)$$

Given two faces  $f_{1;s_1}$  and  $f_{2;s_2}$  and a vertex  $v_s$ , we introduce another multi-index object that we denote by  $\epsilon_{v_s f_{1;s_1} f_{2;s_2}}$  defined as

$$\epsilon_{v_s f_{1;s_1} f_{2;s_2}} = \begin{cases} 1, & (s = s_1 = s_2) \wedge (v_s \in f_{1;s_1}) \wedge (v_s \in f_{2;s_2}), \\ 0, & \text{otherwise.} \end{cases} \quad (21)$$

The case  $f_{1;s_1} = f_{2;s_2}$  could also occur. A first observation is that  $\epsilon_{v_s f_{1;s_1} f_{2;s_2}} = \epsilon_{v_s f_{s_1}} \epsilon_{v_s f_{s_2}}$  in the case when  $v_s \in f_{1;s_1}$  and  $v_s \in f_{2;s_2}$ . Looking at the diagonal, *i.e.*  $f_{1;s_1} = f_{2;s_2}$ ,  $\epsilon_{v_s f_{1;s} f_{1;s}} = 1$  if and only if  $v_s^2 \in f_{1;s}$ .

We are in position to re-express the interaction weights  $\mathbf{V}_{\bullet;4;s}$  in (15). Fix a color  $s$ , the weight of a vertex kernel of  $v_s$  of the kind  $\mathbf{V}_{\bullet;4;s}$  can be written as

$$\text{model} + : \quad \frac{\eta_+}{2} \sum_{f_{s'}} \epsilon_{v_s, f_{s'}} |p_{f_{s'}}|^{2a},$$

$$\text{model } \times : \quad \frac{\eta_{\times}}{2} \sum_{f_{s'}, f_{s''}} \epsilon_{v_s, f_{s'}, f_{s''}} |p_{f_{s'}}|^{2a} |p_{f_{s''}}|^{2a}. \quad (22)$$

We stress, at this point, that the two models  $+$  and  $\times$  will be studied separately, then there is no confusion to adopt a single notation as:

$$\text{model } \bullet : \quad \frac{\eta}{2} (\epsilon p)_{v_s}. \quad (23)$$

The weight of degree 2 vertices (in both models) which belong to  $\mathcal{V}_{2;\xi;s}$  is of the form  $Z_{\xi} \sum_{f_s} \epsilon_{v_s, f_s} |p_{f_s}|^{2\xi} = Z_{\xi} (\epsilon p)_{v_s}$ , where  $\xi = a, 2a, b$ .

Let us introduce:

- the set  $\mathcal{V}_{4;s}$  of vertices with kernel  $\mathbf{V}_{4;s}$ ,  $\mathcal{V}_4 = \sqcup_{s=1}^d \mathcal{V}_{4;s}$  (disjoint union notation),
- the set  $\mathcal{V}_{\bullet;4;s}$  of vertices with vertex kernel  $\mathbf{V}_{\bullet;4;s}$ ,  $\bullet = +, \times$ ,  $\mathcal{V}_{\bullet;4} = \sqcup_{s=1}^d \mathcal{V}_{\bullet;4;s}$ ,
- the set  $\mathcal{V}_2$  of mass vertices with kernel  $\mathbf{V}_2$ , the set  $\mathcal{V}_{2;\xi;s}$  of vertices with kernels  $\mathbf{V}_{2;\xi;s}$ ,  $\mathcal{V}_{2;s} = \cup_{\xi} \mathcal{V}_{2;\xi;s}$ .

We denote the cardinalities  $|\mathcal{V}_{4;s}| = V_{4;s}$ ,  $|\mathcal{V}_4| = V_4$ ,  $|\mathcal{V}_{\bullet;4;s}| = V_{\bullet;4;s}$ ,  $|\mathcal{V}_{\bullet;4}| = V_{\bullet;4}$ ,  $\bullet = +, \times$ ;  $|\mathcal{V}_{2;\xi;s}| = V_{2;\xi;s}$ ,  $V_{2;\xi} = \sum_s V_{2;\xi;s}$ . Then,  $\mathcal{V} = \sqcup_{s=1}^d (\mathcal{V}_{4;s} \cup \mathcal{V}_{\bullet;4;s} \cup \mathcal{V}_{2;s})$ ,  $|\mathcal{V}| = V$ .

Using the Schwinger parametric form of the propagator kernel as

$$\tilde{C}_{\bullet}(\mathbf{P}) = \int_0^{\infty} d\alpha e^{-\alpha(\sum_{\xi} \mathbf{P}^{2\xi} + \mu)}, \quad (24)$$

integrating all deltas from propagators and vertex operators, we put the amplitude (16) in the form

$$\begin{aligned} A_{\mathcal{G}} &= \kappa(\lambda, \eta_{\bullet}, Z_{\xi}) \sum_{p_{f_s}} \int \left[ \prod_{l \in \mathcal{L}} d\alpha_l e^{-\alpha_l \mu} \right] \left[ \prod_{f_s \in \mathcal{F}_{\text{ext}}} e^{-(\sum_{l \in f_s} \alpha_l) \sum_{\xi} |p_{f_s}^{\text{ext}}|^{2\xi}} \right] \\ &\quad \times \left[ \prod_{f_s \in \mathcal{F}_{\text{int}}} e^{-(\sum_{l \in f_s} \alpha_l) \sum_{\xi} |p_{f_s}|^{2\xi}} \right] \left[ \prod_{s=1}^d \prod_{v_s \in \mathcal{V}_{\bullet;4;s} \cup \mathcal{V}_{2;s}} (\epsilon \tilde{p})_{v_s} \right], \end{aligned} \quad (25)$$

where  $\kappa(\lambda, \eta_{\bullet}, Z_{\xi})$  includes symmetry factors and coupling constants,  $p_{f_s}^{\text{ext}}$  are external momenta which are not summed, whereas  $p_{f_s}$  are internal momenta and are summed. In the last line,  $\tilde{p}_{f_s}$  refers to an internal or an external momentum. The sum over infinite values of momenta produces divergent amplitudes (25). In the next section, we will address the nature of these divergences through a power counting theorem.

## 4 Power counting theorems for $p^{2a}\phi^4$ -models

For simplicity, we will study a connected graph amplitude without  $\mathcal{V}_{2;\xi;s}$  vertices. To add these vertices towards the end can be easily done.

**Multiscale analysis.** We slice the propagator in a geometric progression with the parameter  $M > 1$ , and then bound each slice of the propagator:

$$\tilde{C}_{\bullet}(\mathbf{P}) = \int_0^{\infty} d\alpha e^{-\alpha(\sum_{\xi} \mathbf{P}^{2\xi} + \mu)} = \sum_{i=0}^{\infty} C_{\bullet,i}(\mathbf{P}),$$

$$\begin{aligned}
C_{\bullet,0}(\mathbf{P}) &= \int_1^\infty d\alpha e^{-\alpha(\sum_\xi \mathbf{P}^{2\xi} + \mu)} \leq K, \\
C_{\bullet,i}(\mathbf{P}) &= \int_{M^{-2(i+1)}}^{M^{-2i}} d\alpha e^{-\alpha(\sum_\xi \mathbf{P}^{2\xi} + \mu)} \leq K' M^{-2i} e^{-M^{-2i}(\sum_\xi \mathbf{P}^{2\xi} + \mu)} \\
&\leq K M^{-2i} e^{-\delta M^{-i}(\sum_\xi \sum_{s=1}^d \sum_{l=1}^D |p_{s;l}|^\xi + \mu)} \leq K M^{-2i} e^{-\delta M^{-i}(\sum_\xi \sum_s |p_s|^\xi + \mu)}, \tag{26}
\end{aligned}$$

$|p_s|^\xi = \sum_{l=1}^D |p_{s;l}|^\xi$ , for some constants  $K$ ,  $K'$  and  $\delta$ .

The slice decomposition yields the standard interpretation that high values of  $i$  select high momenta of order  $\sim M^i$  and this refers to the UV (this coincides with small distances on the group  $U(1)^D$ ). Meanwhile, low momenta are picked around the slice  $i = 0$ , and correspond to the IR. Note that, since we are dealing with a compact group, the latter limit is harmless. Introduce a cut-off  $\Lambda$  on the slices  $i$ , and then cut off the propagators as  $C_\bullet^\Lambda = \sum_{i=0}^\Lambda C_{\bullet,i}$ . We will not display  $\Lambda$  in the following expression.

Cutting off all propagators in (16), the amplitude  $A_{\mathcal{G}}$  becomes  $\sum_{\boldsymbol{\mu}} A_{\mathcal{G};\boldsymbol{\mu}}$  where  $\boldsymbol{\mu} = \{i_l\}_{l \in \mathcal{L}}$  is a multi-index called momentum assignment which collects the propagator indices  $i_l \in [0, \Lambda]$ , and

$$A_{\mathcal{G};\boldsymbol{\mu}} = \kappa(\lambda, \eta_\bullet) \sum_{p_{v;s}} \left[ \prod_{l \in \mathcal{L}} C_{\bullet,i_l}(\mathbf{P}_{v(l)}; \mathbf{P}'_{v'(l)}) \right] \left[ \prod_{s=1}^d \prod_{v_s \in \mathcal{V}_{\bullet,4;s}} (\epsilon \tilde{p})_{v_s} \right]. \tag{27}$$

Using (26), the above expression finds the form

$$\begin{aligned}
|A_{\mathcal{G};\boldsymbol{\mu}}| &\leq \kappa(\lambda, \eta_\bullet) K^L K_1^V K_2^{F_{\text{ext}}} \left[ \prod_{l \in \mathcal{L}} M^{-2i_l} \right] \\
&\times \sum_{p_{f_s}} \left[ \prod_{f_s \in \mathcal{F}_{\text{int}}} e^{-\delta(\sum_{l \in f_s} M^{-i_l}) \sum_\xi |p_{f_s}|^\xi} \right] \left[ \prod_{s=1}^d \prod_{v_s \in \mathcal{V}_{\bullet,4;s}} (\epsilon \tilde{p})_{v_s} \right], \tag{28}
\end{aligned}$$

where  $K_{1,2}$  are constants.

$A_{\mathcal{G};\boldsymbol{\mu}}$  is the focus of our attention and is the quantity that must be bounded by an optimization procedure. A standard procedure detailed in [122] will allow one to sum over the assignments  $\boldsymbol{\mu}$  after renormalization.

The next definition can be found in [122]. It paves the way to the notion of locality of the theory through the definition of quasi-local subgraphs. Let  $\mathcal{G}$  be a graph, with line set  $\mathcal{L}$ . Fix  $i$  a slice index and define  $\mathcal{G}^i$  to be the subgraph of  $\mathcal{G}$  built with propagator lines with indices obeying  $\forall \ell \in \mathcal{L}(\mathcal{G}^i) \cap \mathcal{L}, i_\ell \geq i$ . It might happen that  $\mathcal{G}^i$  disconnects in several components; we denote these connected components  $G_k^i$  and call them quasi-local subgraphs. It is important to give a characterization of the quasi-local subgraphs. Given  $g$ , a subgraph of  $\mathcal{G}$  with internal line set  $\mathcal{L}(g)$  and external line set  $\mathcal{L}_{\text{ext}}(g)$ . Consider a momentum assignment  $\boldsymbol{\mu}$  of  $\mathcal{G}$ , and define  $i_g(\boldsymbol{\mu}) = \inf_{\ell \in \mathcal{L}(g)} i_\ell$  and  $e_g(\boldsymbol{\mu}) = \sup_{\ell \in \mathcal{L}_{\text{ext}}(g)} i_\ell$ . We can identify  $g$  with a quasi-local subgraph of  $\mathcal{G}$  if and only if  $i_g(\boldsymbol{\mu}) > e_g(\boldsymbol{\mu})$ .

The set  $\{G_k^i\}$  of quasi-local subgraphs of  $\mathcal{G}$  is partially ordered under inclusion. The inclusion can be put in a form of an abstract tree (with vertices the  $G_k^i$ 's) called the Gallavotti-Nicolò (GN) tree [123]. We perform the internal momenta sums in (28) in an optimal way, and show that the result can be expressed in terms of the quasi-local subgraphs. This

condition, called the compatibility condition with the GN tree, turns out to be crucial when performing the sum over the momentum attribution.

All external momenta must be at a lower scale than internal momenta, thus for any external faces  $f_s$  and internal face  $f_{s'}$ ,  $p_{f_s}^{\text{ext}} \ll p_{f_{s'}}^{\text{ext}}$ . We bound all factors or terms with  $p_{f_s}^{\text{ext}}$  and obtain:

$$|A_{\mathcal{G};\mu}| \leq K_3 \left[ \prod_{l \in \mathcal{L}} M^{-2i_l} \right] \sum_{p_{f_s}} \left[ \prod_{f_s \in \mathcal{F}_{\text{int}}} e^{-\delta(\sum_{l \in f_s} M^{-i_l}) \sum_{\xi} |p_{f_s}|^{\xi}} \right] \left[ \prod_{s=1}^d \prod_{v_s \in \mathcal{V}_{\bullet;4;s}} (\epsilon p^{2a})_{v_s} \right], \quad (29)$$

where  $K_3 = \kappa(\lambda, \eta_{\bullet}) K^L K_1^V K_2^{F_{\text{ext}}} K'$ , and  $K'$  is a constant obtained from the bound over the external momenta present in the vertex kernel  $\prod_{s=1}^d \prod_{v_s \in \mathcal{V}_{\bullet;s}} (\epsilon \tilde{p})_{v_s}$ ; note that  $\epsilon$  in (28) is now restricted to internal faces in (29).

Performing the sum over internal momenta  $p_{f_s}$  must be done in a way to get the lowest possible divergence in (29). This is an optimization procedure that we detail now.

We determine the behavior of some momentum sums. The following results have been detailed in appendix A. For constants,  $B > 0$ ,  $c > 0$ ,  $b > 0$ ,  $a > 0$  and  $a' > 0$ , and an integer  $n \geq 0$ , we have

$$\sum_{p_1, \dots, p_D=1}^{\infty} \left( \sum_{l=1}^D p_l^c \right)^n e^{-B \sum_{l=1}^D (p_l^b + p_l^a)} = k B^{-\frac{(cn+D)}{b}} e^{-B^{1-\frac{a}{b}}} (1 + O(B^{\frac{1}{b}})), \quad (30)$$

$$\sum_{p_1, \dots, p_D=1}^{\infty} \left( \sum_{l=1}^D p_l^c \right)^n e^{-B(\sum_{l=1}^D (p_l^b + p_l^a + p_l^{a'}))} = k B^{-\frac{(cn+D)}{b}} e^{-B^{2-\frac{(a+a')}{b}}} (1 + O(B^{\frac{1}{b}})), \quad (31)$$

for a constant  $k$ . At this point, we make two assumptions on the parameters  $a, a', b$ :

- for the model  $+$ ,  $a \leq b$ ,

$$\sum_{p_1, \dots, p_D=1}^{\infty} \left( \sum_{l=1}^D p_l^c \right)^n e^{-B \sum_{l=1}^D (p_l^b + p_l^a)} = k B^{-\frac{(cn+D)}{b}} (1 + O(B^{\frac{1}{b}}) + O(B^{1-\frac{a}{b}})); \quad (32)$$

- for the model  $\times$ ,  $a + a' \leq 2b$ ,

$$\sum_{p_1, \dots, p_D=1}^{\infty} \left( \sum_{l=1}^D p_l^c \right)^n e^{-B(\sum_{l=1}^D (p_l^b + p_l^a + p_l^{a'}))} = k B^{-\frac{(cn+D)}{b}} (1 + O(B^{\frac{1}{b}}) + O(B^{2-\frac{(a+a')}{b}})). \quad (33)$$

Finally, the integration of internal momenta can be performed in the amplitudes.

**Model  $+$  -** Given a face  $f$  (the subscript  $s$  is not useful at this stage), we target the line  $l_f$  such that  $i_{l_f} = \min_{l \in f} i_l = i_f$ . After the integration, it will generate the lowest factor  $M^{i_f \times m}$ , where  $m$  is yet to be determined.

In the product  $\prod_{s=1}^d \prod_{v_s \in \mathcal{V}_{+;4;s}} (\epsilon p^{2a})_{v_s}$ , we choose the factor of a given  $p_f$  and perform the sum  $\sum_{p_f} (|p_f|^{2a})^{\rho_f} e^{-\delta M^{-i_f} |p_f|^b}$ , with  $\rho_f$  an integer, such that the bound (29) still holds.

Performing this sum using (32), we get a product of  $M^{\frac{i_f}{b}(2a\rho_f+D)}$  with the lowest possible

power. Take a closed face  $f_s$  of color  $s$ , the integer  $\rho_{f_s}$  counts how many times  $f_s$  passes through vertices of  $\mathcal{V}_{+;4;s}$ . We have

$$\rho_{f_s} = \sum_{v_s \in \mathcal{V}_{+;4;s}} \epsilon_{v_s, f_s}, \quad \rho_+(\mathcal{G}) = \sum_s \sum_{f_s} \rho_{f_s}. \quad (34)$$

We then write a new bound

$$|A_{\mathcal{G}; \mu}| \leq \kappa_1 \left[ \prod_{l \in \mathcal{L}} M^{-2i_l} \right] \sum_{p_{f_s}} \left[ \prod_{f_s \in \mathcal{F}_{\text{int}}} e^{-\delta M^{-i_{f_s}} \sum_{\xi} |p_{f_s}|^{\xi}} \right] \left[ \prod_{s'=1}^d \prod_{f_{s'}} |p_{f_{s'}}|^{2a\rho_{f_{s'}}} \right], \quad (35)$$

where  $\kappa_1$  is a new constant incorporating the previous constant  $K_3$ . Performing the sum over internal momenta, one gets using (32) with  $a \leq b$ ,

$$|A_{\mathcal{G}; \mu}| \leq \kappa_2 \prod_{l \in \mathcal{L}} M^{-2i_l} \prod_{f_s \in \mathcal{F}_{\text{int}}} M^{\frac{i_{f_s}}{b}(2a\rho_{f_s} + D)}, \quad (36)$$

where  $\kappa_2$  is another constant depending on the graph that includes  $\kappa_1$  and new constants coming from the summation over internal momenta.

We re-express the above bound in terms of the quasi-local subgraphs  $G_k^i$ . The product over lines can be written [122] as

$$\prod_{l \in \mathcal{L}} M^{-2i_l} = \prod_{l \in \mathcal{L}} \prod_{(i,k)/l \in \mathcal{L}(G_k^i)} M^{-2} = \prod_{(i,k)} M^{-2L(G_k^i)}. \quad (37)$$

The second product over faces splits in two factors. The first term can be treated as:

$$\prod_{f_s \in \mathcal{F}_{\text{int}}} M^{\frac{D}{b}i_{f_s}} = \prod_{f_s \in \mathcal{F}_{\text{int}}} \prod_{(i,k)/l_{f_s} \in \mathcal{L}(G_k^i)} M^{\frac{D}{b}} = \prod_{(i,k)} \prod_{f_s \in \mathcal{F}_{\text{int}} \cap G_k^i} M^{\frac{D}{b}} = \prod_{(i,k)} M^{\frac{D}{b}F_{\text{int}}(G_k^i)}. \quad (38)$$

The last product involving  $\rho_{f_s}$  can be treated as

$$\prod_{f_s \in \mathcal{F}_{\text{int}}} \prod_{(i,k)/l_{f_s} \in G_k^i} M^{\frac{2a}{b}i_{f_s}\rho_{f_s}} = \prod_{(i,k)} \prod_{f_s \in \mathcal{F}_{\text{int}} \cap G_k^i} M^{\frac{2a}{b}\rho_{f_s}} = \prod_{(i,k)} M^{\frac{2a}{b}\rho_+(G_k^i)}, \quad (39)$$

where  $\rho_+(\cdot)$  has been defined in (34).

Now, if we introduce the counter-term and the wave function vertices  $V_{2;a;s}$  and  $V_{2;b;s}$ , they might bring an additional momentum enhancement to faces. We want to keep the definition of  $\rho_{f_s}$  as in (34) and we must now add to it the contributions of the 2-point vertices of any types. Hence  $\rho_{f_s} \rightarrow \rho_{f_s} + \rho_{2;a;f_s} + \rho_{2;b;f_s}$ , where  $\rho_{2;\xi;f_s} = \sum_{v_s \in \mathcal{V}_{2;\xi;s}} \epsilon_{v_s, f_s}$  is the number of times that  $f_s$  visits  $\mathcal{V}_{2;\xi;s}$  vertices,  $\xi = a, b$ . To the above power counting, we should therefore add the following factor

$$\prod_{f_s \in \mathcal{F}_{\text{int}}} \prod_{(i,k)/l_{f_s} \in G_k^i} M^{i_{f_s}[\frac{2a}{b}\rho_{2;a;f_s} + \frac{2b}{b}\rho_{2;b;f_s}]} = \prod_{(i,k)} \prod_{f_s \in \mathcal{F}_{\text{int}} \cap G_k^i} M^{[\frac{2a}{b}\rho_{2;a;f_s} + 2\rho_{2;b;f_s}]}. \quad (40)$$



Note that a vertex of  $\mathcal{V}_{2;\xi;s}$  has a single strand with enhanced momentum  $p_s^{2\xi}$ ,  $\xi = a, b$ . When a face uses that strand, the corresponding vertex contributes exactly once to the power counting. Then,

$$\rho_{2;\xi} = \sum_{f_s \in F_{\text{int}}(G_k^i)} \rho_{2;\xi;f_s} \quad (41)$$

counts the number of vertices of  $\mathcal{V}_{2;\xi;s}$  in  $G_k^i$ . In the end, we have

$$\prod_{(i,k)} \prod_{f_s \in \mathcal{F}_{\text{int}} \cap G_k^i} M^{[\frac{2a}{b}\rho_{2;a;f_s} + 2\rho_{2;b;f_s}]} = \prod_{(i,k)} M^{\frac{2a}{b}\rho_{2;a}(G_k^i) + 2\rho_{2;b}(G_k^i)}. \quad (42)$$

Changing  $M \rightarrow M^b$ , we obtain a power counting of the amplitude (36) for the model  $+$ , under the condition  $a \leq b$ , as

$$|A_{\mathcal{G};\boldsymbol{\mu}}| \leq \kappa \prod_{(i,k) \subset N^2} M^{\omega_{d;+}(G_k^i)}, \quad (43)$$

where  $\kappa$  is a constant and the degree of divergence of  $G_k^i$  is given by

$$\omega_{d;+}(G_k^i) = -2bL(G_k^i) + DF_{\text{int}}(G_k^i) + 2a\rho_+(G_k^i) + \sum_{\xi=a,b} 2\xi\rho_{2;\xi}(G_k^i). \quad (44)$$

Putting  $a$  to 0 leads to the ordinary power counting theorem of usual tensor field theories.

**Model  $\times$**  - The analysis is very similar to the above. We count how many times a face  $f_s$  passes through all vertices of the type  $\mathcal{V}_{\times;s}$  and this defines the following quantities

$$\varrho_{f_s} = \sum_{v_{s'}, f_{s''}} \epsilon_{v_{s'} f_s f_{s''}}, \quad \rho_{\times}(\mathcal{G}) = \sum_s \sum_{f_s} \varrho_{f_s}. \quad (45)$$

With a similar calculation as above, using (33) with  $3a \leq 2b$ , introducing also vertices of  $\mathcal{V}_{2;\xi;s}$ ,  $\xi = a, 2a, b$ , and  $\rho_{2;\xi;f_s}$  as the number of times that a closed face  $f_s$  runs through vertices of  $\mathcal{V}_{2;\xi;s}$  and  $\rho_{2;\xi}$  still obeys (41), we obtain the power counting of the model  $\times$  as

$$|A_{\mathcal{G};\boldsymbol{\mu}}| \leq \kappa \prod_{(i,k) \subset N^2} M^{\omega_{d;\times}(G_k^i)}, \quad (46)$$

where  $\kappa$  is a constant and the degree of divergence of  $G_k^i$  is given by

$$\omega_{d;\times}(G_k^i) = -2bL(G_k^i) + DF_{\text{int}}(G_k^i) + 2a\rho_{\times}(G_k^i) + \sum_{\xi=a,2a,b} 2\xi\rho_{2;\xi}(G_k^i). \quad (47)$$

From (44) and (47) and for convenience, we can use unified notations  $\omega_{d;\bullet}$  with  $\bullet = +, \times$ , with the sum of  $\xi$  being appropriately chosen.

## 5 Analyses of the potentially renormalizable models

In this section, we explore the parameter spaces of potentially renormalizable models  $+$  and  $\times$ .

In the analyses below, we need the number of internal faces of a connected graph  $\mathcal{G}$ , in any rank  $d \geq 3$  tensorial model, which is given in [90]:

$$F_{\text{int}} = -\frac{2}{(d^-)!}(\omega(\mathcal{G}_{\text{color}}) - \omega(\partial\mathcal{G})) - (C_{\partial\mathcal{G}} - 1) - \frac{d^-}{2}N_{\text{ext}} + d^- - \frac{d^-}{4}(4 - 2n) \cdot V, \quad (48)$$

where  $d^- = d - 1$  with  $d$  being the rank of the tensor field,  $\mathcal{G}_{\text{color}}$  is the colored extension of  $\mathcal{G}$ ,  $\partial\mathcal{G}$  denotes the boundary of  $\mathcal{G}$  [80], with  $C_{\partial\mathcal{G}}$  the number of connected components of  $\partial\mathcal{G}$ ,  $N_{\text{ext}}$  is the number of external legs of the graph,  $V_k$  is the number of vertices of coordination number  $k$ ,  $V = \sum_k V_k$  is the total number of vertices in  $\mathcal{G}$ , and  $n \cdot V = \sum_k k V_k$  is the number of half lines emanating from vertices.  $\omega(\mathcal{G}_{\text{color}}) = \sum_{J_{\mathcal{G}_{\text{color}}}} g_{\tilde{J}_{\mathcal{G}_{\text{color}}}}$ ,  $\omega(\partial\mathcal{G}) = \sum_{J_{\partial\mathcal{G}}} g_{J_{\partial\mathcal{G}}}$  with genus  $g_J$ , the genus of a ribbon graph  $J$  called jacket [21]. A jacket is nothing but a particular embedding of the bipartite colored graph  $\mathcal{G}$ . The jackets of  $\mathcal{G}_{\text{color}}$  are denoted  $J_{\mathcal{G}_{\text{color}}}$  and they must be “closed” to define a closed surface  $\tilde{J}_{\mathcal{G}_{\text{color}}}$  on which a genus  $g_{\tilde{J}_{\mathcal{G}_{\text{color}}}}$  could be identified. The boundary graph  $\partial\mathcal{G}$  itself maps to a rank  $d - 1$  colored tensor graph.  $\partial\mathcal{G}$  therefore has jackets denoted  $J_{\partial\mathcal{G}}$ .

The quantity  $\omega(\mathcal{G}_{\text{color}})$  is called the degree of the colored tensor graph  $\mathcal{G}_{\text{color}}$ . It replaces the genus and allows one to define a large  $N$  expansion for colored tensor models [21]. A graph  $\mathcal{G}$  is called a melon if and only if its colored extension  $\mathcal{G}_{\text{color}}$  is a melon and that is if  $\omega(\mathcal{G}_{\text{color}}) = 0$  (all jackets  $\tilde{J}_{\mathcal{G}_{\text{color}}}$  are planar). We shall need a few properties of the quantity  $\omega(\mathcal{G}_{\text{color}}) - \omega(\partial\mathcal{G})$  withdrawn from [81] that we will recall at some point.

Let us recall the following terminology: a “bridge” in a graph is a line such that cutting that line adds another connected component to this graph. The “cut of a bridge” means the removal of the bridge from the graph and letting two external legs where its extremities were incident. A graph is called one-particle reducible (1PR) graph if it has bridges, otherwise it is called one-particle irreducible (1PI).

**Lemma 1** ( $\rho_{\bullet}$  and  $\rho_{2;\xi}$  for 1PR graph). *Let  $\mathcal{G}$  be a graph with bridges (or a 1PR graph) such that cutting the bridges gives the family  $\{\mathcal{G}_j\}$  of subgraphs. then*

$$\rho_{\bullet}(\mathcal{G}) = \sum_j \rho_{\bullet}(\mathcal{G}_j), \quad \rho_{2;\xi}(\mathcal{G}) = \sum_j \rho_{2;\xi}(\mathcal{G}_j), \quad (49)$$

where  $\bullet = +$ , and  $\xi = a, b$ , or  $\bullet = \times$ , and  $\xi = a, 2a, b$ .

*Proof.* This follows from the fact that through a bridge no closed face passes. The quantities  $\rho_{\bullet}(\mathcal{G})$  and  $\rho_{2;\xi}(\mathcal{G})$  can be computed with the block diagonal matrix  $\epsilon_{vf}$  using vertices and closed faces in each connected component  $\mathcal{G}_j$ . □

The following proposition is easy to prove.

**Lemma 2** (Bounds on  $\rho_{2;\xi}$ ). *Let  $\mathcal{G}$  be a graph of the model  $\bullet$ . Then  $\rho_{2;\xi}(\mathcal{G}) \leq V_{2;\xi}$ . If  $\mathcal{G}$  is 1PI then*

$$\rho_{2;\xi}(\mathcal{G}) = V_{2;\xi}(\mathcal{G}). \quad (50)$$

## 5.1 Models +

Consider the “contraction” operation of a degree-2 vertex  $v$  (belonging to  $\mathcal{V}_2$  or to  $\mathcal{V}_{2;s}$ ) on the graph  $\mathcal{G}$  which removes  $v$  and replaces it by a propagator line with the same external momenta. Consider the graph  $\tilde{\mathcal{G}}$  resulting from the contractions of all degree-2 vertices in  $\mathcal{G}$ . Note that if  $\mathcal{G}$  is 1PR or 1PI then so is  $\tilde{\mathcal{G}}$  and the number of degree-4 vertices and external legs coincide in both graphs. We define the number  $Br$  of c-bridges (chain-bridges) of  $\mathcal{G}$  to be the number of bridges in  $\tilde{\mathcal{G}}$ . Note a c-bridge of  $\mathcal{G}$  can be very well associated with a bridge  $\mathcal{G}$ . We also introduce  $V_4 + V_{+;4} = V_{(4)}$ .

**Lemma 3** (Bound of  $\rho_+$ ). *Let  $\mathcal{G}$  be a graph with  $N_{\text{ext}} > 0$  external legs. Then,  $\rho_+(\mathcal{G}) \leq V_{+;4}$ . If  $\mathcal{G}$  is melonic*

- $V_{(4)} = 1$ , then  $\rho_+(\mathcal{G}) = 0$ .
  - $V_{(4)} > 1$ , then  $\rho_+(\mathcal{G}) \leq V_{(4)} - \frac{N_{\text{ext}}}{2} - Br$ ,
- where  $Br$  is the number of c-bridges in the graph  $\mathcal{G}$ .

*Proof.* The first statement is clear from the combinatorial procedure counting at most  $V_{+;4}$  for  $\rho_+(\mathcal{G})$  for an arbitrary graph. Now this bound can be refined for a melonic  $N_{\text{ext}}$ -point graph. If  $V_{(4)} = 1$ , then either  $N_{\text{ext}} = 4$ , and then  $\rho_+(\mathcal{G}) = 0$ , or  $N_{\text{ext}} = 2$ , and we have a melonic tadpole or a melonic graph with one c-bridge which gives again  $\rho_+(\mathcal{G}) = 0$ .

A 1PI graph  $\mathcal{G}$  with 4 valent vertices can have at most 2 external legs per vertex. Consider a melonic graph  $\mathcal{G}$  and its colored extension  $\mathcal{G}_{\text{color}}$ : then each vertex in  $\mathcal{G}_{\text{color}}$  comes with a partner (see for instance Figure 1 in [81]). Note that the two partner vertices belong to the same vertex in  $\mathcal{G}$ . If one vertex  $v$  has a propagator  $l$  and its partner  $\tilde{v}$  has no propagator (hence has an external leg) then  $l$  must be a bridge. Focusing on 1PI bipartite melons, then either  $v$  and  $\tilde{v}$  have both propagators or have both external legs. The presence of  $N_{\text{ext}}$  external legs in 1PI bipartite melons implies that these external legs must be hooked to  $N_{\text{ext}}/2$  vertices. Take any vertex  $v_s$  with color  $s$  where an external leg is incident, then an external leg is also incident to  $\tilde{v}_s$ . None of the open faces with color  $0s$ , which can be enhanced, could bring any contribution to  $\rho_+(\mathcal{G})$ . Repeating the argument for  $N_{\text{ext}}/2$  vertices, we see that these vertices could not be part of the optimization procedure computing  $\rho_+(\mathcal{G})$  and so  $\rho_+(\mathcal{G}) \leq V_{(4)} - N_{\text{ext}}/2$ .

Now we treat the case of a 1PR graph  $\mathcal{G}$ . Consider its resulting  $\tilde{\mathcal{G}}$  after the contraction of all of its degree-2 vertices. Cut all bridges in  $\tilde{\mathcal{G}}$  to obtain a family of 1PI subgraphs. On each component  $\tilde{\mathcal{G}}_j$  the bound  $\rho_+(\tilde{\mathcal{G}}_j) \leq V_{(4)}(\tilde{\mathcal{G}}_j) - \frac{N_{\text{ext}}(\tilde{\mathcal{G}}_j)}{2}$  holds. Summing this relation over 1PI subgraphs and using Lemma 1, we get

$$\rho_+(\tilde{\mathcal{G}}) = \sum_j \rho_+(\tilde{\mathcal{G}}_j) \leq \sum_j [V_{(4)}(\tilde{\mathcal{G}}_j) - \frac{N_{\text{ext}}(\tilde{\mathcal{G}}_j)}{2}] = V_{(4)} - \frac{1}{2}N_{\text{ext}} - \# \text{bridges} , \quad (51)$$

where we used that each bridge cut brings two additional external legs compared to  $N_{\text{ext}}$ . Finally, we can use the relation  $\rho_+(\mathcal{G}) = \rho_+(\tilde{\mathcal{G}})$  because degree-2 vertices are not involved in the counting of  $\rho_+$  and  $\# \text{bridges} = Br$ . In summary, we can also use (51) for 1PI graph with  $Br = 0$ . □

As an illustration of Lemma 3, consider the graphs of Figure 4. Consider the melonic graph at the left hand side.  $\frac{N_{\text{ext}}}{2} = 3$  vertices which have external legs will not contribute to

$\rho_+(\mathcal{G})$ . Hence,  $\rho_+(\mathcal{G}) \leq V_{(4)} - \frac{N_{\text{ext}}}{2}$ . On the other hand, consider the non-melonic graph on the right hand side. 3 vertices which have external legs contribute to  $\rho_+(\mathcal{G})$ .

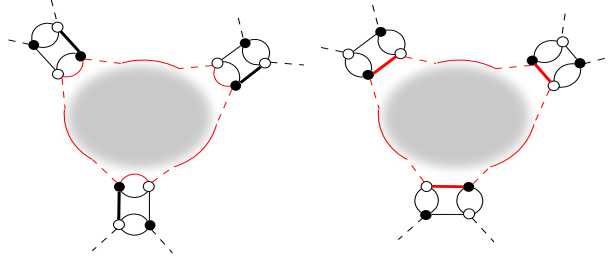


Figure 4: Examples of  $N_{\text{ext}} = 6$ -point functions in rank  $d = 3$  of a melonic and a non-melonic type.

For a melonic graph, Lemma 3 gives in fact two bounds. The bound  $\rho_+(\mathcal{G}) \leq V_{+,4}$  is sharper than the other, if and only if

$$V_4 \geq \frac{N_{\text{ext}}}{2} + Br. \quad (52)$$

**Potentially renormalizable models.** We restrict now to primitively divergent graphs which can be considered connected and with  $Br = 0$ , in other words to 1PI graphs. The degree of divergence of this model is, by combining (44) and (48) and using  $2L = n \cdot V - N_{\text{ext}}$ ,  $a \leq b$ ,

$$\begin{aligned} \omega_{d,+}(\mathcal{G}) &= -\frac{2D}{(d^-)!}(\omega(\mathcal{G}_{\text{color}}) - \omega(\partial\mathcal{G})) - D(C_{\partial\mathcal{G}} - 1) - \frac{1}{2}[(D d^- - 2b)N_{\text{ext}} - 2D d^-] \\ &\quad + \frac{1}{2}[-2D d^- + (D d^- - 2b)n] \cdot V + 2a\rho_+ + 2a\rho_{2;a} + 2b\rho_{2;b}. \end{aligned} \quad (53)$$

From Lemma 3, we have

$$\begin{aligned} \Delta_+^{\text{melon}} &= \begin{cases} 0, & V_{(4)} = 1 \\ V_{(4)} - \frac{N_{\text{ext}}}{2} - \rho_+(\mathcal{G}^{\text{melon}}) \geq 0, & V_{(4)} > 1 \end{cases} \\ \Delta_+ &= V_{+,4} - \rho_+(\mathcal{G}) \geq 0. \end{aligned} \quad (54)$$

The case  $V_{(4)} > 1$  is the most important one when we study all orders of perturbation and we will focus on that. Using the Lemma 2, and further inserting that  $\omega(\mathcal{G}_{\text{color}}) = 0$  and  $\omega(\partial\mathcal{G}) = 0$  for melonic graphs,

$$\begin{aligned} \omega_{d,+}(\mathcal{G}^{\text{melon}}) &\leq -D(C_{\partial\mathcal{G}} - 1) - \frac{1}{2}[(D d^- - 2b + 2a)N_{\text{ext}} - 2D d^-] \\ &\quad - 2bV_2 - 2(b-a)V_{2;a} + (D d^- - 4b + 2a)V_{(4)} - 2a\Delta_+^{\text{melon}} \\ &\leq -D(C_{\partial\mathcal{G}} - 1) - \frac{1}{2}[(D d^- - 2b + 2a)N_{\text{ext}} - 2D d^-] \\ &\quad - 2bV_2 - 2(b-a)V_{2;a} + (D d^- - 4b + 2a)V_{(4)}. \end{aligned} \quad (55)$$

There is another bound for melonic graphs:

$$\begin{aligned}
\omega_{d,+}(\mathcal{G}^{\text{melon}}) &\leq -D(C_{\partial\mathcal{G}} - 1) - \frac{1}{2} [(Dd^- - 2b)N_{\text{ext}} - 2Dd^-] \\
&\quad - 2bV_2 - 2(b-a)V_{2;a} + (Dd^- - 4b)V_4 + (Dd^- - 4b + 2a)V_{+;4} \\
&\leq -D(C_{\partial\mathcal{G}} - 1) - [bN_{\text{ext}} - Dd^-] \\
&\quad - 2bV_2 - 2(b-a)V_{2;a} + (Dd^- - 4b)\left(V_4 - \frac{N_{\text{ext}}}{2}\right) + (Dd^- - 4b + 2a)V_{+;4}. \quad (56)
\end{aligned}$$

Either choosing (56) or (55) as a sharper bound, leads to the same result.

Meanwhile, for non-melonic graphs, using  $\omega(\mathcal{G}_{\text{color}}) - \omega(\partial\mathcal{G}) \geq \frac{1}{2}(d^- - 1)d^-!$  [81], we get

$$\begin{aligned}
\omega_{d,+}(\mathcal{G}^{\text{non-melon}}) &\leq -D(d^- - 1) - D(C_{\partial\mathcal{G}} - 1) - \frac{1}{2} [(Dd^- - 2b)N_{\text{ext}} - 2Dd^-] \\
&\quad - 2bV_2 - 2(b-a)V_{2;a} + (Dd^- - 4b)V_4 + (Dd^- - 4b + 2a)V_{+;4} - 2a\Delta_+ \\
&\leq -D(d^- - 1) - D(C_{\partial\mathcal{G}} - 1) - \frac{1}{2} [(Dd^- - 2b)N_{\text{ext}} - 2Dd^-] \\
&\quad - 2bV_2 - 2(b-a)V_{2;a} + (Dd^- - 4b)V_4 + (Dd^- - 4b + 2a)V_{+;4}. \quad (57)
\end{aligned}$$

For renormalizable models, we require the coefficients of vertices to be negative. This is demanding that, since  $a > 0$ ,  $b > 0$ ,

$$Dd^- - 4b + 2a \leq 0, \quad b \geq a, \quad (58)$$

which give for  $a$ ,

$$a \leq 2b - \frac{1}{2}Dd^-. \quad (59)$$

We see that the condition  $a \leq b$  coming from the sum over internal momenta has been naturally incorporated in the analysis. Then, to achieve just-renormalizability, we use  $a = 2b - \frac{1}{2}Dd^- \geq 0$  (and  $a \leq b$  implies that  $b \leq \frac{1}{2}Dd^-$ ) given in (59) into (55) and (57), and see if the conditions

$$\omega_{d,+}(\mathcal{G}^{\text{melon}})|_{N_{\text{ext}} \geq 6} < 0, \quad \omega_{d,+}(\mathcal{G}^{\text{non-melon}})|_{N_{\text{ext}} \geq 6} < 0 \quad (60)$$

can be accomplished. These conditions translate into

$$\begin{aligned}
\omega_{d,+}(\mathcal{G}^{\text{melon}})|_{N_{\text{ext}} \geq 6} &\leq \\
&\left[ -D(C_{\partial\mathcal{G}} - 1) + Dd^- - bN_{\text{ext}} - 2bV_2 - 2(b-a)V_{2;a} \right] \Big|_{N_{\text{ext}} \geq 6} < 0, \quad (61)
\end{aligned}$$

$$\begin{aligned}
\omega_{d,+}(\mathcal{G}^{\text{non-melon}})|_{N_{\text{ext}} \geq 6} &\leq \\
&\left[ D - D(C_{\partial\mathcal{G}} - 1) - \left(\frac{1}{2}Dd^- - b\right)N_{\text{ext}} - 2bV_2 - 2(b-a)V_{2;a} - 2aV_4 \right] \Big|_{N_{\text{ext}} \geq 6} < 0. \quad (62)
\end{aligned}$$

As  $N_{\text{ext}}$  increases,  $\omega_{d,+}$  decreases, so  $\omega_{d,+}$  is maximum at  $N_{\text{ext}} = 6$  for melonic graphs;  $\omega_{d,+}$  is maximum at  $N_{\text{ext}} = 6$  as long as  $b < \frac{Dd^-}{2}$ , for non-melonic graphs. Thus, the conditions for having convergent  $N_{\text{ext}} = 6$ -pt functions are:

$$\omega_{d,+}(\mathcal{G}^{\text{melon}})|_{N_{\text{ext}}=6} \leq -D(C_{\partial\mathcal{G}} - 1) + Dd^- - 6b - 2bV_2 - 2(b-a)V_{2;a}$$

$$\begin{aligned}
&\leq D d^- - 6b < 0, \\
\omega_{d,+}(\mathcal{G}^{\text{non-melon}})|_{N_{\text{ext}}=6} &\leq D - D(C_{\partial\mathcal{G}} - 1) - 3Dd^- + 6b - 2bV_2 - 2(b-a)V_{2;a} - 2aV_4 \\
&\leq D - 3Dd^- + 6b < 0.
\end{aligned} \tag{63}$$

The above inequalities further reduce to

$$\frac{Dd^-}{6} < b < \frac{D(3d^- - 1)}{6}. \tag{65}$$

Note here that  $\frac{D(3d^- - 1)}{6} < \frac{Dd^-}{2}$  is always true for  $D > 0$ , thus we have improved the bound on  $b$ . Under (65), the degree of divergence for  $N_{\text{ext}} \geq 6$  is maximum at  $N_{\text{ext}} = 6$  and strictly negative. Furthermore, we demand that  $a > 0$  and so that  $b > \frac{Dd^-}{4}$ . We finally get the bound

$$\boxed{\frac{Dd^-}{4} < b < \frac{D(3d^- - 1)}{6}}. \tag{66}$$

Now we use (66) to find a bound on  $a = 2b - \frac{1}{2}Dd^-$  (59) as

$$\boxed{0 < a < \frac{D(3d^- - 2)}{6}} \tag{67}$$

Combining (67) and (66) for given  $D$  and  $d^- \geq 2$ , we obtain the ranges of values of  $a$  and  $b$  in Table 1 which could lead to just-renormalizable models:

	$d^- = 2$	$d^- = 3$	$d^- = 4$	$d^- = 5$
$D = 1$	$0 < a < \frac{2}{3}$ $\frac{1}{2} < b < \frac{5}{6}$	$0 < a < \frac{7}{6}$ $\frac{3}{4} < b < \frac{4}{3}$	$0 < a < \frac{5}{3}$ $1 < b < \frac{11}{6}$	$0 < a < \frac{13}{6}$ $\frac{5}{4} < b < \frac{7}{3}$
$D = 2$	$0 < a < \frac{4}{3}$ $1 < b < \frac{5}{3}$	$0 < a < \frac{5}{2}$ $\frac{3}{2} < b < \frac{8}{3}$	$0 < a < \frac{10}{3}$ $2 < b < \frac{11}{3}$	$0 < a < \frac{13}{2}$ $\frac{5}{2} < b < \frac{14}{3}$
$D = 3$	$0 < a < 2$ $\frac{3}{2} < b < \frac{5}{2}$	$0 < a < \frac{7}{2}$ $\frac{9}{4} < b < 4$	$0 < a < 5$ $3 < b < \frac{11}{2}$	$0 < a < \frac{13}{2}$ $\frac{15}{4} < b < 7$
$D = 4$	$0 < a < \frac{8}{3}$ $2 < b < \frac{10}{3}$	$0 < a < \frac{14}{3}$ $3 < b < \frac{16}{3}$	$0 < a < \frac{20}{3}$ $4 < b < \frac{22}{3}$	$0 < a < \frac{26}{3}$ $5 < b < \frac{28}{3}$

Table 1: Allowed region of the values of  $a$  and  $b$  for potentially just-renormalizable models + with  $d^- \leq 5$  and  $D \leq 4$ .

This table shows that there might be uncountable models which could be just renormalizable. We note that the limit cases  $a = 0$  lead to the renormalizable invariant tensor field theories studied in [86] ( $d = 3, D = 1, b = \frac{1}{2}$ ) and [93] [ $(d = 4, D = 1, b = \frac{3}{4}); (d = 5, D = 1, b = 1); (d = 3, D = 2, b = 1)$ ].

Let us seek further conditions leading to interesting models with  $a > 0$ . One of these conditions is to achieve logarithmic divergence for non-melonic graphs at  $N_{\text{ext}} = 4$ . For this, achieving

$$\omega_{d,+}(\mathcal{G}^{\text{non-melon}})|_{N_{\text{ext}}=4} = 0 \tag{68}$$

entails

$$\boxed{b = \frac{1}{2}D(d^- - \frac{1}{2}), \quad a = \frac{1}{2}D(d^- - 1)} \quad (69)$$

which is consistent with (66), since  $\frac{1}{2}D(d^- - \frac{1}{2}) < \frac{D(3d^- - 1)}{6}$  for  $D > 0$  and  $\frac{Dd^-}{4} < \frac{1}{2}D(d^- - \frac{1}{2})$  for  $d^- > 1$ . In Table 2, we explicitly show the valid values of  $a$  and  $b$  given in (69).

	$d^- = 2$	$d^- = 3$	$d^- = 4$	$d^- = 5$
$D = 1$	$a = \frac{1}{2}$	$a = 1$	$a = \frac{3}{2}$	$a = 2$
	$b = \frac{3}{4}$	$b = \frac{5}{4}$	$b = \frac{7}{4}$	$b = \frac{9}{4}$
$D = 2$	$a = 1$	$a = 2$	$a = 3$	$a = 4$
	$b = \frac{3}{2}$	$b = \frac{5}{2}$	$b = \frac{7}{2}$	$b = \frac{9}{2}$
$D = 3$	$a = \frac{3}{2}$	$a = 3$	$a = \frac{9}{2}$	$a = 6$
	$b = \frac{9}{4}$	$b = \frac{15}{4}$	$b = \frac{21}{4}$	$b = \frac{27}{4}$
$D = 4$	$a = 2$	$a = 4$	$a = 6$	$a = 8$
	$b = 3$	$b = 5$	$b = 7$	$b = 9$

Table 2: Values of  $a$  and  $b$  for potentially just-renormalizable theories with  $\omega_{d,+}(\mathcal{G}^{\text{non-melon}})|_{N_{\text{ext}}=4} = 0$  with  $d^- \leq 5$  and  $D \leq 4$ .

Table 1 and Table 2 are consistent for just-renormalizable models with the superficial degree of divergence which does not depend on  $V_4$ , with logarithmic divergence for graphs with  $N_{\text{ext}} = 4$ , and with convergent graphs with  $N_{\text{ext}} \geq 6$ . Let us discuss the behavior of melonic graphs. Concentrating on  $N_{\text{ext}} = 4$ , we evaluate  $\omega_{d,+}(\mathcal{G}^{\text{melon}})|_{N_{\text{ext}}=4}$  keeping in mind (66) and obtain

$$\omega_d(\mathcal{G}^{\text{melon}})|_{N_{\text{ext}}=4} \leq Dd^- - 4b, \quad (70)$$

which gives

$$\omega_d(\mathcal{G}^{\text{melon}})|_{N_{\text{ext}}=4} < 0. \quad (71)$$

Therefore, we have convergent melonic graphs at  $N_{\text{ext}} = 4$ . Divergent non-melonic graphs at  $N_{\text{ext}} = 4$  dominate all melonic graphs.

Insisting on having a derivative coupling in the direct space, that is on  $(U(1)^D)^d$ , we impose that  $a$  and  $b$  are integers. In that situation, we have the obvious solutions to make  $D$  a multiple of 4. Having covered the parameter space for finding interesting models, we will prove that, in section 6, all models for generic  $(d, D)$  (including those of Table 2) are in fact just-renormalizable.

## 5.2 Models $\times$

We work under the same definition and conditions as in section 5.1, where  $V_{(4)}$  presently denotes  $V_4 + V_{\times;4}$ .

**Lemma 4** (Bound of  $\rho_{\times}$ ). *Let  $\mathcal{G}$  be a graph with  $N_{\text{ext}}$  external legs and  $Br$   $c$ -bridges. We have  $\rho_{\times}(\mathcal{G}) \leq 2V_{\times;4}$ .*

*If  $\mathcal{G}$  is such that*

*-a-  $V_{(4)} = 1$  and  $N_{\text{ext}} = 4$ , then  $\rho_{\times}(\mathcal{G}) = 0$*

- b-  $V_{(4)} = 1, N_{\text{ext}} = 2, \rho_{\times}(\mathcal{G}) \leq 1$
- c-  $V_{(4)} > 1$ , then  $\rho_{\times}(\mathcal{G}) \leq 2V_{(4)} - \frac{N_{\text{ext}}}{2} - Br$ .
- If  $\mathcal{G}$  is melonic and
- d-  $V_{(4)} = 1, N_{\text{ext}} = 2$  then  $\rho_{\times}(\mathcal{G}) = 0$ .
- e-  $V_{(4)} > 1$ , then  $\rho_{\times}(\mathcal{G}) \leq 2V_{(4)} - N_{\text{ext}} - 2Br$ .

*Proof.* The first statement should not bring any difficulties. Now let us consider a general 1PI graph. Assume  $V_{(4)} = 1$  and  $N_{\text{ext}} = 4$ , then  $\rho_{\times}(\mathcal{G}) = 0$ , there are no closed faces and so nothing to count. Now if  $V_{(4)} = 1, N_{\text{ext}} = 2$ , two cases might happen. Either the graph is melonic, and there are no enhanced faces *i.e.*  $\rho_{\times}(\mathcal{G}) = 0$ , or the graph is non-melonic and the vertex might still contribute or not to  $\rho_{\times}(\mathcal{G})$ , thus  $\rho_{\times}(\mathcal{G}) \leq 1$ . Then we have shown that a, b, d, are true for any 1PI graphs. For 1PR graph, we simply observe that the presence of bridge at the external legs will not affect the counting of internal faces visiting the vertex counting in  $V_{(4)}$ . Thus a,b and d are valid in this case.

A 1PI graph, with  $V_{(4)} > 1$ , has at most 2 external legs per vertex. Consider a vertex having exactly 1 external leg: then this vertex will contribute at most 1 to  $\rho_{\times}$ . If a vertex has 2 external legs, then 2 cases may occur: either the 2 legs are on the same external face which cannot contribute to  $\rho_{\times}$  or the legs are incident to partner vertices. In the latter case, there are 2 external faces of that vertex which cannot contribute to  $\rho_{\times}$ . Hence, the upper bound for  $\rho_{\times}(\mathcal{G})$  is  $2V_{(4)} - N_{\text{ext}}/2$ .

For a 1PR graph  $\mathcal{G}$ , we cut all bridges to obtain 1PI subgraphs of the graph  $\tilde{\mathcal{G}}$ . On each component  $\tilde{\mathcal{G}}_j$ , we use the 1PI general bound  $\rho_{\times}(\tilde{\mathcal{G}}_j) \leq 2V_{(4)}(\tilde{\mathcal{G}}_j) - \frac{1}{2}N_{\text{ext}}(\tilde{\mathcal{G}}_j)$ . As we perform in the proof of Lemma 3, we can show that the sum over the components brings  $\rho_{\times}(\mathcal{G}) = \rho_{\times}(\tilde{\mathcal{G}}) \leq 2V_{(4)} - \frac{N_{\text{ext}}}{2} - Br$ .

For a melonic graph, the above bounds must be refined. According to the same discussion in the proof of Lemma 3, we know that for a 1PI melonic graph, each vertex having external legs must have  $N_{\text{ext}} = 2$ . (If  $N_{\text{ext}} = 4$ , then the vertex gets disconnected and this is the case with  $V_{(4)} = 1$ .) These two external legs must be on partner vertices  $v$  and  $\tilde{v}$ . Hence the enhanced faces on this vertex are necessarily external and cannot contribute to  $\rho_{\times}(\mathcal{G})$ . Repeating the argument for all vertices with external legs, we get  $\rho_{\times}(\mathcal{G}) \leq 2(V_{(4)} - \frac{N_{\text{ext}}}{2}) = 2V_{(4)} - N_{\text{ext}}$ .

Consider a melonic 1PR graph  $\mathcal{G}$ . Using again the same strategy, we cut all the bridges in  $\tilde{\mathcal{G}}$ , and apply the relation  $\rho_{\times}(\tilde{\mathcal{G}}_j) \leq 2V_{(4)}(\tilde{\mathcal{G}}_j) - N_{\text{ext}}(\tilde{\mathcal{G}}_j)$  for each 1PI component, we get

$$\rho_{\times}(\tilde{\mathcal{G}}^{\text{melon}}) = \sum_j \rho_{\times}(\tilde{\mathcal{G}}_j) \leq \sum_j [2V_{(4)}(\tilde{\mathcal{G}}_j) - N_{\text{ext}}(\tilde{\mathcal{G}}_j)] = 2V_{(4)} - N_{\text{ext}} - 2Br, \quad (72)$$

which together with  $\rho_{\times}(\mathcal{G}^{\text{melon}}) = \rho_{\times}(\tilde{\mathcal{G}}^{\text{melon}})$  is the second relation for melonic graphs for  $V_{(4)} > 1$ . □

The bounds of Lemma 4 should be chosen wisely when bounding the degree of divergence of the graph. Furthermore, again the generic case of  $V_{(4)} > 1$  will be the important one that we will concentrate on.

**Potentially renormalizable models.** We study only primitively divergent graphs and fix  $Br = 0$ . Combining (47) and (48) and using  $2L = n \cdot V - N_{\text{ext}}$ , we obtain the bound for the



degree of divergence in this model, at  $3a \leq 2b$ ,

$$\begin{aligned} \omega_{d;\times}(\mathcal{G}) &= -\frac{2D}{(d^-)!}(\omega(\mathcal{G}_{\text{color}}) - \omega(\partial\mathcal{G})) - D(C_{\partial\mathcal{G}} - 1) - \frac{1}{2}[(Dd^- - 2b)N_{\text{ext}} - 2Dd^-] \\ &\quad + \frac{1}{2}[-2Dd^- + (Dd^- - 2b)n] \cdot V + 2a\rho_{\times} + \sum_{\xi=a,2a,b} 2\xi\rho_{2;\xi}. \end{aligned} \quad (73)$$

Using the Lemma 4, and further inserting that  $\omega(\mathcal{G}_{\text{color}}) = 0$  and  $\omega(\partial\mathcal{G}) = 0$  for melonic graphs, and  $\omega(\mathcal{G}_{\text{color}}) - \omega(\partial\mathcal{G}) \geq \frac{1}{2}(d^- - 1)d^-!$  for non-melonic graphs, the following bound is true:

$$\begin{aligned} \omega_{d;\times}(\mathcal{G}^{\text{melon}}) &\leq -D(C_{\partial\mathcal{G}} - 1) - \frac{1}{2}[(Dd^- - 2b + 4a)N_{\text{ext}} - 2Dd^-] \\ &\quad - 2bV_2 - 2 \sum_{\xi=a,2a} (b - \xi)V_{2;\xi} + (Dd^- - 4b + 4a)V_{(4)} - 2a\Delta_{\times}^{\text{melon}}, \end{aligned} \quad (74)$$

$$\begin{aligned} \omega_{d;\times}(\mathcal{G}^{\text{non-melon}}) &\leq -D(d^- - 1) - D(C_{\partial\mathcal{G}} - 1) - \frac{1}{2}[(Dd^- - 2b + 2a)N_{\text{ext}} - 2Dd^-] \\ &\quad - 2bV_2 - 2 \sum_{\xi=a,2a} (b - \xi)V_{2;\xi} + (Dd^- - 4b + 4a)V_{(4)} - 2a\Delta_{\times}^{\text{non-melon}}, \end{aligned} \quad (75)$$

where we define

$$\begin{aligned} \Delta_{\times}^{\text{melon}} &= 2V_{(4)} - N_{\text{ext}} - \rho_{\times}(\mathcal{G}^{\text{melon}}) \geq 0, \\ \Delta_{\times}^{\text{non-melon}} &= 2V_{(4)} - \frac{N_{\text{ext}}}{2} - \rho_{\times}(\mathcal{G}^{\text{non-melon}}) \geq 0, \end{aligned} \quad (76)$$

and get the inequalities from Lemma 4. Thus, we obtain

$$\begin{aligned} \omega_{d;\times}(\mathcal{G}^{\text{melon}}) &\leq -D(C_{\partial\mathcal{G}} - 1) - \frac{1}{2}[(Dd^- - 2b + 4a)N_{\text{ext}} - 2Dd^-] \\ &\quad - 2bV_2 - 2 \sum_{\xi=a,2a} (b - \xi)V_{2;\xi} + (Dd^- - 4b + 4a)V_{(4)}, \end{aligned} \quad (77)$$

$$\begin{aligned} \omega_{d;\times}(\mathcal{G}^{\text{non-melon}}) &\leq -D(d^- - 1) - D(C_{\partial\mathcal{G}} - 1) - \frac{1}{2}[(Dd^- - 2b + 2a)N_{\text{ext}} - 2Dd^-] \\ &\quad - 2bV_2 - 2 \sum_{\xi=a,2a} (b - \xi)V_{2;\xi} + (Dd^- - 4b + 4a)V_{(4)}. \end{aligned} \quad (78)$$

Seeking renormalizable models, we require

$$Dd^- - 4b + 4a \leq 0, \quad 2a \leq b, \quad (79)$$

where the second condition, more stringent than  $3a \leq 2b$ , will be kept. This gives for  $a$ ,

$$a \leq b - \frac{1}{4}Dd^-, \quad a \leq \frac{b}{2}. \quad (80)$$

To achieve just-renormalizability, we use  $a = b - \frac{1}{4}Dd^-$  (which implies  $b \leq \frac{Dd^-}{2}$ ), (80), in (77) and (78) and require that, for a number of external legs higher than 4, we have convergence:

$$\omega_{d;\times}(\mathcal{G}^{\text{melon}})|_{N_{\text{ext}} \geq 6} < 0,$$

$$\omega_{d;\times}(\mathcal{G}^{\text{non-melon}})|_{N_{\text{ext}} \geq 6} < 0. \quad (81)$$

From (77) and (78), we have:

$$\begin{aligned} \omega_{d;\times}(\mathcal{G}^{\text{melon}})|_{N_{\text{ext}} \geq 6} \leq \\ \left[ -D(C_{\partial\mathcal{G}} - 1) + Dd^- - bN_{\text{ext}} - 2bV_2 - \frac{1}{2}Dd^-V_{2;a} - (Dd^- - 2b)V_{2;2a} \right] \Big|_{N_{\text{ext}} \geq 6}, \end{aligned} \quad (82)$$

$$\begin{aligned} \omega_{d;\times}(\mathcal{G}^{\text{non-melon}})|_{N_{\text{ext}} \geq 6} \leq \\ \left[ D - D(C_{\partial\mathcal{G}} - 1) - \frac{1}{4}Dd^-N_{\text{ext}} - 2bV_2 - \frac{1}{2}Dd^-V_{2;a} - (Dd^- - 2b)V_{2;2a} \right] \Big|_{N_{\text{ext}} \geq 6}. \end{aligned} \quad (83)$$

The maximum value for  $\omega_{d;\times}(\mathcal{G})$  is reached at  $N_{\text{ext}} = 6$ , so we can always write an upper bound and further require convergence:

$$\omega_{d;\times}(\mathcal{G}^{\text{melon}})|_{N_{\text{ext}}=6} \leq Dd^- - 6b < 0, \quad (84)$$

$$\omega_{d;\times}(\mathcal{G}^{\text{non-melon}})|_{N_{\text{ext}}=6} \leq -D\left(\frac{3}{2}d^- - 1\right) < 0. \quad (85)$$

We note here that  $d^- > \frac{2}{3}$  (85) is trivially satisfied in our study in which we only consider tensors with rank  $d \geq 3$ . Hence, for just renormalizability, we impose

$$\frac{Dd^-}{6} < b \leq \frac{Dd^-}{2}, \quad a = b - \frac{1}{4}Dd^-. \quad (86)$$

However (86) also entails  $a > -\frac{Dd^-}{12}$ . Restricting to  $a > 0$ , the bound of  $b$  given can be improved. For just-renormalizability (*i.e.*, the equality in (80), and (81) together with  $a > 0$ ), we impose

$$\boxed{\frac{Dd^-}{4} < b \leq \frac{Dd^-}{2}, \quad a = b - \frac{1}{4}Dd^- > 0} \quad (87)$$

whose values for given positive integer values of  $D$  and  $d$  are given in Table 3.

	$d^- = 2$	$d^- = 3$	$d^- = 4$	$d^- = 5$
$D = 1$	$0 < a \leq \frac{1}{2}$ $\frac{1}{2} < b \leq 1$	$0 < a \leq \frac{3}{4}$ $\frac{3}{4} < b \leq \frac{3}{2}$	$0 < a \leq 1$ $1 < b \leq 2$	$0 < a \leq \frac{5}{4}$ $\frac{5}{4} < b \leq \frac{5}{2}$
$D = 2$	$0 < a \leq 1$ $1 < b \leq 2$	$0 < a \leq \frac{3}{2}$ $\frac{3}{2} < b \leq 3$	$0 < a \leq 2$ $2 < b \leq 4$	$0 < a \leq \frac{5}{2}$ $\frac{5}{2} < b \leq 5$
$D = 3$	$0 < a \leq \frac{3}{2}$ $\frac{3}{2} < b \leq 3$	$0 < a \leq \frac{9}{4}$ $\frac{9}{4} < b \leq \frac{9}{2}$	$0 < a \leq 3$ $3 < b \leq 6$	$0 < a \leq \frac{15}{4}$ $\frac{15}{4} < b \leq \frac{15}{2}$
$D = 4$	$0 < a \leq 2$ $2 < b \leq 4$	$0 < a \leq 3$ $3 < b \leq 6$	$0 < a \leq 4$ $4 < b \leq 8$	$0 < a \leq 5$ $5 < b \leq 10$

Table 3: Allowed region of the values of  $a$  and  $b$  for potentially just-renormalizable models  $\times$  with  $d^- \leq 5$  and  $D \leq 4$ .

Let us understand what is entailed by the just-renormalizability condition  $Dd^- - 4b + 4a = 0$ , at  $N_{\text{ext}} = 4$ . We have

$$\begin{aligned}\omega_{d;\times}(\mathcal{G}^{\text{non-melon}})|_{N_{\text{ext}}=4} &\leq -D(d^- - 1) - D(C_{\partial\mathcal{G}} - 1) - \frac{1}{2} \left[ \frac{Dd^-}{2} \cdot 4 - 2Dd^- \right] \\ &\quad - 2bV_2 - \frac{1}{2}Dd^-V_{2;a} - (Dd^- - 2b)V_{2;2a} \\ &\leq -D(d^- - 1) < 0,\end{aligned}\tag{88}$$

since we only consider tensors of rank  $d \geq 3$ . Thus, non-melonic graphs with  $N_{\text{ext}} = 4$  are found all convergent. Similarly for melonic graphs, requiring just-renormalizability means  $Dd^- - 4b + 4a = 0$ , leading to

$$\begin{aligned}\omega_{d;\times}(\mathcal{G}^{\text{melon}})|_{N_{\text{ext}}=4} &\leq -D(C_{\partial\mathcal{G}} - 1) - \frac{1}{2} \left[ (2a + \frac{Dd^-}{2})4 - 2Dd^- \right] \\ &\quad - 2bV_2 - \frac{1}{2}Dd^-V_{2;a} - (Dd^- - 2b)V_{2;2a} \leq -4a < 0.\end{aligned}\tag{89}$$

Therefore, all melonic graphs with  $N_{\text{ext}} = 4$  are also convergent.

Further, we analyze graphs of  $N_{\text{ext}} = 2$  under the same condition and find

$$\omega_{d;\times}(\mathcal{G}^{\text{melon}})|_{N_{\text{ext}}=2} \leq -D(C_{\partial\mathcal{G}} - 1) - \frac{1}{2} [2b \cdot 2 - 2Dd^-]\tag{90}$$

$$-2bV_2 - \frac{1}{2}Dd^-V_{2;a} - (Dd^- - 2b)V_{2;2a} \leq -2b + Dd^- < \frac{Dd^-}{2}$$

$$\begin{aligned}\omega_{d;\times}(\mathcal{G}^{\text{non-melon}})|_{N_{\text{ext}}=2} &\leq -D(d^- - 1) - D(C_{\partial\mathcal{G}} - 1) - \frac{1}{2} \left[ \frac{Dd^-}{2} \cdot 2 - 2Dd^- \right] \\ &\quad - 2bV_2 - \frac{1}{2}Dd^-V_{2;a} - (Dd^- - 2b)V_{2;2a} \leq \frac{1}{2}D(2 - d^-) \leq 0,\end{aligned}\tag{91}$$

where we used (87), and  $d^- \geq 2$ . In summary, at  $N_{\text{ext}} = 2$ , both melonic and non-melonic graphs might be divergent. A closer look shows that non-melonic graphs can be at most logarithmically divergent at rank  $d \leq 3$ . Furthermore, as observe above, if we increase  $D$  or  $d^-$ , we see that melons could be again the dominant amplitudes.

We conclude that, for potentially just-renormalizable models  $\times$ , *i.e.*, under (80) and (81), only graphs with  $N_{\text{ext}} = 2$  might be divergent.

Let us emphasize that the model  $\times$  appears as a new type of renormalizable theory. Indeed, the coupling constants  $\lambda$  and  $\rho_+$  do not get any corrections, *i.e.*, do not get renormalized, but degree-2 vertices will do. In ordinary QFT and invariant tensor field theory, when a model acquires this property it becomes super-renormalizable, that is, there is a finite number of graphs which contribute to the flow of the mass. That is for example the case, of the scalar  $P(\phi)_2$ -model and even non-local super renormalizable tensor field theories [93, 89]. However, in the present case, as we will see in the following, the model  $\times$  at  $d = 3$  will have an infinite number of graphs which will contribute to the mass renormalization. We attribute this property to the presence of enhanced interactions in the model.

As a concrete study in section 7, we will focus on  $a = \frac{1}{2}$ ,  $b = 1$  for  $D = 1$  and  $d^- = 2$  as satisfied in Table 3.

## 6 Rank $d$ just-renormalizable models +

In this section, we analyze a class of model + which will be proved renormalizable for arbitrary  $d$  and  $D$ . We provide the list of their primitively divergent graphs and proceed to the expansion of those around their local and diverging part. Our goal is to show that the divergent parts in this expansion recasts as a coupling and so a subtracting scheme can be performed. Dealing exclusively with graphs with external legs, we have  $C_{\partial\mathcal{G}} \geq 1$ . Note also that the theory has bipartite graphs such that  $N_{\text{ext}}$  is an even number.

### 6.1 List of divergent graphs

Consider an arbitrary model in the class of models + at fix  $(d, D)$ , with  $a = D(d^- - 1)/2, b = D(d^- - \frac{1}{2})/2$ . Using (55) and (57), in the same notations and conditions introduced above, the superficial degree of divergence is given by:

$$\omega_{d,+}(\mathcal{G}^{\text{melon}}) \leq -D \left[ (C_{\partial\mathcal{G}} - 1) + \frac{1}{2}((d^- - \frac{1}{2})N_{\text{ext}} - 2d^-) + (d^- - \frac{1}{2})V_2 + \frac{1}{2}V_{2;a} + (d^- - 1)\Delta_+^{\text{melon}} \right], \quad (92)$$

$$\begin{aligned} \omega_{d,+}(\mathcal{G}^{\text{non-melon}}) &\leq -D \left[ (d^- - 1) + (C_{\partial\mathcal{G}} - 1) + \frac{1}{2}(\frac{1}{2}N_{\text{ext}} - 2d^-) \right. \\ &\quad \left. + (d^- - \frac{1}{2})V_2 + \frac{1}{2}V_{2;a} + (d^- - 1)V_4 + (d^- - 1)\Delta_+ \right]. \end{aligned} \quad (93)$$

We have already shown that for any graph such that  $N_{\text{ext}} \geq 6$ , the amplitude is convergent. At  $N_{\text{ext}} = 4$ , non-melonic graphs have maximal degree of divergence 0 (logarithmic divergence) and melonic graphs converge.

The following cases occur

(i)  $N_{\text{ext}} = 4$ ,

$$\omega_{d,+}(\mathcal{G}^{\text{melon}}) \leq -D(d^- - 1) < 0, \quad (94)$$

$$\begin{aligned} \omega_{d,+}(\mathcal{G}^{\text{non-melon}}) &\leq -D \left[ (C_{\partial\mathcal{G}} - 1) + (d^- - \frac{1}{2})V_2 + \frac{1}{2}V_{2;a} + (d^- - 1)V_4 \right. \\ &\quad \left. + (d^- - 1)\Delta_+ \right] \leq 0. \end{aligned}$$

For non-melonic graphs, the upper bound saturates only if  $C_{\partial\mathcal{G}} = 1, V_4 = V_2 = V_{2;a} = 0$ , and  $\Delta_+ = 0$ , *i.e.*  $\rho_+(\mathcal{G}^{\text{non-melon}}) = V_{+;4}$ .

(ii)  $N_{\text{ext}} = 2$ : we can combine  $V_{(4)} > 1$  and  $V_{(4)} = 1$  at  $N_{\text{ext}} = 2$  from Lemma 3. Thus we can write a single bound,  $V_{(4)} \geq 1$  as

$$\omega_{d,+}(\mathcal{G}^{\text{melon}}) \leq -D \left[ (C_{\partial\mathcal{G}} - 1) - \frac{1}{2} + (d^- - \frac{1}{2})V_2 + \frac{1}{2}V_{2;a} + (d^- - 1)\Delta_+^{\text{melon}} \right] \leq \frac{D}{2}. \quad (95)$$

Whenever  $C_{\partial\mathcal{G}} - 1 > 0$ , or  $V_2 > 0$ ,  $V_{2;a} > 1$ , or  $\Delta_+^{\text{melon}} > 0$ , the graph becomes convergent. The only way to achieve a divergence with  $\omega_d(\mathcal{G}^{\text{melon}}) = \frac{D}{2}$  is to set the above quantities to 0. Note that, for a graph with  $N_{\text{ext}} = 2$ ,  $\Delta_+^{\text{melon}} = 0$  means

$\rho_+(\mathcal{G}^{\text{melon}}) = V_{(4)} - 1$  from Lemma 3. But we also have the bound  $\rho_+(\mathcal{G}^{\text{melon}}) \leq V_{+;4}$ , therefore writing  $\rho_+(\mathcal{G}^{\text{melon}}) = V_{+;4} - p$ ,  $p \geq 0$ , implies that  $V_4 = 1 - p \geq 0$ . Thus  $p = 0$ , yields  $(\rho_+(\mathcal{G}^{\text{melon}}) = V_{+;4}, V_4 = 1)$  or  $p = 1$  and then  $(\rho_+(\mathcal{G}^{\text{melon}}) = V_{+;4} - 1, V_4 = 0)$ .

The case  $\omega_d(\mathcal{G}^{\text{melon}}) = 0$  might occur for  $C_{\partial\mathcal{G}} - 1 = 0$ ,  $V_2 = 0$ ,  $\Delta_+^{\text{melon}} = 0$ , and  $V_{2;a} = 1$ . Then  $\Delta_+^{\text{melon}} = 0$  means that one of the following two cases occurs,  $(\rho_+(\mathcal{G}^{\text{melon}}) = V_{+;4}, V_4 = 1)$  or  $(\rho_+(\mathcal{G}^{\text{melon}}) = V_{+;4} - 1, V_4 = 0)$  can be produced.

For a non-melonic graph, we have,  $V_{(4)} \geq 0$ ,

$$\begin{aligned} \omega_{d;+}(\mathcal{G}^{\text{non-melonic}}) &\leq -D \left[ (C_{\partial\mathcal{G}} - 1) - \frac{1}{2} \right. \\ &\quad \left. + (d^- - \frac{1}{2})V_2 + \frac{1}{2}V_{2;a} + (d^- - 1)V_4 + (d^- - 1)\Delta_+ \right] \leq \frac{D}{2}, \end{aligned} \quad (96)$$

and, the only way to achieve divergence is to set  $C_{\partial\mathcal{G}} = 1$ ,  $V_2 = 0$ ,  $V_4 = 0$ , and  $\Delta_+ = 0$ . The last condition translates as  $\rho_+(\mathcal{G}^{\text{melon}}) = V_{+;4}$ . Likewise, we can have  $\omega_{d;+}(\mathcal{G}^{\text{non-melonic}}) = \frac{D}{2}$  for  $V_{2;a} = 0$ , or  $\omega_{d;+}(\mathcal{G}^{\text{non-melonic}}) = 0$  for  $V_{2;a} = 1$ .

We have thus completed the proof of the following statement:

**Proposition 1** (List of primitively divergent graphs for model +). *The  $p^{2a}\phi^4$ -model + with parameters  $a = D(d^- - 1)/2, b = D(d^- - \frac{1}{2})/2$  for two integers  $d > 2$  and  $D > 0$ , has primitively divergent graphs with  $(\Omega(\mathcal{G}) = \omega(\mathcal{G}_{\text{color}}) - \omega(\partial\mathcal{G}))$ :*

$\mathcal{G}$	$N_{\text{ext}}$	$V_2$	$V_{2;a}$	$V_4$	$\rho_+$	$C_{\partial\mathcal{G}} - 1$	$\Omega(\mathcal{G})$	$\omega_d(\mathcal{G})$
	4	0	0	0	$V_{+;4}$	0	1	0
I	2	0	0	0	$V_{+;4}$	0	1	$\frac{D}{2}$
II	2	0	0	0	$V_{+;4} - 1$	0	0	$\frac{D}{2}$
III	2	0	0	1	$V_{+;4}$	0	0	$\frac{D}{2}$
IV	2	0	1	0	$V_{+;4}$	0	1	0
V	2	0	1	0	$V_{+;4} - 1$	0	0	0
VI	2	0	1	1	$V_{+;4}$	0	0	0

Table 4: List of primitively divergent graphs of the  $p^{2a}\phi^4$ -model +.

Some divergent 2-point graphs are illustrated in Figures 6 and 7 in appendix B specializing to  $d = 3$  and  $D = 1$ . They will contribute to the mass renormalization for this model. Secondly, consider the 4-point amplitudes associated with the graphs of Figure 8 in appendix B. These will contribute to the renormalization of couplings  $\eta_+$  or  $\lambda$  depending on the external momentum data of the correlators. We can construct an infinite family of divergent 4-point graphs in this model.

At the end of this section, the proof of the next theorem will be completed:

**Theorem 1.** *The  $p^{2a}\phi^4$  model + with parameters  $a = D(d^- - 1)/2, b = D(d^- - \frac{1}{2})/2$  for arbitrary rank  $d \geq 3$  and dimension  $D > 0$  with action defined by (2) is just-renormalizable at all orders of perturbation theory.*

## 6.2 Renormalization

The subsequent part of the renormalization program consists in the proof that the divergent and local part of all divergent amplitudes can be recast as terms which are present in the Lagrangian of the model + of section 6.1 with fixed parameter  $a = D(d^- - 1)/2$  and  $b = D(d^- - 1/2)/2$ . For that purpose, we perform a Taylor expansion of the amplitudes of graphs listed in Table 4 and show that the divergent terms in that expansion are associated with either the mass, counter-terms  $CT_{2;\xi}$ ,  $\xi = a, b$ , or interaction terms plus convergent remainders.

**Renormalization of marginal 4-point functions.** Marginal 4-point functions are given by the first line of Table 4. Given a connected and bipartite boundary graph of a 4-point graph, it is simple to realize that the pattern of its external momenta should follow either the pattern of  $\mathbf{V}_{4;s}$  or of  $\mathbf{V}_{+,4;s}$  (15) (see Figure 2). The locality principle of the present model tells us to consider a graph issued from the expansion of correlators of the form (17) or (18) which translate as

$$\langle \phi_{12\dots d} \bar{\phi}_{1'2\dots d} \phi_{1'2'\dots d'} \bar{\phi}_{12'\dots d'} \rangle, \quad (97)$$

$$\langle |p_1^{\text{ext}}|^{2a} \bar{\phi}_{1'2\dots d} \phi_{1'2'\dots d'} \bar{\phi}_{12'\dots d'} \rangle, \quad (98)$$

with  $|p_1^{\text{ext}}|^{2a}$  an external momentum with color  $s = 1$ . In the following, we will concentrate on an expansion of a graph with external data of the form of the operator  $\mathbf{V}_{+,4;s=1}$ . In other words, we will focus on  $s = 1$  and a graph coming from the expansion of the correlator (98). However, as it will be clear, our analysis is without loss of generality since the method can be extended to  $\mathbf{V}_{4;1}$  and then to  $\mathbf{V}_{+,4;s}$ , for any color  $s$ .

Consider a 4-point graph with 4 external propagators attached to it with external momenta governed by the pattern of (98). This 4-point graph carries  $2d$  momentum labels; these are associated with  $2d$  external faces, which we denote by

$$f \in \mathcal{F}_{\text{ext}} = \{f_{[1]}, f_2, \dots, f_d, f_{1'}, f_{2'}, \dots, f_{d'}\},$$

where we emphasize the face which is enhanced by a square bracket (say  $[1]$ ). Let  $A_4(\{p_f^{\text{ext}}\})$  be the amplitude of such a graph. Two types of scale indices have to be considered in this amplitude: the external scales  $j_l$  associated with external fields and which correspond to external propagators with labels  $l$  and the (internal) scale  $i$  of the  $G_k^i$  graph. In short, a quasi-local graph  $G_k^i$  implies that  $j_l \ll i$ .

We have from (25)

$$\begin{aligned} A_4(\{p_{f_s}^{\text{ext}}\}) &= \kappa(\eta_+) \sum_{p_{f_s}} \int \left[ \prod_{l \in \mathcal{L}} d\alpha_l e^{-\alpha_l \mu} \right] \left[ \prod_{f_s \in \mathcal{F}_{\text{ext}}} e^{-(\sum_{l \in f_s} \alpha_l) \sum_{\xi} |p_{f_s}^{\text{ext}}|^{2\xi}} \right] \\ &\times \left[ \prod_{f_s \in \mathcal{F}_{\text{int}}} e^{-(\sum_{l \in f_s} \alpha_l) \sum_{\xi} |p_{f_s}|^{2\xi}} \right] |p_{f_{[1]}}^{\text{ext}}|^{2a} \left[ \prod_{s=1}^d \prod_{v_s \in \mathcal{V}_{+,4;s}} (\epsilon \tilde{p}^{2a})_{v_s} \right], \\ (\epsilon \tilde{p}^{2a})_{v_s} &:= \sum_{f_{s'}} \epsilon_{v_s, f_{s'}} (\tilde{p}_{f_{s'}})^{2a}, \end{aligned} \quad (99)$$

where  $\kappa(\eta_+)$  includes symmetry factors and coupling constants. We recall that  $p_{f_s}^{\text{ext}}$  are external momenta, and the last line shows  $\tilde{p}_{f_s}$  which refers to an internal or an external momentum. Let us concentrate on the range of the parameters  $\alpha$ : for an internal line  $l$ , that we will now denote  $\ell$ ,  $\alpha_\ell \in [M^{-(2b)i_\ell}, M^{-(2b)(i_\ell-1)}]$ ; for an external line  $l$ , now denoted  $l_{\text{ext}}$ ,  $\alpha_{l_{\text{ext}}} \in [M^{-(2b)j_{l_{\text{ext}}}}, M^{-(2b)(j_{l_{\text{ext}}}-1)}]$ . We are interested in a regime when  $j_{l_{\text{ext}}} \ll i \leq i_\ell$ .

A Taylor expansion over an external face amplitude gives

$$\begin{aligned} e^{-(\sum_{l \in f} \alpha_l) \sum_\xi |p_f^{\text{ext}}|^{2\xi}} &= e^{-(\alpha_{l_{\text{ext}}} + \alpha_{l_{\text{ext}}'}) \sum_\xi |p_f^{\text{ext}}|^{2\xi}} [1 - R_f] \\ R_f &= \left( \sum_{\ell \in f} \alpha_\ell \right) \left( \sum_\xi |p_f^{\text{ext}}|^{2\xi} \right) \int_0^1 e^{-t(\sum_{\ell \in f} \alpha_\ell) \sum_\xi |p_f^{\text{ext}}|^{2\xi}} dt, \end{aligned} \quad (100)$$

where  $\sum_{\ell \in f} \alpha_\ell$  is small ( $\alpha_\ell \sim \mathcal{O}(\frac{1}{|p_{f_s}|^{2\xi}}) \sim M^{-(2\xi)i_\ell}$ ). We insert that expansion for each external face in (99) and obtain:

$$\begin{aligned} A_4(\{p_f^{\text{ext}}\}) &= \kappa(\eta_+) \sum_{p_f} \int \left[ \prod_{l \in \mathcal{L}} d\alpha_l e^{-\alpha_l \mu} \right] |p_{f_{[1]}}^{\text{ext}}|^{2a} \left[ \prod_{f \in \mathcal{F}_{\text{ext}}} e^{-(\alpha_{l_{\text{ext}}} + \alpha_{l_{\text{ext}}'}) \sum_\xi |p_f^{\text{ext}}|^{2\xi}} \right] \\ &\times \left[ 1 - \sum_{f \in \mathcal{F}_{\text{ext}}} R_f + \sum_{f, f' \in \mathcal{F}_{\text{ext}}} R_f R_{f'} + \dots \right] \left[ \prod_{f \in \mathcal{F}_{\text{int}}} e^{-(\sum_{\ell \in f} \alpha_\ell) \sum_\xi |p_f|^{2\xi}} \right] \prod_{s=1}^d \prod_{v_s \in \mathcal{V}_{+;4;s}} [(\epsilon \tilde{p}^{2a})_{v_s}]. \end{aligned} \quad (101)$$

The dots are higher order products in the  $R_f$ 's. From Table 4,  $\rho_+$  (34) must be equal to  $V_{+;4}$ . Hence, in each vertex kernel, we must collect and integrate one momentum of a closed face. A divergent 4-point graph satisfying the first row of Table 4 must be such that no external momenta can be found within  $\prod_{s=1}^d \prod_{v_s \in \mathcal{V}_{+;4;s}} [(\epsilon \tilde{p}^{2a})_{v_s}]$ .

We write the 0th order in expansion in  $R_f$  as:

$$\begin{aligned} A_4(\{p_f^{\text{ext}}\}; 0) &= \kappa(\eta_+) \sum_{p_f} \int \left[ \prod_l d\alpha_l e^{-\alpha_l \mu} \right] |p_{f_{[1]}}^{\text{ext}}|^{2a} \prod_{f \in \mathcal{F}_{\text{ext}}} \left[ e^{-(\alpha_{l_{\text{ext}}} + \alpha_{l_{\text{ext}}'}) \sum_\xi |p_f^{\text{ext}}|^{2\xi}} \right] \\ &\times \left[ \prod_{f \in \mathcal{F}_{\text{int}}} e^{-(\sum_{\ell \in f} \alpha_\ell) \sum_\xi |p_f|^{2\xi}} \right] \left[ \prod_{s=1}^d \prod_{v_s \in \mathcal{V}_{+;4;s}} (\epsilon \tilde{p}^{2a})_{v_s} \right], \\ &= \kappa(\eta_+) \left[ \int \left[ \prod_{l_{\text{ext}}} d\alpha_{l_{\text{ext}}} e^{-\alpha_{l_{\text{ext}}} \mu} \right] |p_{f_{[1]}}^{\text{ext}}|^{2a} \prod_{f \in \mathcal{F}_{\text{ext}}} e^{-(\alpha_{l_{\text{ext}}} + \alpha_{l_{\text{ext}}'}) \sum_\xi |p_f^{\text{ext}}|^{2\xi}} \right] \\ &\times \left[ \sum_{p_f} \int \left[ \prod_\ell d\alpha_\ell e^{-\alpha_\ell \mu} \right] \prod_{f \in \mathcal{F}_{\text{int}}} \left[ e^{-(\sum_{\ell \in f} \alpha_\ell) \sum_\xi |p_f|^{2\xi}} \right] \left[ \prod_{s=1}^d \prod_{v_s \in \mathcal{V}_{+;4;s}} (\epsilon \tilde{p}^{2a})_{v_s} \right] \right]. \end{aligned} \quad (102)$$

The factor involving external lines can be re-expressed as

$$\begin{aligned} &\int \left[ \prod_{l_{\text{ext}}} d\alpha_{l_{\text{ext}}} e^{-\alpha_{l_{\text{ext}}} \mu} \right] |p_{f_{[1]}}^{\text{ext}}|^{2a} \prod_{f \in \mathcal{F}_{\text{ext}}} e^{-(\alpha_{l_{\text{ext}}} + \alpha_{l_{\text{ext}}'}) \sum_\xi |p_f^{\text{ext}}|^{2\xi}} = \\ &\int \left[ \prod_{l_{\text{ext}}} d\alpha_{l_{\text{ext}}} \right] |p_{f_{[1]}}^{\text{ext}}|^{2a} \\ &\times e^{-\alpha_{l_{\text{ext}1}} [\sum_\xi (|p_{f_{[1]}}^{\text{ext}}|^{2\xi} + |p_{f_2}^{\text{ext}}|^{2\xi} + \dots + |p_{f_d}^{\text{ext}}|^{2\xi}) + \mu]} e^{-\alpha_{l_{\text{ext}2}} [\sum_\xi (|p_{f_{1'}}^{\text{ext}}|^{2\xi} + |p_{f_2}^{\text{ext}}|^{2\xi} + \dots + |p_{f_d}^{\text{ext}}|^{2\xi}) + \mu]} \end{aligned}$$

$$\times e^{-\alpha_{l_{\text{ext}3}} [\sum_{\xi} (|p_{f_{1'}}^{\text{ext}}|^{2\xi} + |p_{f_{2'}}^{\text{ext}}|^{2\xi} + \dots + |p_{f_{d'}}^{\text{ext}}|^{2\xi}) + \mu]} e^{-\alpha_{l_{\text{ext}4}} [\sum_{\xi} (|p_{f_{[1]}}^{\text{ext}}|^{2\xi} + |p_{f_{2'}}^{\text{ext}}|^{2\xi} + \dots + |p_{f_{d'}}^{\text{ext}}|^{2\xi}) + \mu]} . \quad (103)$$

Observe that the above expression describes 4 propagators glued in a way to produce the pattern of a vertex of type  $\mathbf{V}_{+,4;1}$ . The term associated with the sum over internal momenta is log-divergent. Therefore, the amplitude  $A_4(\{p_f^{\text{ext}}\}; 0)$  will renormalize the coupling  $\eta_+$ .

We now prove that the remainders appearing in (101) lead to convergence by improving the power counting. The first remainder calling a single term  $R_f$  is of the form:

$$\begin{aligned} R_4 &= \kappa(\eta_+) \sum_{p_f} \int \left[ \prod_l d\alpha_l e^{-\alpha_l \mu} \right] |p_{f_{[1]}}^{\text{ext}}|^{2a} \left[ \prod_{f \in \mathcal{F}_{\text{ext}}} e^{-(\alpha_{l_{\text{ext}}} + \alpha_{l_{\text{ext}'})} \sum_{\xi} |p_f^{\text{ext}}|^{2\xi} \right] \\ &\times \left[ - \sum_{f \in \mathcal{F}_{\text{ext}}} \left( \sum_{\ell \in f} \alpha_{\ell} \right) \left( \sum_{\xi} |p_f^{\text{ext}}|^{2\xi} \right) \int_0^1 e^{-t(\sum_{\ell \in f} \alpha_{\ell}) \sum_{\xi} |p_f^{\text{ext}}|^{2\xi}} dt \right] \\ &\times \left[ \prod_{f \in \mathcal{F}_{\text{int}}} e^{-(\sum_{\ell \in f} \alpha_{\ell}) \sum_{\xi} |p_f|^{2\xi}} \right] \prod_{s=1}^d \prod_{v_s \in \mathcal{V}_{+,4;s}} [(\epsilon \tilde{p}^{2a})_{v_s}]. \end{aligned} \quad (104)$$

Using  $i(G_k^i) = \inf_{\ell \in G_k^i} i_{\ell}$  and  $e(G_k^i) = \sup_{\ell \in G_k^i} j_{\ell}$ , and recalling  $\alpha_{\ell} \in [M^{-(2b)i_{\ell}}, M^{-(2b)(i_{\ell}-1)}]$  and  $\alpha_{l_{\text{ext}}} \in [M^{-(2b)j_{l_{\text{ext}}}}, M^{-(2b)(j_{l_{\text{ext}}}-1)}]$ ,  $(\sum_{\ell \in f} \alpha_{\ell}) |p_f^{\text{ext}}|^{2b} \leq k_0 M^{-(2b)(i(G_k^i) - e(G_k^i))}$ , then  $R_4$  is bounded as,

$$|R_4| \leq K \prod_{(i,k)} M^{-(2b)(i(G_k^i) - e(G_k^i))} M^{\omega_{d;+}(G_k^i)}, \quad (105)$$

for some constant  $K$  (which includes  $\kappa(\eta_+)$  and  $k_0$ , a constant depending on the graph and a constant which bounds the integral in  $t$ ). The factor  $M^{-(2b)(i(G_k^i) - e(G_k^i))}$  improves the power counting (which is already logarithmic) and will be the source of decay to show that the sum over scale attributions is convergent in the way established in [122]. Inspecting the higher order products in  $R_f$ 's, one realizes that they are obviously more convergent and so do not need further discussion.

If we remove  $|p_{f_{[1]}}^{\text{ext}}|^{2a}$  from the amplitude (99), we will be in presence of an amplitude coming from (97). The boundary data of the resulting amplitude will be of the form  $\mathbf{V}_{4;1}$ . Repeating step by step the previous analysis, we obtain at 0-th order of the expansion a renormalization of the coupling  $\lambda$  and all remainders will lead exactly to the same convergence with power counting given by (105). It is direct to see that the argument extends to any color  $s$ .

As a result of this analysis, we can comment that, although the renormalized coupling  $\lambda$  does not receive any melonic corrections, it receives contributions from the coupling  $\eta_+$ . This is a new property of the perturbative Renormalization Group equations of this model.

**Renormalization of divergent 2-point functions.** We study 2-point functions that obey  $\omega_{d;+}(\mathcal{G}) = 0, \frac{D}{2}$  and characterized by the rows I through VI of Table 4. First, we will focus on the row I and point out the differences with II and III at particular steps of the discussion. We will sketch the analysis for the rows IV, V and VI.

A 2-point graph has a unique boundary which is given by the invariant  $\text{Tr}_2(\phi^2)$  of Figure 2. Because the vertices are enhanced, it may happen that the external data of a two-point



graph is not of the form of a mass term, but rather a form of  $CT_{2;a}$ . A careful discussion will be made about this in the text.

Consider an amplitude  $A_2(\{p_f^{\text{ext}}\})$  associated with a 2-point graph obeying the row I of Table 4. This graph has  $d$  external faces that we label by

$$f \in \mathcal{F}_{\text{ext}} = \{f_1, f_2, \dots, f_d\}.$$

Keeping the same notations as above (see paragraph after (99)),  $l_{\text{ext}}$  labels external propagators with scale index  $j_{l_{\text{ext}}}$ ,  $\ell$  labels internal lines with scale index  $i_\ell$ .

A Taylor expansion of the external face factors out in the same form as (100) and leads us to the following expansion of the 2-point amplitude:

$$\begin{aligned} A_2(\{p_f^{\text{ext}}\}) &= \kappa(\eta_+) \sum_{p_f} \int [\prod_l d\alpha_l e^{-\alpha_l \mu}] \left[ \prod_{f \in \mathcal{F}_{\text{ext}}} e^{-(\alpha_{l_{\text{ext}}} + \alpha_{l_{\text{ext}}'}) \sum_\xi |p_f^{\text{ext}}|^{2\xi}} \right] \\ &\times \left[ 1 - \sum_{f \in \mathcal{F}_{\text{ext}}} R_f + \sum_{f, f' \in \mathcal{F}_{\text{ext}}} R_f R_{f'} + \dots \right] \left[ \prod_{f \in \mathcal{F}_{\text{int}}} e^{-(\sum_{\ell \in f} \alpha_\ell) \sum_\xi |p_f|^{2\xi}} \right] \left[ \prod_{s=1}^d \prod_{v_s \in \mathcal{V}_{+;4;s}} [(\epsilon \tilde{p}^{2a})_{v_s}] \right]. \end{aligned} \quad (106)$$

The 0th order term in the expansion in  $R_f$ ,

$$\begin{aligned} A_2(\{p_f^{\text{ext}}\}; 0) &= \kappa(\eta_+) \sum_{p_f} \int [\prod_l d\alpha_l e^{-\alpha_l \mu}] \\ &\times \left[ \prod_{f \in \mathcal{F}_{\text{ext}}} e^{-(\alpha_{l_{\text{ext}}} + \alpha_{l_{\text{ext}}'}) \sum_\xi |p_f^{\text{ext}}|^{2\xi}} \right] \prod_{f \in \mathcal{F}_{\text{int}}} \left[ e^{-(\sum_{\ell \in f} \alpha_\ell) \sum_\xi |p_f|^{2\xi}} \right] \prod_{s=1}^d \prod_{v_s \in \mathcal{V}_{+;4;s}} [(\epsilon \tilde{p}^{2a})_{v_s}] \\ &= \kappa(\eta_+) \left[ \int [\prod_{l_{\text{ext}}} d\alpha_{l_{\text{ext}}}] e^{-\alpha_{l_{\text{ext}1}} [\sum_\xi (\sum_s |p_{f_s}^{\text{ext}}|^{2\xi}) + \mu]} e^{-\alpha_{l_{\text{ext}2}} [\sum_\xi (\sum_s |p_{f_s}^{\text{ext}}|^{2\xi}) + \mu]} \right] \\ &\times \left[ \sum_{p_f} \int [\prod_\ell d\alpha_\ell e^{-\alpha_\ell \mu}] \prod_{f \in \mathcal{F}_{\text{int}}} \left[ e^{-(\sum_{\ell \in f} \alpha_\ell) \sum_\xi |p_f|^{2\xi}} \right] \left[ \prod_{s=1}^d \prod_{v_s \in \mathcal{V}_{+;4;s}} (\epsilon \tilde{p}^{2a})_{v_s} \right] \right]. \end{aligned} \quad (107)$$

Let us discuss the vertex density. A graph fulfilling the requirements of the row I of Table 4, must be such that  $\rho_+ = V_{+;4}$ . The same argument as in the case of 4-point functions applies: there are no external momenta in the product of vertex kernels and all momenta will be summed. The first factor involving external momenta represents two propagators glued together by a degree-2 vertex; the second factor gives by our power counting a degree of divergence  $\frac{D}{2}$ . Hence the term (107) renormalizes the mass term.

Concerning a graph satisfying the rows II and III, we know that  $\rho_+ = V_{(4)} - 1$  and that the graph is melonic. Lemma 3 explained in its proof that for 1PI melonic graphs, external legs must be hooked on partner vertices. Hence a 2-point primitively divergent (1PI) melonic graph has at least a vertex  $v_{0;s}$  which will not contribute to  $\rho_+$ . Two cases might occur:

(II) The vertex  $v_{0;s}$  must belong to  $\mathcal{V}_{+;4;s}$ , then an extra factor of  $|p_{f_s}^{\text{ext}}|^{2a}$  must be added to the boundary data. This makes that graph of the form of  $\mathcal{V}_{2;a;s}$ . Now, adding all colored symmetric contribution with respect to  $s$  of this graph term renormalizes the coupling  $Z_a$ ;

(III) The vertex  $v_{0;s}$  must belong to  $\mathcal{V}_4$ , then the boundary data is that of a mass and so (107) again renormalizes the mass term.

The remainders of (106) are now treated for the row I of our table. The first order remainder involving the sum  $\sum_f R_f$  can be bounded as follows

$$\begin{aligned}
R_2 &= -\kappa(\eta_+) \left[ \int \left[ \prod_{l_{\text{ext}}} d\alpha_{l_{\text{ext}}} e^{-\alpha_{l_{\text{ext}}} \mu} \right] \prod_{f \in \mathcal{F}_{\text{ext}}} e^{-(\alpha_{l_{\text{ext}}} + \alpha_{l_{\text{ext}}'}) \sum_{\xi} |p_f^{\text{ext}}|^{2\xi}} \right] \\
&\times \sum_{f \in \mathcal{F}_{\text{ext}}} \left[ \int \left[ \prod_{\ell} d\alpha_{\ell} e^{-\alpha_{\ell} \mu} \right] \left( \sum_{\ell \in f} \alpha_{\ell} \right) \left( \sum_{\xi} |p_f^{\text{ext}}|^{2\xi} \right) \int_0^1 e^{-t(\sum_{\ell \in f} \alpha_{\ell}) \sum_{\xi} |p_f^{\text{ext}}|^{2\xi}} dt \right] \\
&\times \sum_{p_f} \prod_{f \in \mathcal{F}_{\text{int}}} \left[ e^{-(\sum_{\ell \in f} \alpha_{\ell}) \sum_{\xi} |p_f|^{2\xi}} \right] \prod_{s=1}^d \prod_{v_s \in \mathcal{V}_{+;4;s}} [(\epsilon \tilde{p}^{2a})_{v_s}] \\
|R_2| &\leq K \prod_{(i,k)} M^{-2b(i(G_k^i) - e(G_k^i))} M^{\omega_{d,+}(G_k^i) = \frac{D}{2}}, \tag{108}
\end{aligned}$$

where we used the same scheme leading to (105), for some constant  $K$ . For a constant  $C \geq 1$ ,  $-D(d^- - \frac{1}{2})C + \frac{D}{2} \leq -D(d^- - 1) \leq -D < 0$  ensures the convergence of the remainder. All higher order remainders can be proved more convergent. From this point, the summation over scale attributions can be again performed after subtractions. The case of an amplitude of the rows II and III of the table can be addressed in similar way.

Let us now discuss the rows IV, V, and VI. In these cases,  $\rho_{2;a} = 1 = V_{2;a}$  which means that the enhanced momenta  $|p_{f_s}|^{2a}$  associated with the vertex which is counted in  $V_{2;a} = 1$  is necessarily integrated. Hence the analysis of the rows IV, V, and VI are completely similar to what we have done for the rows I, II, and III, respectively. As a last remark, we stress that there are no corrections to the wave function  $Z_b$  because all amplitudes at first order are already convergent. Hence we can put the coupling  $Z_b$  to 0.

In conclusion,

- the expansion of marginal 4-point functions around their local part gives a log-divergent terms which renormalize the coupling constants  $\eta_+$  or  $\lambda$ .
- the expansion of  $\frac{D}{2}$ -divergent or log-divergent 2-point graphs around their local parts yield a  $\frac{D}{2}$ -divergent or log-divergent term renormalizing either the mass or  $Z_a$ ;
- all remainders are convergent and will bring enough decay for ensuring the final summability over scale attributions. From this point, the procedure for performing this last sum over attributions is standard and will secure the renormalization at all orders of perturbation theory according to techniques developed in [122]. Thus, Theorem 1 holds.

## 7 A rank $d = 3$ renormalizable model $\times$

We adopt the same strategy as in the previous section, to prove the renormalizability of a model  $\times$ . After listing its primitively divergent connected graphs, we proceed with the renormalization procedure. The same conditions  $C_{\partial\mathcal{G}} \geq 1$  and  $N_{\text{ext}}$  even must be true.

## 7.1 List of divergent graphs

We are interested in a rank  $d = 3$  model  $\times$  with  $a = \frac{1}{2}$ ,  $b = 1$  and  $D = 1$ . This choice  $b = 1$  gives a Laplacian in the kinetic term, and an integer power of the interaction  $|p|\phi^4$ , thus this model seems natural (that we can think as a single derivative coupling). The interactions are of the same form as given in Figure 5 with the sole difference that we enhance by a product of  $|p|$  both edges in the melonic interaction.

We start from (77) and (78), the superficial degree of divergence for generic graphs:

$$\omega_{d;\times}(\mathcal{G}^{\text{melon}}) \leq -(C_{\partial\mathcal{G}} - 1) - \frac{1}{2}(2N_{\text{ext}} - 4) - 2V_2 - V_{2;a} - \Delta_{\times}^{\text{melon}}, \quad (109)$$

$$\omega_{d;\times}(\mathcal{G}^{\text{non-melon}}) \leq -1 - (C_{\partial\mathcal{G}} - 1) - \frac{1}{2}(N_{\text{ext}} - 4) - 2V_2 - V_{2;a} - \Delta_{\times}^{\text{non-melon}}. \quad (110)$$

We observe that both counter-terms  $CT_{2;2a}$  and  $CT_{2;b}$  disappear from the power counting. As degree-2 vertices, they are neutral for the power counting.

Our previous analysis shows that, for any  $N_{\text{ext}} \geq 4$ , the amplitude is convergent. We concentrate on the remaining case  $N_{\text{ext}} = 2$ . From Lemma 4, we can still combine the analysis of  $V_{(4)} = 1$  and  $V_{(4)} > 1$  at  $N_{\text{ext}} = 2$  and have

$$\begin{aligned} \omega_{d;\times}(\mathcal{G}^{\text{melon}}) &\leq -(C_{\partial\mathcal{G}} - 1) - 2V_2 - V_{2;a} - \Delta_{\times}^{\text{melon}} \leq 0, \\ \omega_{d;\times}(\mathcal{G}^{\text{non-melon}}) &\leq -(C_{\partial\mathcal{G}} - 1) - 2V_2 - V_{2;a} - \Delta_{\times}^{\text{non-melon}} \leq 0. \end{aligned} \quad (111)$$

The only way to achieve logarithmic divergence is to have exactly:  $C_{\partial\mathcal{G}} = 1$ ,  $V_2 = 0 = V_{2;a}$ . For a non-melonic graph, we further impose  $\Delta_{\times}^{\text{non-melon}} = 0$  from which we infer  $\rho_{\times} = 2V_{(4)} - 1$ . Knowing that  $\rho_{\times} \leq 2V_{\times;4}$ , this leads us to  $(\rho_{\times} = 2V_{\times;4} - 1; V_4 = 0)$ . The case of a melonic graph yields  $\Delta_{\times}^{\text{melon}} = 0$  which gives  $\rho_{\times} = 2V_{(4)} - 2$ , which together with  $\rho_{\times} \leq 2V_{\times;4}$  yields two possibilities: either  $(\rho_{\times} = 2V_{\times;4}; V_4 = 1)$  or  $(\rho_{\times} = 2V_{\times;4} - 2; V_4 = 0)$ .

We have the following proposition.

**Proposition 2** (List of primitively divergent graphs for model  $\times$ ). *The  $p^{2a}\phi^4$ -model  $\times$  with parameters  $D = 1, d = 3, a = \frac{1}{2}, b = 1$ , has the following primitively divergent graphs which obey  $(\Omega(\mathcal{G}) = \omega(\mathcal{G}_{\text{color}}) - \omega(\partial\mathcal{G}))$*

$\mathcal{G}$	$N_{\text{ext}}$	$V_2$	$V_{2;a}$	$V_4$	$\rho_{\times}$	$C_{\partial\mathcal{G}} - 1$	$\Omega(\mathcal{G})$	$\omega_d(\mathcal{G})$
I	2	0	0	0	$2V_{\times;4} - 1$	0	1	0
II	2	0	0	0	$2V_{\times;4} - 2$	0	0	0
III	2	0	0	1	$2V_{\times;4}$	0	0	0

Table 5: List of primitively divergent graphs of the  $p^{2a}\phi^4$ -model  $\times$ .

In appendix C, we have illustrated an infinite family of 2-point graphs with log-divergent amplitudes, see Figures 9, 10 and 11. Thus, this theory is not super-renormalizable in the usual sense because it possesses an infinite family of corrections to the mass,  $Z_a$  and  $Z_{2a}$  couplings. It does not also fit the definition of a just-renormalizable theory because all

corrections of the coupling  $\lambda$  and  $\eta_\times$  are finite. Again this is a specific feature brought by the enhancement of non-local tensor interactions.

With the above analysis, we can now prove that the following theorem holds.

**Theorem 2.** *The  $p^{2a}\phi^4$  model  $\times$  with parameters  $D = 1, d = 3, a = \frac{1}{2}, b = 1$ , with action defined by (2) is renormalizable at all orders of perturbation.*

## 7.2 Renormalization

We follow a similar scheme as developed in section 6.2. We sketch the expansion of amplitudes of the graphs listed in Table 5 and check that their local parts indeed take the form of the terms in the Lagrangian of the model  $\times$  of section 7.1. Doing a Taylor expansion the amplitudes, we will also show that the subleading orders are convergent.

**Renormalization of divergent 2-point functions.** In the model  $\times$ , we only have 2-point log-divergent graphs as listed in Table 5. For type I and II graphs, note that  $\rho_\times < 2V_{\times;4}$ , therefore one or two edges of their boundary graph are touched by external faces which are enhanced. This entails that the boundaries of these graphs are equipped with  $|p_{f[1]}^{\text{ext}}|^{2a}$  and  $|p_{f[1]}^{\text{ext}}|^{4a}$  and therefore of the form of  $CT_{2;a}$ ,  $CT_{2;2a}$ , respectively. On the other hand, for a log-divergent graph of the type III, we have  $\rho_\times = 2V_{\times;4}$  and its boundary graph does not have any enhanced edges and so takes the form of the mass term.

In the following, we only address the 2-point graphs of type I and II and will give the main points leading to the treatment of type III graphs.

Let us consider the amplitude  $A_2(\{p_f^{\text{ext}}\})$  of 2-point non-melonic and melonic graphs obeying, respectively, the rows I and II of Table 5. These graphs have 3 external faces labeled by  $f \in \mathcal{F}_{\text{ext}} = \{f_{[1]}, f_2, f_3\}$ , with an enhanced color 1 strand. By an argument of symmetry, our following study will give the same result for a graph with another enhanced color.

We perform a Taylor expansion of external face factors as given in (100) and the amplitude  $A_2(\{p_f^{\text{ext}}\})$  takes a similar form as (106); we replace  $\kappa(\eta_+)$  with  $\kappa(\eta_\times)$  and have extra term  $|p_{f[1]}^{\text{ext}}|^{2\xi}$  present, where  $\xi = a$  for the type I and  $\xi = 2a$  for type II graph. Then the 0th order term in the expansion in  $R_f$  expresses as

$$\begin{aligned} A_2(\{p_f^{\text{ext}}\}; 0) &= \kappa(\eta_\times) \left[ \int \left[ \prod_{l_{\text{ext}}} d\alpha_{l_{\text{ext}}} \right] |p_{f[1]}^{\text{ext}}|^{2\xi} \right. \\ &\times e^{-\alpha_{l_{\text{ext}1}} \sum_\xi (|p_{f[1]}^{\text{ext}}|^{2\xi} + |p_{f_2}^{\text{ext}}|^{2\xi} + |p_{f_3}^{\text{ext}}|^{2\xi} + \mu)} e^{-\alpha_{l_{\text{ext}2}} \sum_\xi (|p_{f[1]}^{\text{ext}}|^{2\xi} + |p_{f_2}^{\text{ext}}|^{2\xi} + |p_{f_3}^{\text{ext}}|^{2\xi} + \mu)} \left. \right] \\ &\times \left[ \sum_{p_f} \int \left[ \prod_\ell d\alpha_\ell e^{-\alpha_\ell \mu} \right] \prod_{f \in \mathcal{F}_{\text{int}}} \left[ e^{-(\sum_\ell \alpha_\ell) \sum_\xi |p_f|^{2\xi}} \right] \left[ \prod_{s=1}^d \prod_{v_s \in \mathcal{V}_{\times;4;s}} (\epsilon \tilde{p}^{2a})_{v_s} \right] \right]. \quad (112) \end{aligned}$$

It is explicit here from the pattern of the external data, that this amplitude takes the form of the  $CT_{2;\xi}$  term. We identify then the factor associated with the internal data as having a degree of divergence  $\omega_{d;\times} = 0$ , given by our power counting analysis in section 7.1. Adding all colored symmetric contribution with respect to  $s$  of this graph, the sum of these amplitudes renormalizes the coupling  $Z_\xi$ .

We now treat the higher orders in the Taylor expansion in the form  $\sum_f R_f$  of  $A_2(\{p_f^{\text{ext}}\})$ . The first order remainder involving the sum  $\sum_f R_f$  can be bounded in the same vein as (108) and we find

$$|R_2| \leq K \prod_{(i,k)} M^{-2b(i(G_k^i) - e(G_k^i))} M^{\omega_{d,+}(G_k^i)=0}, \quad (113)$$

for some constant  $K$ . We are guaranteed of the convergence of this remainder, and that all higher order remainders can be shown more convergent. We are ensured about the summability over scale attributions in this case.

For the log-divergent graphs III, the analysis is similar except that we do not have extra external momenta contributions  $|p_{f[1]}^{\text{ext}}|^{2\xi}$  appearing, as discussed earlier.

We conclude that,

- the expansion of log-divergent 2-point graphs around their local parts yield log-divergent terms renormalizing  $Z_a$ ,  $Z_{2a}$  and the mass.

- all remainders are convergent and bring a sufficient decay for ensuring the summability over scale attribution. This means that renormalization at all orders of perturbation theory according to [122] can be achieved. Therefore, we conclude that Theorem 2 holds.

- there is no wave function renormalization associated with  $Z_b$  for the model  $\times$  because all amplitudes at the leading order are already convergent.

Without much work, we observe that several other models listed in Table 3 are renormalizable at  $d = 3$ , just like the present model is (up to a change of (109), (110), (111), Table 5 and (113)). More surprising perhaps, at fix  $D$ , we even suspect that it might have a continuum of renormalizable theories for a range of values of  $b$ .

## 8 Conclusion

We have addressed the perturbative (at all orders) multi-scale renormalization analysis of the so-called enhanced quartic melonic tensor field theory at any rank  $d$  of the tensor fields and for any group  $(U(1)^D)^d$ . Studied in the momentum space, the models are endowed with powers of momenta in the interaction terms which are roughly of the form  $p^{2a}\phi^4$ ,  $a > 0$ , and which might be associated with derivative couplings. The case  $a = 0$  being well-studied in the literature can be recovered at this limit. Through the enhancing procedure, amplitudes which were suppressed in models at  $a = 0$  now participate in the analysis at  $a > 0$ .

In order to achieve renormalizability in enhanced models, the propagators need a more general form than the usual Laplacian dynamics: we thus assume the propagators to be of the form  $(\sum_\xi |p|^{2\xi} + \mu)^{-1}$ ,  $\xi = a, 2a, b$  strictly positive. Two types of models were introduced and studied in parallel in this work: an asymmetric model  $+$  and a symmetric model  $\times$ . From the multi-scale analyses of these models, we identify new combinatorial quantities which allow us to write down a power counting theorem in terms of quasi-local subgraphs. At any rank  $d > 2$ , group dimension  $D \geq 1$ , we have found intervals of values for  $a$  and  $b$  for which both models are potentially renormalizable at all orders of perturbation theory. Let us give a summary of the particularities of each model.

For arbitrary  $d$  and  $D$ , which specify the rest of the parameters, we find a two-dimensional grid  $((\mathbb{N} - \{0, 1, 2\}) \times (\mathbb{N} - \{0\}))$  of just-renormalizable models  $+$ . As expected, the amplitudes

of non-melonic diagrams start to contribute to the flow and dominate the melonic amplitudes in each model. In fact, all the 4-point melonic diagrams become convergent. We found that the enhanced coupling  $\eta_+$  will contribute to the flow of the melonic coupling  $\lambda$  whereas the opposite is not possible. Introducing enhanced interactions of  $\text{Tr}_4(p^{2a}\phi^4)$  influences the study of the 2-point function as it requires to introduce a particular counter-term of the form  $\text{Tr}_2(p^{2a}\phi^2)$ .

The model  $\times$  is also renormalizable for a tuned set of parameters. Again, melonic and non-melonic amplitudes can be of the same divergence degree, as expected with enhanced interactions. However, something puzzling happens in this model: all 4-point amplitudes prove to be finite and only 2-point amplitudes may diverge. There are infinitely many 2-point divergent amplitudes. The detailed study of the 2-point graphs imposes us to include two counter-terms for removing all divergences:  $\text{Tr}_2(p^{2a}\phi^2)$  and  $\text{Tr}_2(p^{4a}\phi^2)$ . Thus, the flow of this model is uniquely driven by 2-point functions. Then, the model belongs neither to the class of just-renormalizable models nor to the class of super-renormalizable models in the language of usual QFT. We conjecture that there are several other renormalizable models of this kind.

We recall that enhanced tensor models are introduced from attempts to escape the branched polymer phase of colored tensor models. If enhanced tensor models are turned into field theories, then the large  $N$ -limit becomes the UV-limit (large  $p$ ). As far as the present study is concerned, the perturbative renormalizability of the enhanced models of the type presented here might not immediately tell us anything about new limits or new phases of these enhanced models. Having renormalizability rather ensures us that the field theory counterparts of these models are long-lived, defined through several layers of momentum scales, and might be UV-complete. This is definitely an important and encouraging point to keep up with their study.

Another important aim that could be certainly reached from our analysis is the computation of the perturbative  $\beta$ -functions for these models. There are several arguments putting forward that ordinary  $\phi^4$  tensor field theories are perturbatively asymptotically free [47, 93]. The main ingredient leading to asymptotic freedom is the presence of a wave-function renormalization which dominates the renormalized coupling constant. Nevertheless, the models addressed in this paper seem to belong to another class, simply because of the presence of the several couplings  $Z_\xi$ ,  $\xi = a, 2a$ , and the fact that  $Z_b$  does not get any radiative corrections. For the model  $+$ , we realize that the RG equations might be more involved than one might think because of the number of couplings in the theory. Thus, only careful computations of the  $\beta$ -functions of this model could help to understand the UV-behaviour of the model  $+$ .

Beyond perturbation, non-perturbative properties of these models can be sought in the future. In particular, the next steps of the program for enhanced models would be to find UV and IR fixed points which may exist and, from these, perhaps complete trajectories from the UV to the IR. The proof of the perturbative renormalizability is again encouraging for this next level. The FRG approach has been applied to ordinary tensor field theories with interesting results. Extending the methods to the enhanced theory space is again to be done. In particular, if one shows the existence of stable IR fixed points in enhanced tensor field theories, it could give them a firmer underpinning as interesting candidates undergoing a phase transition from discrete-like geometries to some condensate-like geometry.

## Acknowledgements

The research of RT is supported by the Netherlands Organisation for Scientific Research (NWO) within the Foundation for Fundamental Research on Matter (FOM) grant 13VP12. RT thanks Max Planck Institute for Gravitational Physics, Potsdam-Golm (Albert Einstein Institute) for their hospitality while this work was in progress. JBG thanks the Laboratoire de Physique Théorique d'Orsay, Université Paris 11, for its hospitality.

## Appendix

### A Spectral sums

In this appendix, we perform spectral sums over internal momenta. We start from a basic sum and will go for more involved cases in dimension  $D$ . In the following, we use  $B > 0$  as a parameter, and in the text,  $B = M^{-i_l}$ . Targeting upper bounds on  $B^\alpha$ , we focus on the terms with  $\alpha < 0$ .

Noting that for constants  $B > 0$ ,  $a > 0$  and  $b > 0$ , a single sum over a  $p_{s,l}$  behaves like

$$\sum_{p=1}^{\infty} p^a e^{-Bp^b} = kB^{-\frac{(a+1)}{b}} (1 + O(B^{\frac{(a+1)}{b}})), \quad (\text{A.1})$$

where  $k$  is an  $a$ -dependent constant. This relation has been proved for instance in appendix A of [93]. This sum can be generalized as

$$\begin{aligned} \sum_{p=1}^{\infty} p^a e^{-B(p^b+p^c)} &= \sum_{n=0}^{\infty} \frac{(-B)^n}{n!} \sum_{p=1}^{\infty} p^{a+cn} e^{-Bp^b} \\ &= k \sum_{n=0}^{\infty} \frac{(-B)^n}{n!} B^{-\frac{(a+cn+1)}{b}} (1 + O(B^{\frac{(a+cn+1)}{b}})) \\ &= kB^{-\frac{(a+1)}{b}} e^{-B^{1-\frac{c}{b}}} (1 + O(B^{\frac{(a+1)}{b}}) + B^{(1-\frac{c}{b})} O(B^{\frac{(a+c+1)}{b}}) + B^{2(1-\frac{c}{b})} O(B^{\frac{(a+2c+1)}{b}})) \\ &= kB^{-\frac{(a+1)}{b}} e^{-B^{1-\frac{c}{b}}} (1 + O(B^{\frac{(a+1)}{b}})), \end{aligned} \quad (\text{A.2})$$

where we use (A.1) at an intermediate step. For the specific choice  $c \leq b$ , such that  $1 - \frac{c}{b} \geq 0$  the previous result recasts as

$$\sum_{p=1}^{\infty} p^a e^{-B(p^b+p^c)} = kB^{-\frac{(a+1)}{b}} (1 + O(B^{1-\frac{c}{b}})). \quad (\text{A.3})$$

It is not difficult then to use the same routine and get, for  $c + d \leq 2b$ ,

$$\sum_{p=1}^{\infty} p^a e^{-B(p^b+p^c+p^d)} = \sum_{m,n=0}^{\infty} \frac{(-B)^{n+m}}{n!m!} \sum_{p=1}^{\infty} p^{a+cn+dm} e^{-Bp^b}$$

$$\begin{aligned}
&= k \sum_{m,n=0}^{\infty} \frac{(-B)^{n+m}}{n!m!} B^{-\frac{(a+cn+dm+1)}{b}} (1 + O(B^{\frac{(a+cn+dm+1)}{b}})) \\
&= kB^{-\frac{(a+1)}{b}} e^{-B^{2-\frac{(c+d)}{b}}} (1 + O(B^{\frac{(a+1)}{b}})) = kB^{-\frac{(a+1)}{b}} (1 + O(B^{2-\frac{(c+d)}{b}})). \quad (\text{A.4})
\end{aligned}$$

Note that if the above calculations were approximated at  $c \leq b$ , using  $e^{-B(p^b+p^c)} \leq e^{-2Bp^c}$  and, if  $c \leq d \leq b$ ,  $e^{-B(p^b+p^c+p^d)} \leq e^{-3Bp^c}$ , the sum behavior could change (using (A.1) with a modified  $B$ ). Hence using this bounds is not the optimal choice.

We will need a companion sum in dimension  $D$ :

$$\begin{aligned}
&\sum_{p_1, \dots, p_D=1}^{\infty} \left( \sum_{l=1}^D p_l^a \right)^n e^{-B(\sum_{l=1}^D p_l^b)} = \sum_{\sum_i n_i=n} \frac{n!}{\prod_{l=1}^D n_l!} \sum_{p_1, \dots, p_D=1}^{\infty} \prod_{l=1}^D p_l^{an_l} e^{-Bp_l^b} \\
&= c' \sum_{\sum_i n_i=n} \frac{n!}{\prod_{l=1}^D n_l!} B^{-\frac{\sum_l (an_l+1)}{b}} \prod_{l=1}^D (1 + O(B^{\frac{(an_l+1)}{b}})) = c' B^{-\frac{(an+D)}{b}} (1 + O(B^{\frac{1}{b}})), \quad (\text{A.5})
\end{aligned}$$

where  $c' = c^{D2^n}$ . We extend this computation, in the case of multiple powers in the exponential, with  $c \leq b$ :

$$\begin{aligned}
&\sum_{p_1, \dots, p_D=1}^{\infty} \left( \sum_{l=1}^D p_l^a \right)^n e^{-B \sum_{l=1}^D (p_l^b + p_l^c)} = \\
&c' \sum_{\sum_i n_i=n} \frac{n!}{\prod_{l=1}^D n_l!} B^{-\frac{\sum_l (an_l+1)}{b}} e^{-B^{1-\frac{c}{b}}} \prod_{l=1}^D (1 + O(B^{\frac{(an_l+1)}{b}})) \\
&= c' B^{-\frac{(an+D)}{b}} e^{-B^{1-\frac{c}{b}}} (1 + O(B^{\frac{1}{b}})) = c' B^{-\frac{(an+D)}{b}} (1 + O(B^{\frac{1}{b}}) + O(B^{1-\frac{c}{b}})), \quad (\text{A.6})
\end{aligned}$$

where (A.2) and (A.3) have been used. Depending on  $b - c \leq 1$  or otherwise, the two big-O functions can be reduced into one. However, being interested in the leading order, this relation is sufficient to proceed further. Using the same techniques, the last useful sum evaluates as

$$\begin{aligned}
&\sum_{p_1, \dots, p_D=1}^{\infty} \left( \sum_{l=1}^D p_l^a \right)^n e^{-B(\sum_{l=1}^D (p_l^b + p_l^c + p_l^d))} = c' B^{-\frac{(an+D)}{b}} e^{-B^{2-\frac{(c+d)}{b}}} (1 + O(B^{\frac{1}{b}})) \\
&= c' B^{-\frac{(an+D)}{b}} (1 + O(B^{\frac{1}{b}}) + O(B^{2-\frac{(c+d)}{b}})), \quad (\text{A.7})
\end{aligned}$$

where the last equality is obtained for  $c + d \leq 2b$ .

## B Divergences in model + ( $d = 3, D = 1, a = \frac{1}{2}, b = \frac{3}{4}$ )

We consider here a specific model + with parameter given as  $d = 3, D = 1, a = \frac{1}{2}, b = \frac{3}{4}$ . The mass term and interactions are of the form given in Figure 5.



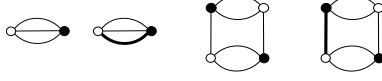


Figure 5: Rank  $d = 3$ , mass, enhanced  $\phi^2$ -interaction, and (simple and enhanced)  $\phi^4$ -interactions.

In this appendix, we illustrate graphs which satisfy the power counting achieved in Table 4 in section 6.1.

The superficial degree of divergence of a graph  $\mathcal{G}$  is given in (44) that we specialize for  $D = 1$ ,  $a = \frac{1}{2}$ , and  $b = \frac{3}{4}$  as

$$\omega_{d,+}(\mathcal{G}) = -\frac{3}{2}L + F_{\text{int}} + \rho_+ + \rho_{2;a} + \frac{3}{2}\rho_{2;b}. \quad (\text{B.8})$$

We use the bipartite colored graph representation of the Feynman graphs of the model. Edges which are dashed are propagators; edges in the interaction vertex can be in bold or not. If they are in bold that means that they receive an enhancement factor of  $p^{2a}$ . The figures illustrating graphs have red lines that facilitate the identification of the face structure of the graphs. Given a colored graph, we emphasize a red cycle (made with alternating edges and dashed edges with red color) that indicates a particular closed face. Naturally, this face will be the source of an enhanced power counting if it contains a bold edge.

We only list here some divergent graphs contributing to the renormalization of the interactions.

(i) We consider 2-point functions,  $N_{\text{ext}} = 2$ .

(i1) We consider  $V_{(4)} = 1$  or divergent tadpoles given in Figure 6. The graphs a and b are melonic with  $V_{(4)} = 1$ ,  $\rho_+ + \rho_{2;a} + \frac{3}{2}\rho_{2;b} = 0$ , and  $\omega_{d,+} = \frac{1}{2}$ , whereas the graph c is non-melonic with  $V_{+,4} = 1$ ,  $\rho_+ = 1$ ,  $\rho_{2;a} + \frac{3}{2}\rho_{2;b} = 0$  and  $\omega_{d,+} = \frac{1}{2}$ . The graphs d and e with  $V_{(4)} = 1$  and  $V_{2;a} = 1$ ,  $\rho_+ + \frac{3}{2}\rho_{2;b} = 0$ ,  $\rho_{2;a} = 1$  are melonic and log-divergent with  $\omega_{d,+} = 0$ ; the graph f is non-melonic with  $V_{+,4} = 1$ ,  $V_{2;a} = 1$ ,  $\rho_+ = 1 = \rho_{2;a}$ ,  $\rho_{2;b} = 0$ , and also log-divergent with  $\omega_{d,+} = 0$ .

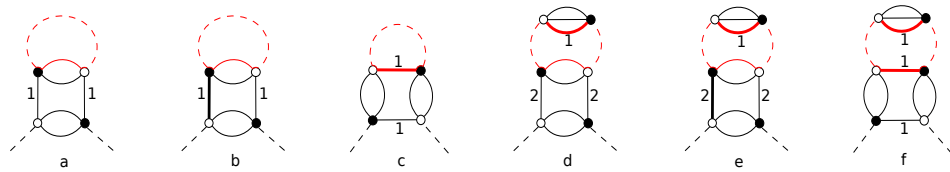


Figure 6: Divergent graphs with  $N_{\text{ext}} = 2$  and  $V_{(4)} = 1$ .

(i2) We consider  $V_{(4)} = 2$  (in particular,  $(V_4, V_{+,4}) = (1, 1)$  or  $(0, 2)$ ) and its generalizations given in Figure 7. Note that if we increase  $V_{+,4}$  in the way of producing c ( $V_{+,4} = 3$  given by the graph b), then we have for arbitrary  $V_{+,4}$ ,  $L = 1 + 2(V_{(4)} - 1) = 2V_{(4)} - 1$ ,  $F_{\text{int}} = 2V_{(4)}$ , and  $\rho_+ = V_{(4)} - 1$ ,  $\rho_{2;a} = 0$ , and  $\rho_{2;b} = 0$ , therefore  $\omega_{d,+} = \frac{1}{2}$ , and is independent of  $V_{(4)}$  (or  $V_{+,4}$ ) which is expected. To these graphs, we can add the enhanced 2-point

function  $V_{2;a} = 1$  to any of the internal lines as illustrated in the graphs d and e. We have for arbitrary  $V_{+;4}$  and  $V_{2;a} = 1$ ,  $L = 2V_{(4)}$ ,  $F_{\text{int}} = 2V_{(4)}$ ,  $\rho_+ = V_{(4)} - 1$ ,  $\rho_{2;a} = 1$ , and  $\rho_{2;b} = 1$  therefore  $\omega_{d;+} = 0$  is independent of  $V_{(4)}$  (or  $V_{+;4}$ ).

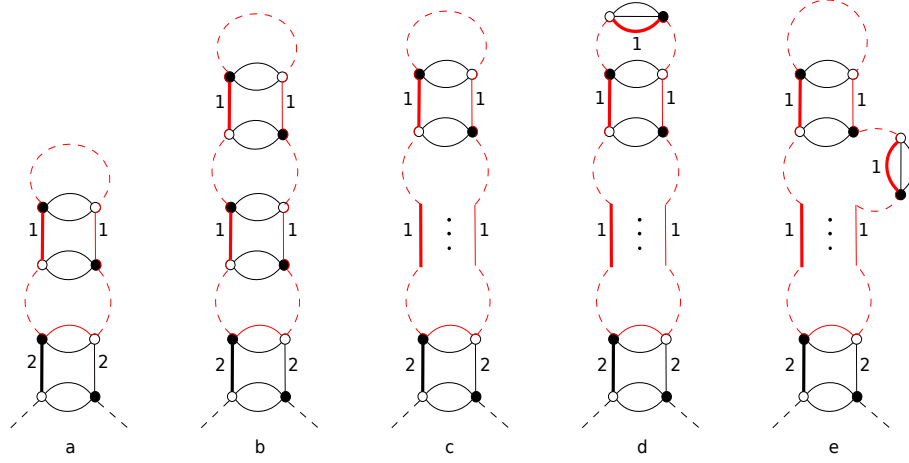


Figure 7: A family of melonic graphs (a,b and c) with  $N_{\text{ext}} = 2$  and  $\omega_{d;+} = \frac{1}{2}$  and a family of log-divergent melonic graphs (d and f) with  $N_{\text{ext}} = 2$ .

(ii) We now consider 4-point functions,  $N_{\text{ext}} = 4$ . First, set  $V_{+;4} = 2$ . The non-melonic graph a of Figure 8 is logarithmic-divergent since  $L = 2$ ,  $F_{\text{int}} = 1$ ,  $\rho_+ = 2$ ,  $\rho_{2;a} = 0$ , and  $\rho_{2;b} = 0$ . This graph generalizes to b and then to c such that  $F_{\text{int}} = 1 + d^-(V_{+;4} - \frac{N_{\text{ext}}}{2}) = -3 + 2V_{+;4}$ ,  $\rho_+ = V_{+;4}$ ,  $\rho_{2;a} = 0$  and  $\rho_{2;b} = 0$ .

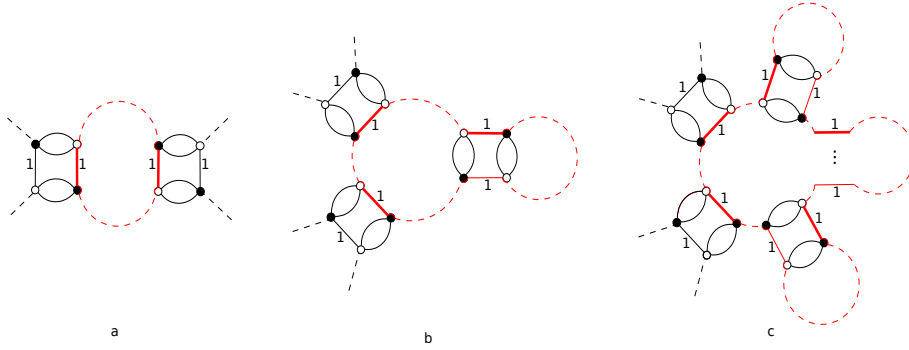


Figure 8: A family of log-divergent non-melonic graphs with  $N_{\text{ext}} = 4$  and  $V_{+;4} \geq 2$ .

## C Divergences in model $\times$ ( $d = 3, D = 1, a = \frac{1}{2}, b = 1$ )

We illustrate some divergent amplitudes in the model  $\times$  with parameters given above. We keep the same meaning of the graphical representation for graphs as in appendix B.

The superficial degree of divergence of a graph  $\mathcal{G}$  has been given in (47) and that we evaluate at  $D = 1, a = \frac{1}{2}$ , and  $b = 1$  as

$$\omega_{d;\times}(\mathcal{G}) = -2L + F_{\text{int}} + \rho_{\times} + \rho_{2;a} + 2\rho_{2;b}. \quad (\text{C.9})$$

We consider 2-point functions,  $N_{\text{ext}} = 2$ .

(1) We consider tadpole graphs with  $V_{(4)} = 1$  given in Figure 9 which are log-divergent. The graphs a and b are melonic whereas the graph c is non-melonic.

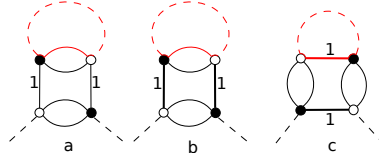


Figure 9: Log-divergent graphs with  $N_{\text{ext}} = 2$  and  $V_{(4)} = 1$ .

(2) Consider now  $V_{(4)} \geq 2$ . Melonic graphs (resp. non-melonic graphs) with  $V_{(4)} = 2$  and their generalizations for  $V_{(4)} > 2$  are given in Figure 10 (resp. Figure 11).

First, focus on the melonic graphs of Figure 10. The melonic graphs, a and d with  $N_{\text{ext}} = 2$  and  $V_{(4)} = 2$  (but  $V_{\times;4} \geq 1$ ) give  $\omega_{d;\times} = 0$ . Increase  $V_{\times;4}$  in a way to have the graphs c and f (intermediate steps are given by graphs b and e, respectively), then we have for arbitrary  $V_{\times;4}$ ,  $F_{\text{int}} = 2V_{(4)}$ ,  $\rho_{\times} = 2(V_{(4)} - 1)$ , therefore  $\omega_{d;\times} = 0$ . With these graphs, we confirm that this model has infinitely many log-divergent 2-point graphs.

Next, consider the non-melonic graphs of Figure 11. For arbitrary  $V_{(4)} = V_{\times;4}$ ,  $F_{\text{int}} = 2(V_{(4)} - 1) + 1$ ,  $\rho_{\times} = 1 + 2(V_{(4)} - 1)$ ,  $\rho_{2;a} = 0$ , and  $\rho_{2;b} = 0$  therefore  $\omega_{d;\times} = 0$ . Again, we see that this model has infinitely many graphs that are divergent.

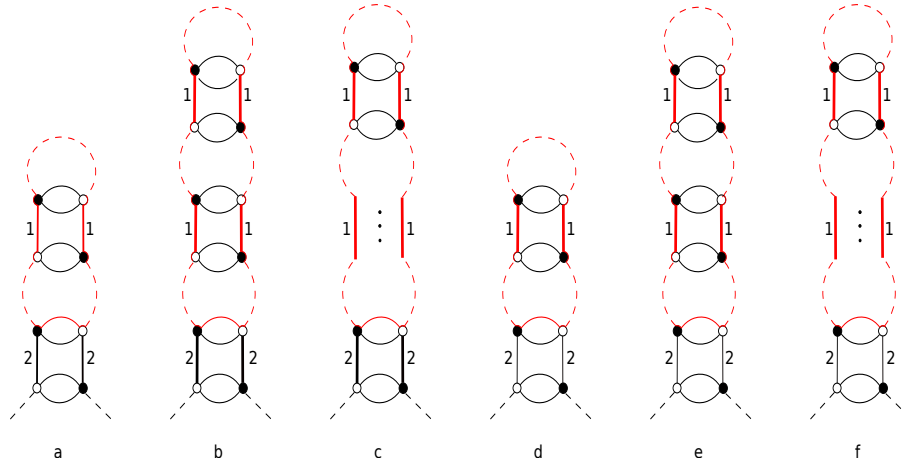


Figure 10: Melonic graphs with  $N_{\text{ext}} = 2$  which give  $\omega_{d;\times} = 0$ .

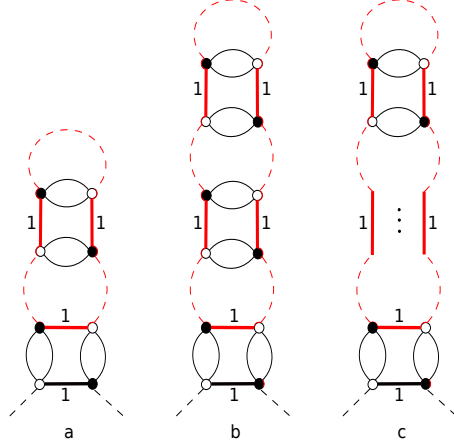


Figure 11: Non-melonic graphs with  $N_{\text{ext}} = 2$  which give  $\omega_{\text{d};\times} = 0$ .

(3) A comparison with the previous model shows that the 4-point non-melonic graph with  $V_{(4)} = V_{\times;4} = 2$  of Figure 12 is convergent  $\omega_{\text{d};\times} = -1$ ,  $F_{\text{int}} = 1$ ,  $\rho_{\times} = 2$ ,  $\rho_{2;a} = 0$ , and  $\rho_{2;b} = 0$ .

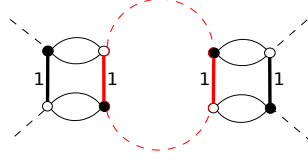


Figure 12: A convergent non-melonic graph with  $N_{\text{ext}} = 4$  and  $V_{(4)} = V_{\times;4} = 2$ .

## References

- [1] J. Ambjorn, B. Durhuus and T. Jonsson, “Three-Dimensional Simplicial Quantum Gravity And Generalized Matrix Models,” *Mod. Phys. Lett. A* **6**, 1133 (1991).
- [2] M. Gross, “Tensor models and simplicial quantum gravity in  $> 2$ -D,” *Nucl. Phys. Proc. Suppl.* **25A**, 144 (1992).
- [3] N. Sasakura, “Tensor model for gravity and orientability of manifold,” *Mod. Phys. Lett. A* **6**, 2613 (1991).
- [4] D. V. Boulatov, “A Model of three-dimensional lattice gravity,” *Mod. Phys. Lett. A* **7**, 1629 (1992) [arXiv:hep-th/9202074];
- [5] H. Ooguri, “Topological lattice models in four-dimensions,” *Mod. Phys. Lett. A* **7**, 2799 (1992) [arXiv:hep-th/9205090].

- [6] T. Regge, "General relativity without coordinates" *Nuovo Cimento* **19.3** (Feb. 1961), pp. 558-571
- [7] H. Hamber, "Quantum Gravitation - The Feynman Path Integral Approach," (Springer Publishing, Berlin & New York, 2009) 342 pp.
- [8] J. Ambjorn, J. Jurkiewicz and R. Loll, "The Universe from scratch," *Contemp. Phys.* **47**, 103 (2006) [hep-th/0509010].
- [9] J. Ambjorn, A. Goerlich, J. Jurkiewicz and R. Loll, "Nonperturbative Quantum Gravity," *Phys. Rept.* **519**, 127 (2012) [arXiv:1203.3591 [hep-th]].
- [10] J. Ambjorn, A. Goerlich, J. Jurkiewicz and R. Loll, "Causal Dynamical Triangulations and the Search for a Theory of Quantum Gravity," *Proceedings of the MG13 Meeting on General Relativity Stockholm University, Sweden, 1-7 July 2012*, pp. 120-137 [arXiv:1305.6680 [gr-qc]].
- [11] P. Di Francesco, P. H. Ginsparg and J. Zinn-Justin, "2-D Gravity and random matrices," *Phys. Rept.* **254**, 1 (1995) [arXiv:hep-th/9306153].
- [12] G. 't Hooft, "A Planar Diagram Theory for Strong Interactions," *Nucl. Phys. B* **72**, 461 (1974).
- [13] V. A. Kazakov, "Bilocal Regularization of Models of Random Surfaces," *Phys. Lett. B* **150**, 282 (1985).
- [14] V. A. Kazakov, I. K. Kostov, A. A. Migdal, "Critical properties of randomly triangulated planar random surfaces," *Phys. Lett. B* **157** 295-300 (1985).
- [15] F. David, "A Model of Random Surfaces with Nontrivial Critical Behavior," *Nucl. Phys. B* **257**, 543 (1985).
- [16] V. G. Knizhnik, A. M. Polyakov and A. B. Zamolodchikov, "Fractal Structure of 2D Quantum Gravity," *Mod. Phys. Lett. A* **3**, 819 (1988).
- [17] F. David, "Conformal Field Theories Coupled to 2D Gravity in the Conformal Gauge," *Mod. Phys. Lett. A* **3**, 1651 (1988).
- [18] J. Distler and H. Kawai, "Conformal Field Theory and 2D Quantum Gravity Or Who's Afraid of Joseph Liouville?," *Nucl. Phys. B* **321**, 509 (1989).
- [19] R. Gurau, "The  $1/N$  expansion of colored tensor models," *Annales Henri Poincare* **12**, 829 (2011) [arXiv:1011.2726 [gr-qc]].
- [20] R. Gurau and V. Rivasseau, "The  $1/N$  expansion of colored tensor models in arbitrary dimension," *Europhys. Lett.* **95**, 50004 (2011) [arXiv:1101.4182 [gr-qc]].
- [21] R. Gurau, "The complete  $1/N$  expansion of colored tensor models in arbitrary dimension," *Annales Henri Poincare* **13**, 399 (2012) [arXiv:1102.5759 [gr-qc]].

- [22] R. Gurau, “Colored Group Field Theory,” *Commun. Math. Phys.* **304**, 69 (2011) [arXiv:0907.2582 [hep-th]].
- [23] R. Gurau, “Topological Graph Polynomials in Colored Group Field Theory,” *Annales Henri Poincare* **11**, 565 (2010) [arXiv:0911.1945 [hep-th]].
- [24] R. Gurau, “Lost in Translation: Topological Singularities in Group Field Theory,” *Class. Quant. Grav.* **27**, 235023 (2010) [arXiv:1006.0714 [hep-th]].
- [25] R. Gurau and J. P. Ryan, “Colored Tensor Models - a review,” *SIGMA* **8**, 020 (2012) [arXiv:1109.4812 [hep-th]].
- [26] V. Bonzom, R. Gurau, A. Riello and V. Rivasseau, “Critical behavior of colored tensor models in the large N limit,” *Nucl. Phys. B* **853**, 174 (2011) [arXiv:1105.3122 [hep-th]].
- [27] R. Gurau, “A generalization of the Virasoro algebra to arbitrary dimensions,” *Nucl. Phys. B* **852**, 592 (2011) [arXiv:1105.6072 [hep-th]].
- [28] V. Bonzom, R. Gurau and V. Rivasseau, “The Ising Model on Random Lattices in Arbitrary Dimensions,” *Phys. Lett. B* **711**, 88 (2012) [arXiv:1108.6269 [hep-th]].
- [29] D. Benedetti and R. Gurau, “Phase Transition in Dually Weighted Colored Tensor Models,” *Nucl. Phys. B* **855**, 420 (2012) [arXiv:1108.5389 [hep-th]].
- [30] A. Tanasa, “Multi-orientable Group Field Theory,” *J. Phys. A* **45**, 165401 (2012) [arXiv:1109.0694 [math.CO]].
- [31] R. Gurau, “The Double Scaling Limit in Arbitrary Dimensions: A Toy Model,” *Phys. Rev. D* **84**, 124051 (2011) [arXiv:1110.2460 [hep-th]].
- [32] R. Gurau, “Universality for Random Tensors,” *Ann. Inst. H. Poincare Probab. Statist.* **50**, no. 4, 1474 (2014) [arXiv:1111.0519 [math.PR]].
- [33] V. Bonzom, R. Gurau and V. Rivasseau, “Random tensor models in the large N limit: Uncoloring the colored tensor models,” *Phys. Rev. D* **85**, 084037 (2012) [arXiv:1202.3637 [hep-th]].
- [34] T. Krajewski, “Schwinger-Dyson Equations in Group Field Theories of Quantum Gravity,” arXiv:1211.1244[math-ph].
- [35] R. Gurau, “The Schwinger Dyson equations and the algebra of constraints of random tensor models at all orders,” *Nucl. Phys. B* **865**, 133 (2012) [arXiv:1203.4965 [hep-th]].
- [36] V. Bonzom, R. Gurau and M. Smerlak, “Universality in p-spin glasses with correlated disorder,” *J. Stat. Mech.* (2013) L02003, [arXiv:1206.5539 [cond-mat.dis-nn]].
- [37] R. Gurau, “The  $1/N$  Expansion of Tensor Models Beyond Perturbation Theory,” *Commun. Math. Phys.* **330**, 973 (2014) [arXiv:1304.2666 [math-ph]].

- [38] S. Dartois, R. Gurau and V. Rivasseau, “Double Scaling in Tensor Models with a Quartic Interaction,” JHEP **1309**, 088 (2013) [arXiv:1307.5281 [hep-th]].
- [39] T. Delepouve, R. Gurau and V. Rivasseau, “Borel summability and the non perturbative  $1/N$  expansion of arbitrary quartic tensor models,” arXiv:1403.0170 [hep-th].
- [40] V. Bonzom, R. Gurau, J. P. Ryan and A. Tanasa, “The double scaling limit of random tensor models,” arXiv:1404.7517 [hep-th].
- [41] S. Dartois, “Random Tensor models: Combinatorics, Geometry, Quantum Gravity and Integrability,” arXiv:1512.01472 [math-ph].
- [42] R. Gurau, “Random Tensors,” Oxford University Press, Oxford, 2016.
- [43] A. Eichhorn and T. Koslowski, “Continuum limit in matrix models for quantum gravity from the Functional Renormalization Group,” Phys. Rev. D **88**, 084016 (2013) [arXiv:1309.1690 [gr-qc]].
- [44] J. Ben Geloun and T. A. Koslowski, “Nontrivial UV behavior of rank-4 tensor field models for quantum gravity,” arXiv:1606.04044 [gr-qc].
- [45] A. Eichhorn and T. Koslowski, “Flowing to the continuum in discrete tensor models for quantum gravity,” arXiv:1701.03029 [gr-qc].
- [46] S. Carrozza and V. Lahoche, “Asymptotic safety in three-dimensional SU(2) Group Field Theory: evidence in the local potential approximation,” Class. Quant. Grav. **34**, no. 11, 115004 (2017) [arXiv:1612.02452 [hep-th]].
- [47] V. Rivasseau, “Quantum Gravity and Renormalization: The Tensor Track,” AIP Conf. Proc. **1444**, 18 (2011) [arXiv:1112.5104 [hep-th]].
- [48] V. Rivasseau, “The Tensor Track, IV,” PoS CORFU **2015**, 106 (2016) [arXiv:1604.07860 [hep-th]].
- [49] S. Dartois, V. Rivasseau and A. Tanasa, “The  $1/N$  expansion of multi-orientable random tensor models,” Annales Henri Poincare **15**, 965 (2014) [arXiv:1301.1535 [hep-th]].
- [50] E. Fusy and A. Tanasa, “Asymptotic expansion of the multi-orientable random tensor model,” The electronic journal of combinatorics **22(1)** (2015), P1.52 [arXiv:1408.5725 [math.CO]].
- [51] V. Lahoche and D. Ousmane Samary, “Functional renormalization group for the U(1)- $T_5^6$  tensorial group field theory with closure constraint,” Phys. Rev. D **95**, no. 4, 045013 (2017) [arXiv:1608.00379 [hep-th]].
- [52] D. Ousmane Samary, C. I. Pérez-Sánchez, F. Vignes-Tourneret and R. Wulkenhaar, “Correlation functions of a just renormalizable tensorial group field theory: the melonic approximation,” Class. Quant. Grav. **32**, no. 17, 175012 (2015) [arXiv:1411.7213 [hep-th]].

- [53] D. O. Samary, “Closed equations of the two-point functions for tensorial group field theory,” *Class. Quant. Grav.* **31**, 185005 (2014) [arXiv:1401.2096 [hep-th]].
- [54] T. Delepouve and R. Gurau, “Phase Transition in Tensor Models,” *JHEP* **1506**, 178 (2015) [arXiv:1504.05745 [hep-th]].
- [55] L. Lionni and J. Thuerigen, “Multi-critical behaviour of 4-dimensional tensor models up to order 6,” arXiv:1707.08931 [hep-th].
- [56] L. Lionni and V. Rivasseau, “Intermediate Field Representation for Positive Matrix and Tensor Interactions,” arXiv:1609.05018 [math-ph].
- [57] V. Rivasseau and F. Vignes-Tourneret, “Constructive tensor field theory: The  $T_4^4$  model,” arXiv:1703.06510 [math-ph].
- [58] V. Rivasseau “Loop Vertex Expansion for Higher Order Interactions,” arXiv:1702.07602 [math-ph].
- [59] T. Krajewski, “Group field theories,” *PoS QGQGS 2011*, 005 (2011) [arXiv:1210.6257 [gr-qc]].
- [60] Sigma Collection, “Invitation to Random Tensors,” Editor R. Gurau, *SIGMA* 12 (2016), **094**, 12 pages  
V. Rivasseau, “Constructive Tensor Field Theory,” *SIGMA* 12 (2016), 085, 31 pages.  
S. Gielen and L. Sindoni, “Quantum Cosmology from Group Field Theory Condensates: a Review,” *SIGMA* 12 (2016), 082, 49 pages.  
J. P. Ryan, “ $(D + 1)$ -Colored Graphs - a Review of Sundry Properties,” *SIGMA* 12 (2016), 076, 27 pages.  
V. Bonzom, “Large  $N$  Limits in Tensor Models: Towards More Universality Classes of Colored Triangulations in Dimension  $d \geq 2$ ,” *SIGMA* 12 (2016), 073, 39 pages.  
S. Carrozza, “Flowing in Group Field Theory Space: a Review,” *SIGMA* 12 (2016), 070, 30 pages.  
V. Rivasseau, “Random Tensors and Quantum Gravity,” *SIGMA* 12 (2016), 069, 17 pages.  
T. Krajewski and R. Toriumi, “Exact Renormalisation Group Equations and Loop Equations for Tensor Models,” *SIGMA* 12 (2016), 068, 36 pages.  
A. Tanasa, “The Multi-Orientable Random Tensor Model, a Review,” *SIGMA* 12 (2016), 056, 23 pages.
- [61] J. Ben Geloun and R. Toriumi, “Parametric representation of rank  $d$  tensorial group field theory: Abelian models with kinetic term  $\sum_s |p_s| + \mu$ ,” *J. Math. Phys.* **56**, no. 9, 093503 (2015) [arXiv:1409.0398 [hep-th]].
- [62] T. Krajewski and R. Toriumi, “Polchinski’s exact renormalisation group for tensorial theories: Gaussian universality and power counting,” *J. Phys. A* **49**, no. 38, 385401 (2016) [arXiv:1511.09084 [gr-qc]].



- [63] T. Krajewski and R. Toriumi, “Exact Renormalisation Group Equations and Loop Equations for Tensor Models,” *SIGMA* **12**, 068 (2016) [arXiv:1603.00172 [gr-qc]].
- [64] A. Eichhorn and T. Koslowski, “Towards phase transitions between discrete and continuum quantum spacetime from the Renormalization Group,” *Phys. Rev. D* **90**, no. 10, 104039 (2014) [arXiv:1408.4127 [gr-qc]].
- [65] D. Benedetti, J. Ben Geloun and D. Oriti, “Functional Renormalisation Group Approach for Tensorial Group Field Theory: a Rank-3 Model,” *JHEP* **1503**, 084 (2015) [arXiv:1411.3180 [hep-th]].
- [66] D. Benedetti and V. Lahoche, “Functional Renormalization Group Approach for Tensorial Group Field Theory: A Rank-6 Model with Closure Constraint,” *Class. Quant. Grav.* **33**, no. 9, 095003 (2016) [arXiv:1508.06384 [hep-th]].
- [67] J. Ben Geloun, R. Martini and D. Oriti, “Functional Renormalization Group analysis of a Tensorial Group Field Theory on  $\mathbb{R}^3$ ,” *Europhys. Lett.* **112**, no. 3, 31001 (2015) [arXiv:1508.01855 [hep-th]].
- [68] J. Ben Geloun, R. Martini and D. Oriti, “Functional Renormalisation Group analysis of Tensorial Group Field Theories on  $\mathbb{R}^d$ ,” *Phys. Rev. D* **94**, no. 2, 024017 (2016) [arXiv:1601.08211 [hep-th]].
- [69] S. Carrozza, V. Lahoche and D. Oriti, “Renormalizable Group Field Theory beyond melons: an example in rank four,” arXiv:1703.06729 [gr-qc].
- [70] R. Gurau and J. P. Ryan, “Melons are branched polymers,” *Annales Henri Poincare* **15**, no. 11, 2085 (2014) [arXiv:1302.4386 [math-ph]].
- [71] V. Bonzom, “New  $1/N$  expansions in random tensor models,” *JHEP* **1306**, 062 (2013) [arXiv:1211.1657 [hep-th]].
- [72] V. Bonzom, T. Delepouve and V. Rivasseau, “Enhancing non-melonic triangulations: A tensor model mixing melonic and planar maps,” *Nucl. Phys. B* **895**, 161 (2015) [arXiv:1502.01365 [math-ph]].
- [73] J. Ben Geloun, “A power counting theorem for a  $p^{2a}\phi^4$  tensorial group field theory”, arXiv:hep-th/1507.00590.
- [74] V. Rivasseau, “Towards Renormalizing Group Field Theory,” *PoS C NCFG2010*, 004 (2010) [arXiv:1103.1900 [gr-qc]].
- [75] V. Rivasseau, “The Tensor Track: an Update,” arXiv:1209.5284 [hep-th].
- [76] V. Rivasseau, “The Tensor Track, III,” arXiv:1311.1461 [hep-th].
- [77] S. Carrozza, “Tensorial methods and renormalization in Group Field Theories,” Springer Theses, 2014 (Springer, NY, 2014), arXiv:1310.3736 [hep-th].
- [78] V. Rivasseau, “The Tensor Theory Space,” arXiv:1407.0284 [hep-th].

- [79] S. Gielen, D. Oriti and L. Sindoni, “Cosmology from Group Field Theory Formalism for Quantum Gravity,” *Phys. Rev. Lett.* **111**, no. 3, 031301 (2013) [arXiv:1303.3576 [gr-qc]].
- [80] J. Ben Geloun and V. Rivasseau, “A Renormalizable 4-Dimensional Tensor Field Theory,” *Commun. Math. Phys.* **318**, 69 (2013) [arXiv:1111.4997 [hep-th]].
- [81] J. Ben Geloun and V. Rivasseau, “Addendum to ‘A Renormalizable 4-Dimensional Tensor Field Theory’,” *Commun. Math. Phys.* **322**, 957 (2013) [arXiv:1209.4606 [hep-th]].
- [82] J. Ben Geloun, J. Magnen and V. Rivasseau, “Bosonic Colored Group Field Theory,” *Eur. Phys. J. C* **70**, 1119 (2010) [arXiv:0911.1719 [hep-th]].
- [83] J. Ben Geloun, T. Krajewski, J. Magnen and V. Rivasseau, “Linearized Group Field Theory and Power Counting Theorems,” *Class. Quant. Grav.* **27**, 155012 (2010) [arXiv:1002.3592 [hep-th]].
- [84] J. Ben Geloun, R. Gurau and V. Rivasseau, “EPRL/FK Group Field Theory,” *Europhys. Lett.* **92**, 60008 (2010) [arXiv:1008.0354 [hep-th]].
- [85] J. Ben Geloun and V. Bonzom, “Radiative corrections in the Boulatov-Ooguri tensor model: The 2-point function,” *Int. J. Theor. Phys.* **50**, 2819 (2011) [arXiv:1101.4294 [hep-th]].
- [86] J. Ben Geloun and D. O. Samary, “3D Tensor Field Theory: Renormalization and One-loop  $\beta$ -functions,” *Annales Henri Poincaré* **14**, 1599 (2013) [arXiv:1201.0176 [hep-th]].
- [87] J. Ben Geloun and E. R. Livine, “Some classes of renormalizable tensor models,” *J. Math. Phys.* **54**, 082303 (2013) [arXiv:1207.0416 [hep-th]].
- [88] J. Ben Geloun, “Two and four-loop  $\beta$ -functions of rank 4 renormalizable tensor field theories,” *Class. Quant. Grav.* **29**, 235011 (2012) [arXiv:1205.5513 [hep-th]].
- [89] S. Carrozza, D. Oriti and V. Rivasseau, “Renormalization of Tensorial Group Field Theories: Abelian  $U(1)$  Models in Four Dimensions,” *Commun. Math. Phys.* **327**, 603 (2014) [arXiv:1207.6734 [hep-th]].
- [90] D. O. Samary and F. Vignes-Tourneret, “Just Renormalizable TGFT’s on  $U(1)^d$  with Gauge Invariance,” *Commun. Math. Phys.* **329**, 545 (2014) [arXiv:1211.2618 [hep-th]].
- [91] S. Carrozza, D. Oriti and V. Rivasseau, “Renormalization of a  $SU(2)$  Tensorial Group Field Theory in Three Dimensions,” *Commun. Math. Phys.* **330**, 581 (2014) [arXiv:1303.6772 [hep-th]].
- [92] D. O. Samary, “Beta functions of  $U(1)^d$  gauge invariant just renormalizable tensor models,” *Phys. Rev. D* **88**, 105003 (2013) [arXiv:1303.7256 [hep-th]].
- [93] J. Ben Geloun, “Renormalizable Models in Rank  $d \geq 2$  Tensorial Group Field Theory,” *Commun. Math. Phys.* **332**, 117 (2014) [arXiv:1306.1201 [hep-th]].

- [94] M. Raasakka and A. Tanasa, “Combinatorial Hopf algebra for the Ben Geloun-Rivasseau tensor field theory,” *Seminaire Lotharingien de Combinatoire* **70** (2014), B70d [arXiv:1306.1022 [gr-qc]].
- [95] S. Carrozza, “Discrete Renormalization Group for SU(2) Tensorial Group Field Theory,” *Ann. Inst. Henri Poincaré Comb. Phys. Interact.* **2** (2015), 49-112 [arXiv:1407.4615 [hep-th]].
- [96] S. Carrozza, “Group field theory in dimension  $4 - \epsilon$ ,” *Phys. Rev. D* **91**, no. 6, 065023 (2015) [arXiv:1411.5385 [hep-th]].
- [97] V. Rivasseau, “Why are tensor field theories asymptotically free?,” *Europhys. Lett.* **111**, no. 6, 60011 (2015) [arXiv:1507.04190 [hep-th]].
- [98] A. Kegeles and D. Oriti, “Generalized conservation laws in non-local field theories,” *J. Phys. A* **49**, no. 13, 135401 (2016) [arXiv:1506.03320 [hep-th]].
- [99] A. Kegeles and D. Oriti, “Continuous point symmetries in Group Field Theories,” *J. Phys. A* **50**, no. 12, 125402 (2017) [arXiv:1608.00296 [gr-qc]].
- [100] R. C. Avohou, J. Ben Geloun and M. N. Hounkonnou, “A Polynomial Invariant for Rank 3 Weakly-Colored Stranded Graphs,” accepted in *Combinatorics, Probability and Computing* [arXiv:1301.1987 [math.CO]].
- [101] J. P. Ryan, “Tensor models and embedded Riemann surfaces,” *Phys. Rev. D* **85**, 024010 (2012) [arXiv:1104.5471 [gr-qc]].
- [102] J. Ben Geloun, “On the finite amplitudes for open graphs in Abelian dynamical colored Boulatov-Ooguri models,” *J. Phys. A* **46**, 402002 (2013) [arXiv:1307.8299 [hep-th]].
- [103] M. R. Casali, P. Cristofori, S. Dartois and L. Grasselli, “Topology in colored tensor models via crystallization theory,” arXiv:1704.02800 [math-ph].
- [104] J. Ben Geloun and S. Ramgoolam, “Tensor Models, Kronecker coefficients and Permutation Centralizer Algebras,” arXiv:1708.03524 [hep-th].
- [105] E. Witten, “An SYK-Like Model Without Disorder,” arXiv:1610.09758 [hep-th].
- [106] R. Gurau, “The complete  $1/N$  expansion of a SYK-like tensor model,” *Nucl. Phys. B* **916**, 386 (2017) [arXiv:1611.04032 [hep-th]].
- [107] I. R. Klebanov and G. Tarnopolsky, “Uncolored random tensors, melon diagrams, and the Sachdev-Ye-Kitaev models,” *Phys. Rev. D* **95**, no. 4, 046004 (2017) [arXiv:1611.08915 [hep-th]].
- [108] C. Krishnan, S. Sanyal and P. N. Bala Subramanian, “Quantum Chaos and Holographic Tensor Models,” *JHEP* **1703**, 056 (2017) [arXiv:1612.06330 [hep-th]].
- [109] F. Ferrari, “The Large D Limit of Planar Diagrams,” arXiv:1701.01171 [hep-th].

- [110] R. Gurau, “Quenched equals annealed at leading order in the colored SYK model,” arXiv:1702.04228 [hep-th].
- [111] V. Bonzom, L. Lionni and A. Tanasa, “Diagrammatics of a colored SYK model and of an SYK-like tensor model, leading and next-to-leading orders,” J. Math. Phys. **58**, no. 5, 052301 (2017) [arXiv:1702.06944 [hep-th]].
- [112] S. Sachdev and J. Ye, “Gapless spin fluid ground state in a random, quantum Heisenberg magnet,” Phys. Rev. Lett. **70** (1993) 3339 [cond-mat/9212030].
- [113] A. Kitaev, <http://online.kitp.ucsb.edu/online/entangled15/kitaev/>
- [114] J. Maldacena and D. Stanford, “Remarks on the Sachdev-Ye-Kitaev model,” Phys. Rev. D **94**, no. 10, 106002 (2016) [arXiv:1604.07818 [hep-th]].
- [115] D. J. Gross and V. Rosenhaus, “A Generalization of Sachdev-Ye-Kitaev,” JHEP **1702**, 093 (2017) [arXiv:1610.01569 [hep-th]].
- [116] L. Freidel, “Group field theory: An Overview,” Int. J. Theor. Phys. **44**, 1769 (2005) [hep-th/0505016].
- [117] D. Oriti, “The group field theory approach to quantum gravity,” arXiv:gr-qc/0607032.
- [118] D. Oriti, “A Quantum field theory of simplicial geometry and the emergence of space-time,” J. Phys. Conf. Ser. **67**, 012052 (2007) [hep-th/0612301].
- [119] H. Grosse and R. Wulkenhaar, “Renormalisation of  $\phi^4$  theory on noncommutative  $\mathbb{R}^4$  in the matrix base,” Commun. Math. Phys. **256**, 305 (2005) [arXiv:hep-th/0401128].
- [120] H. Grosse and R. Wulkenhaar, “Self-Dual Noncommutative  $\phi^4$  -Theory in Four Dimensions is a Non-Perturbatively Solvable and Non-Trivial Quantum Field Theory,” Commun. Math. Phys. **329**, 1069 (2014) [arXiv:1205.0465 [math-ph]].
- [121] H. Grosse, A. Sako and R. Wulkenhaar, “The  $\Phi_4^3$  and  $\Phi_6^3$  matricial QFT models have reflection positive two-point function,” arXiv:1612.07584 [math-ph].
- [122] V. Rivasseau, “From perturbative to constructive renormalization,” Princeton series in physics (Princeton Univ. Pr., Princeton, 1991).
- [123] G. Gallavotti and F. Nicolò, “Renormalization theory in four-dimensional scalar fields. I.” Commun. Math. Phys. **100**, 545 (1985).